

**Evaluating the Effect of a Self-Healing Elastomer on the Self-Healing Properties of Asphalt
Cement**

by

Mike Aurilio

A thesis

presented to the University of Waterloo

in fulfillment of the

thesis requirement for the degree of

Master of Applied Science

in

Civil Engineering

Waterloo, Ontario, Canada, 2020

© Mike Aurilio 2020

Author's Declaration

I hereby declare that I am the sole author of this thesis. This is a true copy of the thesis, including any required final revisions, as accepted by my examiners.

I understand that my thesis may be made electronically available to the public.

Abstract

Asphalt pavements exhibit an interesting behaviour when the traffic loading is removed. The chemical structure of asphalt cement lends itself to the ability to heal damage and improve the longevity of the pavement. This phenomenon was first discovered in the 1960s and makes up an interesting area of research. The area of self-healing materials has been a growing area of research for materials in general, but recently attempts have been made to improve the natural healing capabilities of asphalt cement. Other branches of science have begun using microcapsules dispersed through the matrix to distribute healing agent upon damage. Styrene Butadiene Styrene (SBS) modification of asphalt cement is already a common technology in the pavement industry, and this has inspired the idea to introduce a polymer that has self-healing properties into asphalt cement. This thesis looks at the effect of traditional elastomeric modification on the healing efficiency of asphalt cement and explore the use of a novel self-healing elastomer (SHE) to modify the asphalt cement healing properties. Data in this thesis indicates that the self-healing elastomer used here was unable to improve the healing efficiency of asphalt cement, while SBS has shown some ability to improve crack healing. SBS has also shown a great ability to improve adhesion, which may influence the cohesive healing ability of asphalt cement.

Acknowledgements

I would like to extend my gratitude to Professor Hassan Baaj for his introduction to this interesting topic and guidance during this project. This was a fantastic opportunity to learn and I'm looking forward to applying what I've learned as we work together on future projects. I would also like to thank Dr. Sina Varamini and Dr. Chris Bachmann for agreeing to be part of my thesis review committee.

I want to express my thanks to Donn Bernal who gave me the freedom to pursue this degree while working full-time.

Most importantly, I want to thank my family for their love and support during the completion of this thesis. My brother, Rob, was particularly helpful since he decided to do his PhD at the same time and make this a lot more fun.

Table of Contents

Author’s Declaration	ii
Abstract.....	iii
Acknowledgements	iv
List of Figures	vii
List of Tables	x
List of Abbreviations.....	xi
Chapter 1: INTRODUCTION.....	1
1.1 Background	1
1.2 Problem Statement and Research Questions	2
1.3 Research Hypothesis.....	3
1.4 Thesis Organization	3
Chapter 2: LITERATURE REVIEW	4
2.1 Asphalt Cement Chemistry	4
2.1.1 Viscoelasticity of Asphalt Cement.....	6
2.1.2 Laboratory Aging Methods	8
2.1.3 SBS Modified Asphalt Cement.....	10
2.2 Characterizing Asphalt Cement and Mixture Fatigue.....	12
2.2.1 Asphalt Mixture Testing.....	13
2.2.2 Fatigue Life Predictions with Wohler Curves	14
2.2.3 Damage Rate Analysis with the DGCB Method.....	15
2.2.4 Fracture Mechanics Approaches for Fatigue Characterization	18
2.2.5 Viscoelastic Continuum Damage Model for Fatigue Characterization	21
2.2.6 Asphalt Cement Testing	22
2.2.7 Applying VECD to Asphalt Cement.....	23
2.2.8 Applying Fracture Mechanics to Asphalt Cement	25
2.3 Introduction to Self-Healing Asphalt Pavements	26
2.3.1 Intrinsic Self-Healing of Asphalt Cement	27
2.3.2 Healing of SBS Modified Asphalt Cement	29
2.3.3 Approaches for Developing Self-Healing Asphalt Pavements	30
2.3.4 Capsule Based Self-Healing Materials.....	30
2.3.5 Capsule Based Self-Healing Asphalt Pavements.....	31
2.3.6 Vascular Self-Healing Materials.....	33
2.3.7 Induction Healing of Asphalt Pavements	33
2.3.8 Intrinsic Self-Healing Materials.....	35

2.3.9 Nanoparticles	37
2.4 Characterizing the Self-Healing Properties of Asphalt Cement and Mixtures	37
2.4.1 Self-Healing Properties of Asphalt Mixtures.....	37
2.4.2 Characterizing the Self-Healing Properties of Asphalt Cement	43
2.5 Gaps in Current Research.....	49
2.5.1 Limitations to Healing Characterization.....	49
2.5.2 Limitations to Extrinsic Self-Healing Pavements	50
Chapter 3: PRELIMINARY TESTING OF A SELF-HEALING ASPHALT CEMENT	51
3.1 Material Preparation.....	51
3.2 Testing Methodology	53
3.3 Results and Discussion.....	54
3.4 Chapter Summary	59
Chapter 4: ENHANCED HEALING CHARACTERIZATION OF SBS MODIFIED AND SELF- HEALING ASPHALT CEMENT.....	60
4.1 Performance Grade Asphalt Cement Testing	60
4.2 Master Curves and Black Space Diagrams	62
4.3 DSR Based Cracking Resistance	64
4.4 Healing and Restoration Properties- SLASH Percent Restoration	66
4.5 Healing and Restoration Properties- Healing Ratios	71
4.6 Healing and Restoration Properties- PoliTO Healing Index	77
4.7 Chapter Summary	80
Chapter 5: ADHESIVE HEALING PULL OFF TEST	82
5.1 Background	82
5.2 Methodology	82
5.3 Results and Discussion.....	84
5.4 Chapter Summary	88
Chapter 6: SUMMARY OF WORK AND FUTURE RECOMMENDATIONS.....	89
6.1 Conclusions	89
6.2 Future Work	90
References.....	91
Appendix	99

List of Figures

Figure 2- 1 Example of SAR-AD spider plot of five different asphalt cement sources [11]	5
Figure 2- 2 Examples of possible structures of a) saturates, b) aromatics and c) asphaltenes [,].....	5
Figure 2- 3 Typical master curve construction portraying DSR and BBR data with a fitted rheological model [21].....	8
Figure 2- 4 Master curves (left) and black space diagrams (right) for various levels of asphalt cement aging [8].....	9
Figure 2- 5 Typical master curves (left) and black space diagram (right) for SBS modified asphalt cement [2]	11
Figure 2- 6 Four Point Bending Beam (4PB) number of cycles to failure versus the concentration of SBS [36]	11
Figure 2- 7 The three phases of a cyclically loaded fatigue test [16]	14
Figure 2- 8 Wohler curves for a PG 64-28 with increasing concentrations of SBS [36].....	15
Figure 2- 9 Damage rate analysis and annotations for PG 58-28 in the first measured interval [36].....	17
Figure 2- 10 Illustration of post peak point and calculation of the slope [58]	20
Figure 2- 11 Examples of the effect of temperature on the type of failure observed in LAS testing [72]..	24
Figure 2- 12 Number of cycles to failure for a PG 64-22 [65].....	26
Figure 2- 13 Fatigue Resistance Energy Index for a PG 64-22 [65]	26
Figure 2- 14 Self-healing and fatigue cracking mechanism [13]	28
Figure 2- 15 ESEM images of calcium alginate capsules with various calcium alginate to rejuvenator ratios [84].....	32
Figure 2- 16 Schematic overview of induction healing process [88]	34
Figure 2- 17 Chemical structure and overview of self-healing mechanism of iron-based metal coordination PDMS self-healing polymer [91].....	36
Figure 2- 18 Chemical structure and appearance of final product of zinc-based metal coordination PDMS self-healing polymer [92].....	36
Figure 2- 19 Schematic of Beam-on-elastic-foundation set up developed by Delft University [38]	38
Figure 2- 20 Computed Tomography (CT) images of crack healing for an SMA-11 mixture [94].....	39
Figure 2- 21 Evolution of dynamic modulus versus the number of cycles at 20°C (left) and 60°C (right) [97]	40
Figure 2- 22 Diagram of test set up and procedure used to evaluate calcium alginate capsules containing rejuvenator [99].....	41
Figure 2- 23 Evolution of complex modulus versus the number of cycles (left) and the loading time (right) [79]	42
Figure 2- 24 Evolution of dissipated energy versus the number of cycles (left) and the loading time (right) [79]	43
Figure 2- 25 Example of the data collected using the PoliTO protocol including test parameters [100]...	44
Figure 2- 26 Damage intensity versus pseudo stiffness curves for 50 %S _f (left) and 75 %S _f (right) for rest periods of 1, 5, 10, 15 and 30 minutes [78]	45
Figure 2- 27 Illustration of the sample preparation and test set up for analysing the effect of normal force on self-healing properties [103]	47

Figure 3- 1 Self-healing elastomer as received from the commercial laboratory	51
Figure 3- 2 Self-healing elastomer following a) curing Method B and b) curing Method C	52
Figure 3- 3 Pseudo-stiffness (C) vs damage parameter (S) for (a) the original LASH Test incorporating the cohesive failure damage level, S_f , from [78] and (b) the Simplified-LASH Test [106]	54
Figure 3- 4 Temperature-frequency sweep master curves (left) and temperature-frequency sweep black space diagrams (right)	56
Figure 3- 5 Fourier Transmission Infrared Spectroscopy (ATR-FTIR) reflectance spectra for the self-healing elastomer and unmodified asphalt cement.....	57
Figure 3- 6 Fourier Transmission Infrared Spectroscopy (ATR-FTIR) reflectance spectra for Method A, Method B and Method C	57
Figure 3- 7 Self-healing elastomer following the second and third attempts using curing Method C	58
Figure 4- 1 Master curves modeled using 2S2P1D for the unaged and PAV aged 58-28 and self-healing asphalt cement.....	63
Figure 4- 2 Black space diagrams for the unaged and PAV aged 58-28 and self-healing asphalt cement .	64
Figure 4- 3 Linear Amplitude Sweep data analyzed using the VECD model.....	65
Figure 4- 4 Linear Amplitude Sweep data analyzed using fracture mechanics approach	66
Figure 4- 5 Percent Restoration determined by the SLASH test at different test temperatures	67
Figure 4- 6 Percent Restoration determined by the SLASH test at different levels of laboratory aging	69
Figure 4- 7 Percent restoration determined by the SLASH with different strain levels applied before the rest period at 19°C.....	70
Figure 4- 8 Percent restoration determined by the SLASH with different strain levels applied before the rest period at 13°C.....	70
Figure 4- 9 Linear Amplitude Sweep data analyzed using the VECD model including the rest period	72
Figure 4- 10 Healing ratios calculated using the VECD number of cycles to failure	73
Figure 4- 11 Linear Amplitude Sweep data analyzed using the fracture mechanics approach including the rest period	74
Figure 4- 12 Healing ratios calculated using the fatigue resistance energy index (A: outlier removed for clarity, B: all the data points).....	74
Figure 4- 13 Relationship between VECD number of cycles to failure and FREI healing ratios.....	75
Figure 4- 14 Relationship between VECD number of cycles to failure healing ratio and percent restoration	76
Figure 4- 15 Relationship between FREI healing ratio to failure and percent restoration.....	76
Figure 4- 16 Complex modulus versus time for the calibration test data	79
Figure 4- 17 Complex modulus versus time for the 15% loss in dissipated energy test data	79
Figure 4- 18 Complex modulus versus time for the 50% loss in dissipated energy test data	80
Figure 5- 1 Example of demolded specimen attached to parchment paper prior to testing	83
Figure 5- 2 Single specimen testing before and following test completion.....	83
Figure 5- 3 Healing specimen prior to and following test completion	84
Figure 5- 4 Normal force versus time for the baseline testing of the self-healing asphalt cement (10% SHE and 8% SHE) and unmodified 58-28.....	84
Figure 5- 5 Normal force versus time for the baseline testing of the 58-28 with 2% SBS and 4% SBS....	85
Figure 5- 6 Work required to pull the samples to a gap of 15mm.....	87

Figure 5- 7 Percent restoration for the unmodified 58-28 and self-healing asphalt cement for each gap size tested..... 87

List of Tables

Table 3- 1 Curing times and temperatures for the Self-Healing Elastomer	53
Table 3- 2 LAS number of cycles to failure and percent restoration for unmodified, SHACs and SBS modified asphalt cement	55
Table 4- 1 High temperature test properties measured for the 58-28 and self-healing asphalt cement	61
Table 4- 2 Bending Beam Rheometer test properties measured for the 58-28 and the self-healing asphalt cement.....	62
Table 4- 3 Healing index and dissipated energy loss data for 58-28 replicates	77
Table 4- 4 Healing index and dissipated energy loss data for self-healing asphalt cement replicates	78

List of Abbreviations

4PB	Four Point Bending Beam
AASHTO	American Association of State Highway Transportation Officials
ASTM	American Society for Testing and Materials
ATR	Attenuated Total Reflectance
BBR	Bending Beam Rheometer
BBS	Binder Bond Strength
BOEF	Beam-on-elastic-foundation
CMOD	Crack Mouth Opening Displacement
COD	Crack Opening Displacement
COV	Coefficient of Variation
CT	Computed Tomography
DCT	Disk Shaped Compact Test
DGCB	Département Génie Civil et Bâtiment
DMA	Dynamic Mechanical Analyser
DSR	Dynamic Shear Rheometer
DTT	Direct Tension Test
EPFM	Elastic-Plastic Fracture Mechanics
ESEM	Environmental Scanning Electron Microscope
FREI	Fatigue Resistance Energy Index
FTIR	Fourier Transmission Infrared Spectroscopy
HiMA	Highly Modified Asphalt
HR	Healing Ratio
IDEAL-CT	Indirect Tensile Asphalt Cracking Test
IDT	Indirect Tensile Testing
ISBM	International Symposium on Bituminous Materials
LAS	Linear Amplitude Sweep
LASH	Linear Amplitude Sweep with Healing
LDVW	Lifshitz-Van der Waals
LEFM	Linear-Elastic Fracture Mechanics
MARC	Modified Asphalt Research Center
MGAC	Multiple Stress Creep Recovery Graded Asphalt Cement
MSCR	Multiple Stress Creep Recovery
NCHRP	National Cooperative Highway Research Program
NMR	Nuclear Magnetic Resonance
PAV	Pressure Aging Vessel
PDMS	Polydimethyl Siloxane
PGAC	Performance Graded Asphalt Cement
PLAS	Pure Linear Amplitude Sweep
PMA	Polymer Modified Asphalt
RAP	Reclaimed Asphalt Product
RAS	Reclaimed Asphalt Shingles
RILEM	Reunion Internationale des Laboratoires et Experts des Matériaux
RTFO	Rolling Thin Film Oven
SARA	Saturates, Aromatics, Resins and Asphaltenes
SAR-AD	SARA Determinator
SBS	Styrene Butadiene Styrene
SCB	Semi-Circular Bend Test
SHAC	Self-Healing Asphalt Cement

SHE	Self-Healing Elastomer
SLASH	Simplified Linear Amplitude Sweep with Healing
SMA	Stone Mastic Asphalt
TC	Tension-Compression
TTSP	Time Temperature Superposition
UV	Ultraviolet
VDW	Van der Waal
VECD	Viscoelastic Continuum Damage
WLF	William-Landel-Ferry
WRI	Western Research Institute

Chapter 1: INTRODUCTION

1.1 Background

Flexible pavements, produced using asphalt materials, represent the majority of paved roads driven on by the public in Canada. Approximately 95% of roads paved in Ontario are paved using asphalt [1] and it is equally popular in many parts of the world. Increasing the longevity of pavements in a cost-effective manner has proven to be of great interest public agencies who are responsible for overseeing the procurement of services. Asphalt pavements are prone to several different types of failure including fatigue cracking which occurs overtime as a result of traffic loading. The cracking begins as microcracks before propagating and growing to a size that can lead to failure. Polymer modification of asphalt has proven to be a cost-effective way to improve the resistance to cracking in pavements. Elastomers such as Styrene Butadiene Styrene (SBS) has been shown to greatly increase the strain tolerance of the asphalt and improve cracking resistance at different temperature ranges [2]. SBS improves the elastomeric properties as well as the stiffness leading to a general improvement in all aspects of performance [3].

Asphalt pavements also exhibit an interesting behaviour when the traffic loading is removed. The chemical structure of asphalt cement lends itself to the ability to heal damage and improve the longevity of the pavement. This phenomenon was first discovered in the 1960s and makes up an interesting area of research [4]. Current pavement design methodologies fail to take healing into consideration [5]. The area of self-healing materials has been a growing area of research for materials in general, but recently attempts have been made to improve the natural healing capabilities of asphalt cement. Other branches of science have begun using microcapsules dispersed through the matrix to distribute healing agent upon damage. There have also been interesting examples of polymers produced to heal damage at room temperature. Pavement engineers have begun to draw inspiration from these polymers to produce asphalt mixtures containing microcapsules and induction healing pavements using steel fibers [2].

Polymer modification is already a common technology in the pavement industry, and this means it may be possible to combine this concept with a polymer that has self-healing properties to improve the healing efficiency of asphalt cement. This thesis will look at the effect of traditional elastomeric modification on the healing efficiency of asphalt cement and explore the use of a novel self-healing elastomer (SHE) to modify the asphalt cement healing properties.

1.2 Problem Statement and Research Questions

Improving the fatigue resistance of pavements is a constant concern for pavement engineers and government agencies who own the roads. The development of self-healing asphalt mixtures is a growing area of research, one which can greatly improve the future performance of pavements. By healing damage induced by traffic, the life of the pavement can be extended thus reducing the need to perform maintenance or rehabilitation. This research explores the possibility of utilizing a self-healing elastomer to improve the self-healing properties of asphalt cement which would potentially lead to an improved life span for a pavement.

This thesis will explore the use of a novel self-healing elastomer as a modifier for asphalt cement. The healing properties of this self-healing asphalt cement are evaluated using some chemical analysis, basic asphalt cement testing as well as advanced rheological characterization. These change in rheological properties observed in the self-healing asphalt cement are compared to the change in rheological properties observed following SBS modification. SBS modified asphalt is a common way to improve cracking resistance and serves as an excellent benchmark for the self-healing asphalt cement in this regard. However, the effect of SBS on crack healing is not yet fully understood. The healing properties of the self-healing asphalt cement and SBS modified asphalt cement are evaluated using two different methodologies. The first methodology will attempt to induce damage in the asphalt cement which will recreate the formation of microcracks within a pavement. The second methodology will evaluate the role of adhesion in healing by simulating the interaction of two microcrack interfaces. The validity of these tests will also be explored and discussed.

This research will use the current best practices in evaluating the healing properties of asphalt cement in order to focus on answering the following questions:

- Does the self-healing elastomer improve the self-healing properties of asphalt cement? If so, how does it influence the crack resistance of asphalt cement?
- How does the addition of SBS influence the healing properties of asphalt cement?

The concept of using a self-healing elastomer to modify asphalt cement has rarely been explored, but it presents an interesting way to improve on an existing technique which already increases the cracking resistance of asphalt cement and pavements. Enhancing the natural ability of asphalt cement to heal damage could potentially lead to longer lasting pavements.

1.3 Research Hypothesis

Self-healing elastomers have an intrinsic ability to heal damage due to the presence of highly reversible bonds. The energy required for the bonds to reform often depends on the chemical structure of the polymer, which is tuned for specific applications. Fatigue damage in a pavement will gradually increase over time introducing microcracks into the asphalt cement. The intrinsic ability of asphalt cement to heal damage will cause crack closure when given sufficient rest periods. Dispersion of the self-healing elastomer through the asphalt cement matrix is expected to increase the rate of crack healing by increasing the likelihood of rebonding. The lower molecular weight of the self-healing elastomer relative to the fractions of asphalt cement may also allow it to have increased molecular mobility which may also help to improve crack healing. It is expected that this combination of self-healing elastomer and asphalt cement would have improved healing characteristics when compared to asphalt cement alone.

1.4 Thesis Organization

The contents of this thesis are divided into six chapters:

- Chapter 1 introduces the research objectives and scope of the project.
- Chapter 2 provides a literature review looking at many topics, including: asphalt cement chemistry, fatigue characterization of asphalt cement and mixtures and the mechanism of healing in asphalt pavements.
- Chapter 3 discusses the preliminary testing of SBS and the self-healing asphalt cement in order to evaluate the effect on the healing characteristics of asphalt cement.
- Chapter 4 discusses the in-depth characterization of the materials examined in this thesis through multiple methods including standard PGAC testing, advanced rheological methods and multiple cyclic shear healing tests.
- Chapter 5 discusses the in-depth characterization of the materials examined in this thesis using an adhesion style pull off test to evaluate a healing in a different manner.
- Chapter 6 summarizes the work and provides recommendations for future research.

Chapter 2: LITERATURE REVIEW

2.1 Asphalt Cement Chemistry

Asphalt cement is both naturally occurring and a by product of the crude oil refinery process. Commonly referred to as “bottom of the barrel,” asphalt cement is the heaviest product left over in the fractional distillation process. This process separates out the different hydrocarbon components of crude oil by their boiling point. Asphalt cement consists of the largest hydrocarbon fraction after the lighter hydrocarbons are distilled under atmospheric conditions [6]. A second phase which makes use of a vacuum distillation tower is sometimes required to improve the consistency and make it suitable for use [7]. This residue can go to be modified by oxidative techniques at the refinery or different types of additives downstream at asphalt cement terminals before being sent to hot mix plants for production [8]. It is estimated that only 4% of the crude oil processed in Canada ends up being used for asphalt cement [9].

The rheological characteristics of asphalt cement are controlled by the chemical composition and the interaction between the molecules, which is in turn controlled by the crude source and refinery process [8, 9]. Crude sources themselves are highly variable and the temperatures during the distillation process can control the distribution of hydrocarbon chain molecular weight. Asphalt cement is largely carbon based but can also contain a small quantity of heteroatoms and metals (typically less than 9%) [10]. Understanding the role that the crude source plays in asphalt cement properties has been the priority of National Cooperative Highway Research Program 9-60 being investigated by the Western Research Institute (WRI). This is because refinery process has changed overtime due to the increase in demand for petroleum-based products. Refiners also have much greater access to different crude sources and is important to understand how these changes can impact the quality of asphalt cement. Changes to the Marine Fuel Sulfur Limit in 2020 are also expected to have an impact on the refinery process which may further impact asphalt cement quality [9].

Despite the changes, asphalt cement can still be broken down in the same major fractional groups saturates, aromatics, resins and asphaltenes (referred to as SARA). These fractions can be determined through an automated piece of equipment called SAR-AD (SARA Determinator) which performs chromatography and fractionation by solubility. This piece of equipment developed by WRI is being used to study the relationship between chemical composition and physical properties such as high temperature modulus and low temperature creep stiffness [11]. An example of a SAR-AD spider plot from the NCHRP 9-60 project is shown in Figure 2-1. The plot shows the differing levels of resin and aromatic content from five different asphalt cement sources highlighting the high degree of variability amongst different sources.

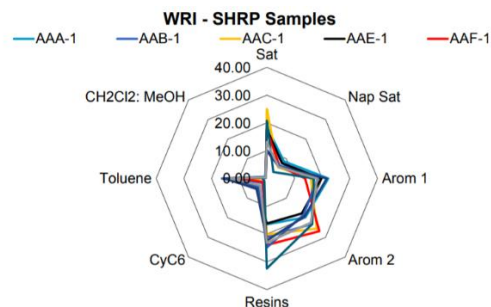


Figure 2- 1 Example of SAR-AD spider plot of five different asphalt cement sources [11]

The saturate fraction of asphalt cement is largely composed of non-polar aliphatic hydrocarbons (Figure 2-2a) with a relatively low molecular weight ranging between 300 to 2000. This fraction can contain waxy and non-waxy structures. The crystallinity of the waxy fraction can have a negative impact on the low temperature properties of asphalt cement [6, 8]. The aromatic fraction (Figure 2-2b) consists of non-polar chains with unsaturated ring structures and range in molecular weight from 300 to 2000. The saturate and aromatic fraction combine to produce what is known as the maltene phase in which the resins and asphaltenes are dispersed. The resins are a group of much larger molecules (molecular weight range of 500 to 50,000) which are highly polar and can contain some heteroatoms. Heteroatoms can increase the polarity which increases the molecular interactions. Thiophenes, indoles, pyrroles, carbazoles, furans, phenols and carboxylic acids are the most common structures resulting from the presence of sulfur, nitrogen and oxygen [6]. The resins coat the asphaltenes which is what allows them to be dispersed in the non-polar maltene phase. Asphaltenes (Figure 2-2c) themselves make up the largest molecules (molecular weight range of 1000 to 100,000) consisting mainly of polyaromatic rings causes them to also be highly polarized. The asphaltenes typically control the stiffness of the asphalt cement [12, 13].

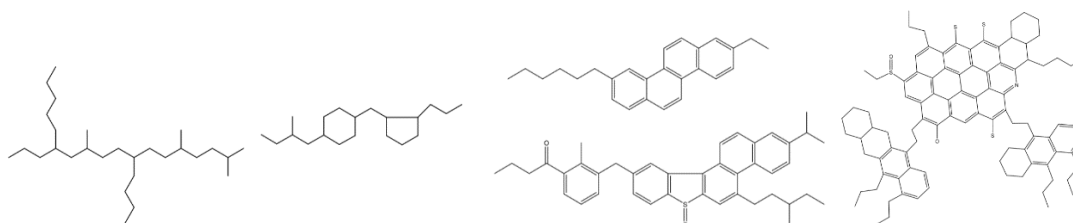


Figure 2- 2 Examples of possible structures of a) saturates, b) aromatics and c) asphaltenes [14, 15]

Changes in asphalt chemistry can occur during the construction phase and life of the pavement. The changes in chemistry will depend on the initial composition of the asphalt cement, but also the pavement's exposure to environmental conditions. Oxidative aging, exposure to ultra-violet light, moisture can lead to changes in the asphalt chemistry which ultimately can impact the long-term performance. Typically, changes in the chemistry result in a stiffening of the asphalt cement which creates a more brittle material. This can

negatively impact the fatigue resistance [6, 8, 16]. The process of mixing asphalt cement with aggregate at the hot mix plant causes a large increase in the stiffness through oxidation. The asphalt cement forms a thin film around the aggregate, and this greatly increases the surface area and exposure to oxygen [6]. Oxidative aging also occurs gradually over the life of the pavement. Temperature and exposure to oxygen both impact the reaction rate, but the rate is clearly much lower over the life of the pavement than in the high temperature process of hot mix preparation. Factors such as local climate can influence the oxidative aging as well as the level of compaction achieved during construction. Poorer compaction can increase the interconnectivity of the air voids increasing the exposure to oxygen [6]. The aging of the asphalt gradually changes the microstructure from a sol-type to a gel-type as the particle size increases. The asphaltene fraction gradually increases while the aromaticity decreases [17]. This change in structure results in the aforementioned change in mechanical properties [8]. Oxidative aging is the primary driver of chemical change and is the factor laboratory testing has been designed to characterize.

2.1.1 Viscoelasticity of Asphalt Cement

Asphalt cement is a viscoelastic material which means that the properties depend on the loading rate and the temperature. A purely elastic material exhibits an immediate return to its original properties when a load is removed while viscous liquid strain increases with an increase in the shear flow rate. A viscoelastic material exhibits both properties under different conditions [8]. Asphalt cement also exhibits thixotropy, which is the time dependent change in viscosity that does not result in permanent changes to the properties [18]. At high temperatures and long loading rates, the asphalt cement exhibits viscous like flow. At low temperatures and quicker loading rates asphalt cement behaves like an elastic solid [6]. These properties are related to the chemical structure and level of molecular mobility within the matrix. Short loading times and low temperature conditions do not give molecules sufficient time to move and hence their elastic behaviour. High temperatures and long loading times give rise to flow and molecular movement which allows asphalt cement to behave more like a viscous liquid [18]. The elastic behaviour explains the increase in stiffness and brittleness observed at low temperatures and high loading rates leading to fatigue and thermal cracking. The flow behaviour at high temperatures can be responsible for rutting in the pavement.

This concept can be easily illustrated by examining the phase angle under sinusoidal loading patterns. As a stress is applied to the sample, the material response will depend on the temperature and rate of loading. A purely elastic material would exhibit an immediate response and the phase angle would be 0° . For a purely viscous material, the phase angle will be 90° because of the lag in the response to loading. Unmodified asphalt cement will have phase angle values around 85° at high temperatures and near 45° at intermediate temperatures indicating a shift to more elastic material as the temperature drops [19].

The concept outlined here is often described as the time-temperature super position principle as the properties of asphalt cement are sensitive to temperature and the loading rate applied. Using the principle, it is possible to develop master curves which can be used to understand a wide range of properties [8]. The complex modulus and phase angle are measured at a wide range of temperatures and frequencies and then the data is shifted to a single curve. Different methods of developing shift factors have been developed in order to do this. A very common shift factor used is the Williams-Landel-Ferry (WLF) equation:

$$\log a_T = -\frac{C_1(T-T_R)}{C_2+(T-T_R)} \quad (1)$$

where $\log a_T$ is the logarithm of the shift factor, C_1 and C_2 are material specific constants and T_R is the reference temperature of interest. The WLF equation is simple to use but assumes that temperature susceptibility is known [20]. Other shift factor equations exist such as the Arrhenius equation and the Kaelble equation which is modified from the WLF equation [8, 19]. The complex modulus and phase angle data is collected using the Dynamic Shear Rheometer, but data from the Bending Beam Rheometer (BBR) can be included by converting the creep stiffness into an approximate complex modulus:

$$G^*(\omega) \approx \frac{S(t)}{3} \quad (2)$$

where G^* is the complex modulus as a function of reduced frequency and $S(t)$ is the creep stiffness. The BBR measures the creep stiffness at six different times and each time can be converted into a frequency to allow for the inclusion of the data. Master curves make excellent tools for evaluating and comparing different asphalt cements. The typical master curve is displayed in Figure 2-3. Also shown in the figure is the Rheological Index, R and crossover frequency. The Rheological Index gives an indication of the rheological type and can be an indicator of the shape of the curve. A flatter curve will have a Rheological Index higher value. The crossover frequency gives an indication of the hardness of the asphalt cement. The hardness increases as the crossover frequency decreases [21].

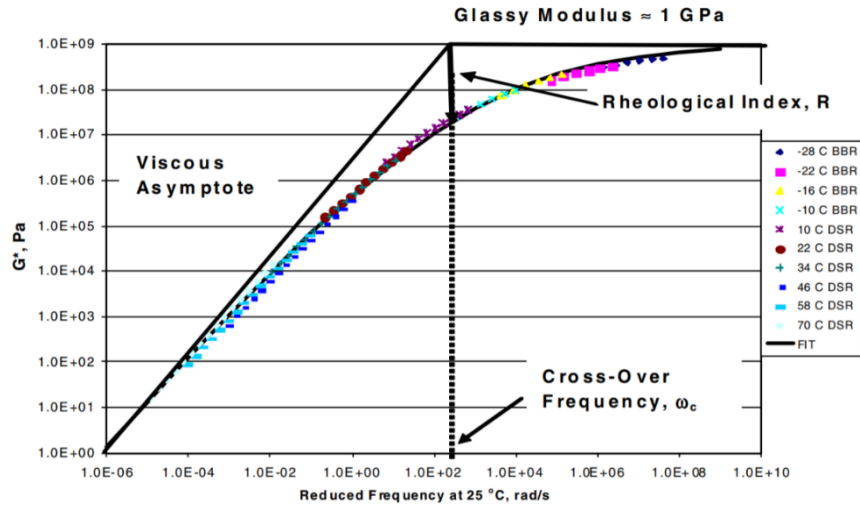


Figure 2- 3 Typical master curve construction portraying DSR and BBR data with a fitted rheological model [21]

2.1.2 Laboratory Aging Methods

Laboratory testing of asphalt cement in North America revolves around the Performance Graded Asphalt Cement (PGAC) system designated as specification M 320 by the American Association of State Highway and Transportation Officials (AASHTO). The system was developed by the Strategic Highway Research Program in order to improve the characterization of asphalt cement [8]. The PGAC system has been updated to the Multiple Stress Creep Recovery Graded Asphalt Cement (MGAC) system which relies on newer testing procedures designed to improve the characterization of polymer modified asphalt cement [22]. The system relies on testing the asphalt cement at different levels of laboratory aging designed to simulate different facets of the asphalt cement life cycle. The Rolling Thin Film Oven (RTFO) test was initially developed to simulate the aging that occurs at the hot mix plant during production. The Pressure Aging Vessel (PAV) is an accelerated aging test designed to simulate 5-7 years of in-service oxidation [6].

Many different styles of short-term aging have been developed, but the RTFO was ultimately accepted as the procedure of choice by AASHTO. The test is conducted by pouring 35 +/- 0.5g of asphalt cement in glass containers and placing them in an oven with rotating rack at 163°C for 85 minutes. A nozzle in the oven blows air directly into the bottles and the rotation of the rack ensures that the asphalt cement is oxidized evenly. The Multiple Stress Creep Recovery (MSCR) test is performed on RTFO aged asphalt cement. Under the old PGAC system, the RTFO aged asphalt cement was tested for the complex modulus and phase angle in order to determine the high temperature critical grade. It has been determined that the high temperature critical grade (which can also be obtained on unaged asphalt cement) correlated poorly with rutting performance, hence the adoption of the MSCR test [23]. Some research has suggested that the

RTFO procedure is insufficient to replicate plant aging. After recovering the asphalt cement from freshly produced mixtures, the stiffness and chemical changes in the RTFO were not comparable to the asphalt cement aged in mixture production [8, 17]. Attempts are being made to improve the quality of the RTFO test, but significant changes are not expected [24].

The shape of a master curve can give insight into the potential performance of asphalt cement. A curve that is flatter in shape is often described as having poorer relaxation properties and could have a higher propensity for cracking issues although this is not always the case. PAV aged material typically has a flatter curve than RTFO and unaged asphalt cement, which contributes to the brittleness. These changes can be observed in Figure 2-4, where the asphalt cement gradually stiffens as the degree of aging increases. The increase is larger at high temperatures than at low temperatures which contributes to the change in the shape of the curve. The black space diagrams in this figure also show a shift towards a more elastic material as the degree of aging increases. This shape change can also be seen when examining the blending between aged asphalt cement and virgin asphalt cement by extracting the asphalt cement from mixes containing reclaimed asphalt product (RAP) [20]. Master curves are a useful tool for examining the change in rheological properties of the aging process.

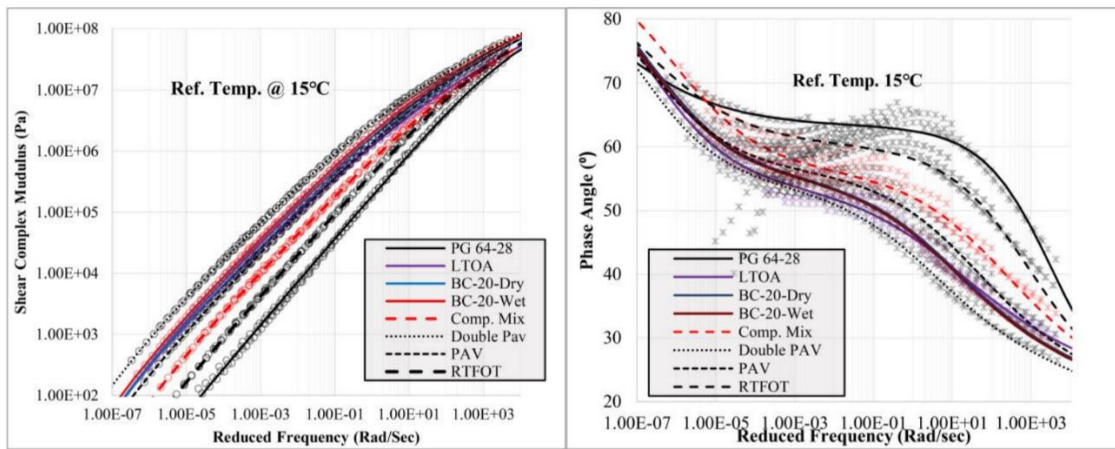


Figure 2- 4 Master curves (left) and black space diagrams (right) for various levels of asphalt cement aging [8]

2.1.3 SBS Modified Asphalt Cement

The use of styrene-butadiene-styrene (SBS) co-block polymer is a common way to improve the fatigue performance of asphalt cement and asphalt mixtures. It increases the stiffness of the asphalt cement and improves the elastomeric response of the material. These attributes improve rutting resistance in addition to the improvement in fatigue cracking resistance [2, 16, 25, 26]. Dispersion of SBS within asphalt cement produces a polymer network [27]. SBS compatibility with asphalt cement depends on the concentration of SBS, chemical composition of the asphalt cement and the microstructure of the SBS. Linear SBS has a lower molecular weight than radial SBS and the lower molecular weight of linear SBS increases the level of dispersion. The aromaticity and asphaltenes interact with the SBS chains resulting in swelling [24, 28]. The amount of swelling can change depending on the asphalt composition and microstructure of the SBS used [29]. This increases the volume fraction of SBS at relatively low concentrations. SBS dispersion is improved in asphalt cement with high aromatic and low asphaltene content [24]. The compatibility also improves as the difference in Hildebrand solubility parameter decreases. The saturate and aromatic fraction of asphalt have very similar Hildebrand values when compared to polystyrene and polybutadiene. SBS generally has good compatibility with asphalt cement because of this [26].

Crosslinking of SBS modified asphalt improves the thermal stability and improves the quality of the SBS network within the asphalt cement. This increases the stiffness of the modified asphalt cement as well as improves the elastomeric response. A crosslinking agent is an additive that can be capable of bonding multiple times with the SBS chains [30].

The change in elastomeric properties can be observed in the master curves and black space diagrams developed from temperature-frequency sweeps on the DSR. It can be clearly observed from the master curves (Figure 2-5a) that the modulus increases and low frequency, which corresponds to high temperatures and decreases slightly at high and intermediate frequencies which corresponds to low and intermediate temperatures, respectively, as the concentration of SBS increases. The increase in modulus at high temperatures accounts for the improved rutting resistance [31] and the decrease in modulus at low and intermediate temperature can be an indicator of improved cracking resistance [32]. The addition of SBS changes the shape of the master curve in a similar way to the increase in oxidative aging despite having a drastically different effect on performance. The black space diagrams (Figure 2-5b) display a plateau region that is characteristic of elastomeric materials [33, 34]. The plateau region can be indicative a good compatibility between asphalt cement and SBS [35]. The master curves and black space diagrams here can be considered typical of SBS modified asphalt cement.

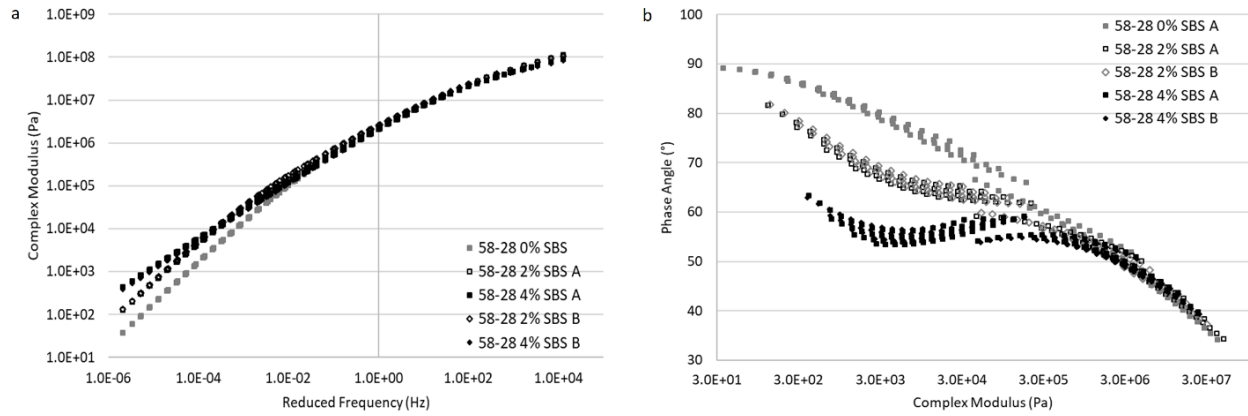


Figure 2- 5 Typical master curves (left) and black space diagram (right) for SBS modified asphalt cement [2]

The positive impact on fatigue has also been clearly demonstrated [16, 22, 36]. Figure 2-6 shows the results of Four Point Bending Beam (4PB) results as the concentration of SBS increases using two different base asphalts and a linear SBS. The number of cycles to failure (N_f) increase as the concentration of SBS increases. This is likely due to the increase in modulus and the increase in elastomeric properties which improve the response to loading.

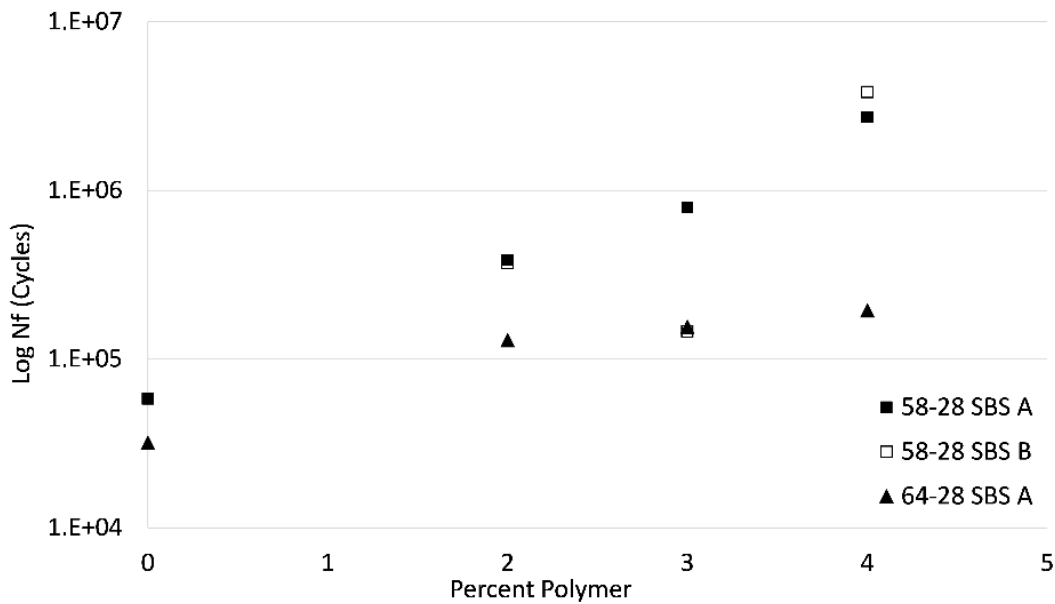


Figure 2- 6 Four Point Bending Beam (4PB) number of cycles to failure versus the concentration of SBS [36]

2.2 Characterizing Asphalt Cement and Mixture Fatigue

Characterizing the cracking resistance of asphalt pavements can be a difficult process. The testing used must accurately find a way to simulate the stresses experienced by the pavement in situ where it is due to low temperature or traffic. There are four types of cracking that can affect pavements. They are thermal, reflection, fatigue and top-down cracking [37]. Fatigue cracking seems to be the primary target of crack healing in pavements. This is due to the relationship between cracking and healing. The healing process has been described as the reverse of the fatigue process [13, 38, 39].

Fatigue cracking is a result of repetitive tensile loading at the bottom of the pavement layer directly above the sublayers as a result of the passage of traffic and typically occurs at intermediate pavement temperatures [40]. The level of strain and the number of load repetitions play a role in determining how much damage will occur [36]. As discussed previously, asphalt mixtures are viscoelastic materials which experience brittle behaviour under high loading and low temperatures. This underscores the necessity of designing a pavement which is either strain tolerant or can minimize the strain and therefore the stresses at the bottom of the pavement [41]. The use of asphalt mixture testing has been commonplace in France for many years and was originally intended to be the third phase of the original Superpave system although it has only begun to be implemented in the United States very recently [36].

Depending on the mixture design, there are multiple ways to improve the fatigue resistance of asphalt pavements. “Enrobé à Module Élevé” which can be loosely translated into high modulus asphalt is a pavement design technique developed in France. The pavement uses very low penetration grade asphalt which would be the equivalent of roughly a PG 82-28 in order to produce a very stiff asphalt mixture. This has been shown to have a very high resistance to fatigue damage by reducing the amount of strain experienced by the pavement [42]. With Superpave designs, the inclusion of performance testing has resulted in a shift towards increasing the asphalt cement content. Researchers in New Jersey found that increasing the asphalt cement content by roughly 0.6% would improve the performance of the mixtures containing RAP to similar levels as the virgin asphalt mixtures [43]. Researchers in Louisiana also found that a similar increase in asphalt cement content was necessary to improve fatigue performance. The increase in asphalt cement content improves the viscous response to loading and compensates for the stiffer mixture [44]. The use of polymer and other modifiers is also a good way to improve the performance of asphalt mixtures. Increasing the concentration of SBS often provides improved performance and this has led to research with Highly Modified Asphalt (HiMA) which uses between 6-8% SBS. The HiMA pavement trials in China, Poland and the United States [45, 46, 47], have shown that this technique offers a great improvement over more practical concentration of SBS.

In addition to adjusting the mixture, the pavement structure can also play a role in improving the fatigue resistance. Thicker pavements will have reduced strains and stresses at the bottom of the pavement which will in turn reduce the amount of cracking. This has led to the development of “perpetual pavements” where the structure incorporates an extra layer by comparison to traditional pavement design [48]. The proper bonding of the asphalt layers and good compaction are also important for minimizing the potential for fatigue cracking necessitating the application of tack coats before paving [49]. Cracking issues can extend far beyond the asphalt cement with mixture design, polymers, and construction quality all playing a role in contributing to performance.

2.2.1 Asphalt Mixture Testing

The characterization of fatigue performance in asphalt mixtures has evolved to become a more important aspect of the pavement design process in the United States in recent years. NCHRP 9-57 evaluated nine different cracking tests which were fit into the four many categories described earlier. The goal of the project was to evaluate the test methods in order to improve the cracking characterization of Superpave mixes. The design of the test and the failure criteria selected can influence the evaluation of the asphalt mixtures [71]. The different style of tests can also be analyzed using the different failure criteria. For example, Four Point Bending Beam data can be analyzed using the traditional failure criteria of that relies on a 50% reduction in modulus or the “Département Génie Civil et Bâtiment” (DGCB) method based on the fatigue damage accumulated per cycle [36].

Cyclic fatigue testing is described has having three distinct phases:

1. Phase I: Adaption Phase
2. Phase II: Quasi-Stationary Phase
3. Phase III: Failure Phase

The three phases can be described by the evolution of the modulus. Phase I is characterized by a sudden drop in the modulus which is not primarily the result of fatigue damage. The modulus also decreases due to the increase in temperature in some tests and the thixotropy of the asphalt mixture. The effect of thixotropy is supported by the quick recovery of properties when the loading is removed [50]. Phase II is the phase where the majority of fatigue damage occurs. This is due to the presence of microcracks which begin to grow. The decrease in modulus is roughly linear depending on the material and test specifics. Phase III is when macro-cracks begin to form, and the material fails [50, 51, 52]. A diagram of the change in modulus versus the number of cycles which illustrates the three phases is displayed in Figure 2-7. These phases can be described together in the failure criteria or analyzed separately.

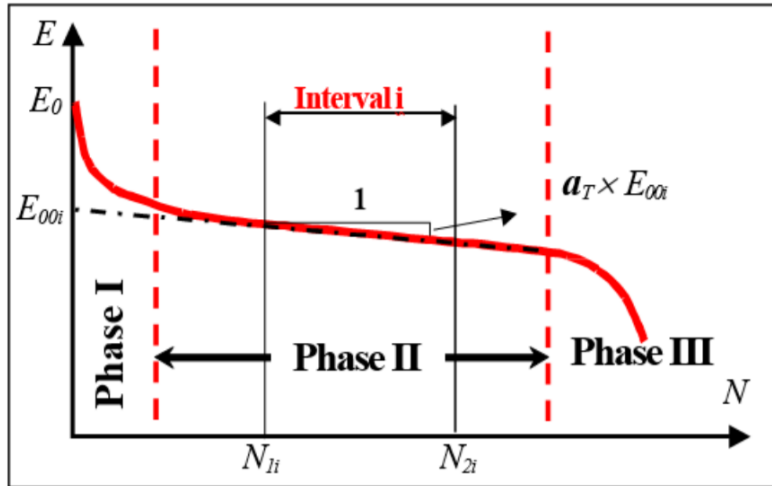


Figure 2- 7 The three phases of a cyclically loaded fatigue test [16]

2.2.2 Fatigue Life Predictions with Wohler Curves

Wohler curves rely on the change in modulus in order to predict the fatigue life of materials. Originally developed for metals, Wohler was the first to relate the magnitude of an applied stress to the number of cycles to failure. It was observed that as the magnitude of cyclic loading increases, the fatigue life in terms of cycles to failure decreases. This is a commonly used technique for asphalt mixtures when testing is performed in strain-controlled modes [53]. Wohler curves are produced by plotting the number of cycles to failure of a material versus the strain amplitude used to induce the failure on a bi-logarithmic scale. The number of cycles to failure is based on the reduction in modulus [54]. The plot is used to find ϵ_6 which is defined as the strain amplitude required to induce failure after 1,000,000 cycles. Tension-Compression style testing has proven to be a more consistent methodology than bending beam style tests due to the homogenous nature of the stresses within the specimen. The results from different types of tests must be verified with field performance separately due to the poor relationship between them. The points of 50% reduction in modulus and 1,000,000 cycles have been chosen arbitrarily and are susceptible to misinterpretation. This analysis can be performed with any fatigue test that applies a cyclic loading or can be presented in terms of number of cycles to failure [50].

Qabur [36] used Wohler curves with Four Point Bending Beam testing in order to verify the improvement in performance provided by SBS. Strain values of 300, 400, 500, 600, 700 and 1000 $\mu\text{m}/\text{m}$ were selected, and failure was determined using a 50% reduction in the modulus. The number of cycles to failure for each concentration of SBS tested can be seen in Figure 2-8. The slope of each curve tends to decrease as the concentration of SBS increases and it was found that the value of ϵ_6 also increased as the concentration increases. This was observed for both the PG 58-28 and the PG 64-28 tested with a linear SBS. Wohler

curves based on the reduction in modulus are a well studied tool and still can be an applicable form of analysis depending on the application.

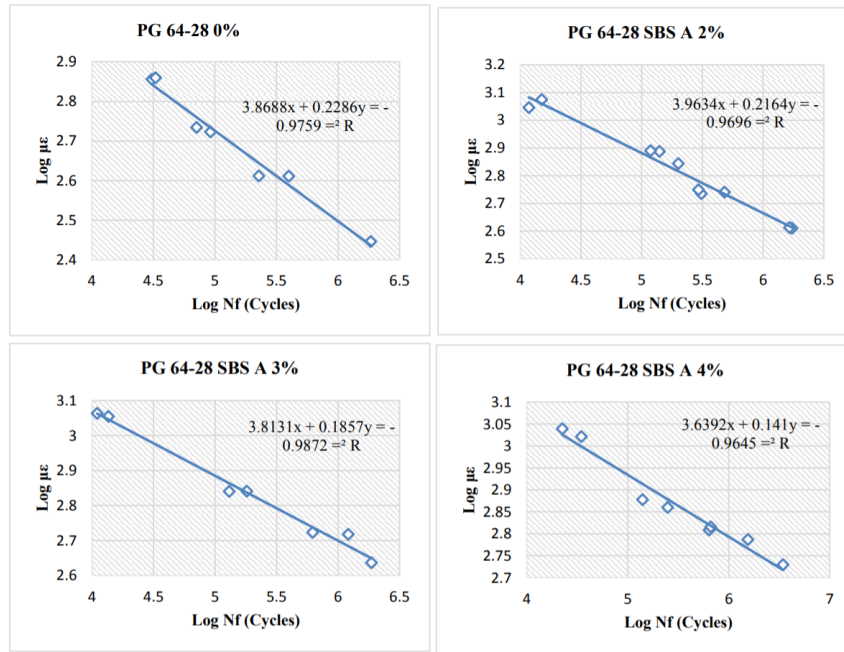


Figure 2- 8 Wohler curves for a PG 64-28 with increasing concentrations of SBS [36]

2.2.3 Damage Rate Analysis with the DGCB Method

The Département Génie Civil et Bâtiment (DGCB) method was developed to analyze the damage rate per loading cycle. The DGCB method assumes that that Phase II is linear or roughly linear and was designed to avoid the bias effects that are seen in Phase I (heating and thixotropy) by applying a correction factor. Doing this is expected to allow for a more precise analysis of the fatigue damage accumulated in the sample. Research led by Di Benedetto et al. [50] was performed on 11 different styles of fatigue test; ranging from beam style (2-, 3- and 4-point bending), tension-compression and indirect tensile test. The damage rate was calculated using the following equation:

$$D_{exp} = 1 - \frac{E_0 - E_N}{E_0} \quad (2)$$

where D_{exp} is defined as the experimental damage parameter, E_0 is the initial modulus and E_N is the current cycle stiffness. The experimental damage factor is then corrected for the bias effects. A linear regression is used in order to determine the initial modulus of different intervals in Phase II. The experimental damage slope is given by the sum of the “true” fatigue slope and the variation in stiffness effected by heating and

thixotropy. The evolution of the bias effects is proportional to the change in dissipated energy and therefore the fatigue slope, a_F , can be written as:

$$a_F = a_T + a_w \frac{C_i(E_0 - E_{00i})}{E_{00i}} \quad (3)$$

where the experimental damage/ slope, a_T , is given by the equation $a_T = D_{exp} \frac{E_0}{E_{00i}}$ and a_w is the slope of the dissipated energy per cycle of the same interval which is normalized by the initial dissipated energy. C_i is a coefficient related to the non-linear damage evolution which occurs during Phase I. The correction factor can be positive or negative. Analysis of the different fatigue testing modes has shown that stress controlled, and strain-controlled tests show different experimental slopes but similar fatigue slopes (a_F). The DGCB method makes it possible to compare different testing approaches by developing a model calibration using a homogenous test like the tension-compression set up. This allows the approximation of beam stiffness by expression the damage law a function of strain amplitude [50].

Qabur [36] also used the DGCB method to analyze the effect of polymer concentration on fatigue performance discussed earlier that was conducted on the 4PB set up. Analysis of the PG 58-28 tested in the study can be seen in Figure 2-9. There is a clear ranking which shows that the increasing polymer concentration reduces the damage rate of the asphalt mixture. The testing showed that the PG 64-28 mixtures had a lower damage rate than the PG 58-28 despite having a lower fatigue life when analyzed using the traditional fatigue failure criteria. Some issues arose which were partially attributed to the non-homogeneity of the test resulting in an imperfect correlation with damage rate and the concentration of polymer. This was seen in the PG 64-28 at 3% SBS, but not with the PG 58-28.

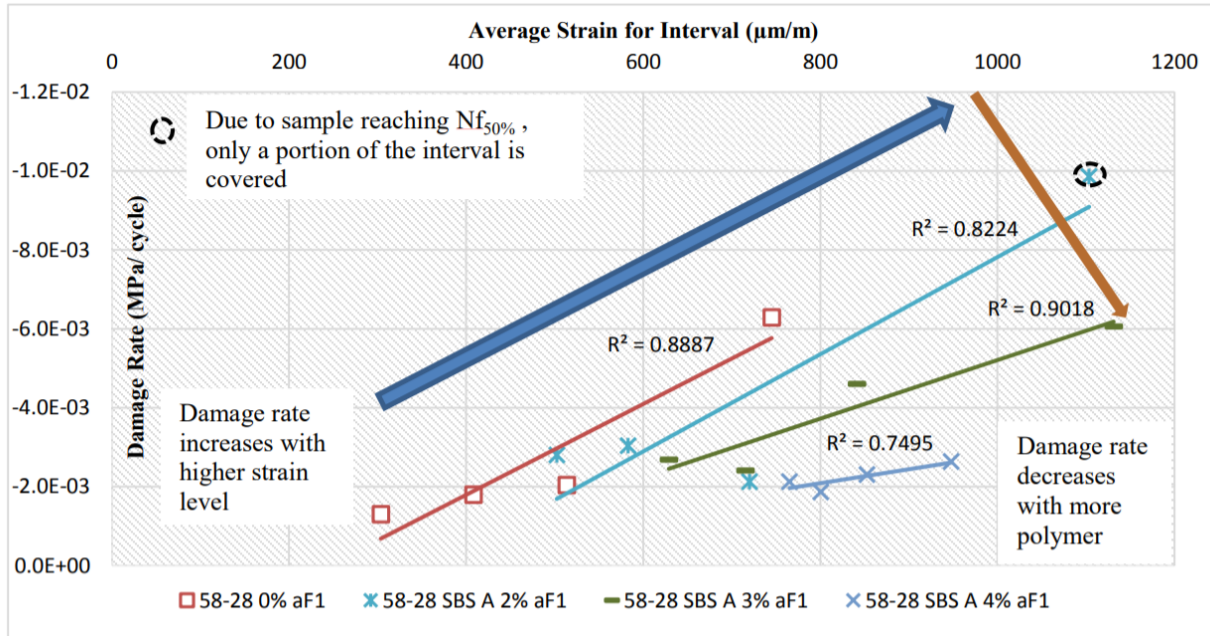


Figure 2- 9 Damage rate analysis and annotations for PG 58-28 in the first measured interval [36]

Baaj et al. [16] used the DGCB method to examine the effect of asphalt cement properties on the asphalt mixture. The researchers examined the properties of mixtures using asphalt cements with different penetration values, different levels of crystallization and different modifiers. The testing was conducted using tension-compression on cylindrical specimens at a frequency of 10 Hz and a temperature of 10°C. Transducers were placed triaxially around the specimen in order to measure the strain in order to evaluate the homogeneity of the loading. They found that damage rates change depending on the interval that is being examined owing to the non-linearity of damage. When looking at asphalt cement penetration, it was determined that the ϵ_6 could not differentiate the fatigue performance but the DGCB method could finding that a stiffer asphalt cement had a lower damage rate. It was also determined that the higher crystallinity improved fatigue performance in the DGCB method and the classical approach. The elastomer modified asphalt cements using SBS were found to have very small damage rates and the addition of a plastomer also improved the damage rate. It should be noted that the asphalt mixtures used in this study all had an asphalt cement content of 6.8% or higher. Baaj and Carter [55] also used a similar set up to evaluate a stone mastic asphalt (SMA) mixture in comparison to standard French mixture designs. They found that the SMA performed better in fatigue than the standard mixes and this was used to conclude that standard pavement design methods do not properly account for superior performance of specialty mixtures like SMA due to the dependence on stiffness.

2.2.4 Fracture Mechanics Approaches for Fatigue Characterization

The use of fracture mechanics is another approach that has been used to evaluate the brittle response to loading observed by asphalt mixtures at low temperatures. The critical stress intensity factor, which is based on the linear-elastic fracture mechanics (LEFM), has been applied to asphalt mixtures. Attempts have also been made to characterize asphalt mixtures using the elastic-plastic fracture mechanics (EPFM) [56]. LEFM assumes that the crack propagation is continuous, but crack growth in asphalt mixtures and pavements is considered discontinuous. The fracture mechanics approach can be applied when the crack is considered continuous [57]. Some researchers have found that the EPFM method is more sensitive to the changes in fracture properties when compared to the LEFM method. The critical stress intensity factor loses significance as the material behaviour becomes non-linear as temperature increases. The J-integral of EPFM better applies to linear and non-linear behaviour [56].

Portillo and Cebon [56] used fracture mechanics to evaluate “idealised” asphalt mixtures with a 3-point single-edge notch beam set up. The beam is used has a notch cut into the side where force will be applied. The force, deflection, crack mouth opening displacement (CMOD) and crack length are all measured with time. High speed cameras were used to monitor the crack growth due to the instantaneous nature of failure observed in this test. Clip gauges were used to monitor the CMOD. Cracking performance was then determined in terms of stress intensity factor, fracture energy and the J-contour integral. The researchers found that the stress intensity factor was independent of temperature and strain rate. It was considered the best descriptor of brittle failure. Fracture energy and the J-contour integral were found to be better suited to characterizing behaviour in the ductile regime although fracture energy was more consistent.

Several recently developed tests take advantage of the fracture mechanics approach in order to estimate the cracking resistance and fatigue performance of asphalt mixtures quickly. One such test is the IDEAL-CT developed by Zhou et al. [58] at the Texas A&M Transportation Institute. The test was developed in response to the literature review completed by NCHRP Report 9-57 which stated the need for a simple cracking test to meet the following criteria [58]:

1. Simplistic
2. Practical
3. Efficient
4. Inexpensive Equipment
5. Good repeatability

6. Sensitivity to different mix parameters
7. Correlation with field performance

The developers of the IDEAL-CT concluded that the test meets all the above criteria. The cracking parameter is based on Paris' Law which is used to describe continuous crack growth [57, 58]. The crack growth rate is defined as:

$$\dot{c} = v_c \left(\frac{G}{G_f} \right)^{n/2} \quad (4)$$

where v_c is the a constant, n is a material constant, G is the energy release rate (defined as $G = K_I^2/E$) and G_f is defined as the fracture energy. K_I is the stress intensity factor and E is the modulus, so substituting for G gives the following equation:

$$\dot{c} = v_c \left(\frac{K_I^2}{E \times G_f} \right)^{n/2} \quad (5)$$

where v_c is the a constant, n is a material constant, G_f is defined as the fracture energy, K_I is the stress intensity factor and E is the modulus. The modulus can be estimated using the applied load and vertical deformation and the stress intensity factor can be determined by the tensile stress and a shape function. After substituting and simplifying, the cracking index can be written as:

$$CT_{Index} = \frac{G_f}{P} \times \left(\frac{l}{D} \right) \quad (6)$$

where G_f is the fracture energy, P is the applied load, l is the measured vertical deformation and D is the diameter of the specimen. This equation can be corrected for the thickness of the specimen being tested if it is not produced in the laboratory. The fracture energy is equal to the area under the load versus displacement curve divided by the area of the cracking face. The modulus is represented by P/l which is the slope of the load-displacement curve and l/D represents a strain tolerance parameter. The cracking index depends on the point where it is measured. As such, the researchers have suggested that the point past the peak equal to 75% of the maximum load is used. This is illustrated in Figure 2-10. The absolute value of the slope at this point is used and calculated using the points 85% and 65% past the peak load. The researchers state that this interval is two times the standard deviation and this assures over 95% probability and this slope is less variable than the tangential slope [58].

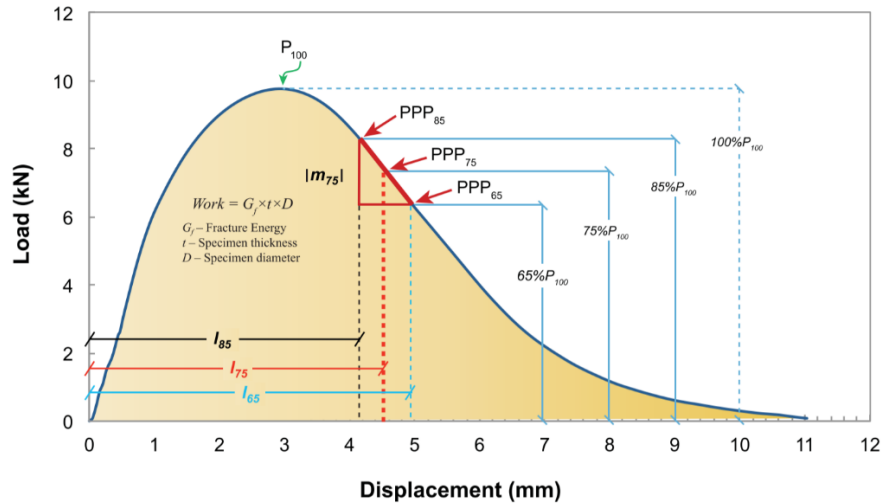


Figure 2- 10 Illustration of post peak point and calculation of the slope [58]

The test is performed at intermediate temperatures by applying a load to a cylindrical sample in a similar way to traditional indirect tensile strength tests with a loading rate of 50 mm/min. The researchers determined that the test showed good sensitivity to RAP and RAS, asphalt cement type, different ageing conditions and air voids. Repeatability was considered good (typically below 25% COV) and a strong correlation to field performance was found [58]. Literature on this test method is limited, but a project using the test to evaluate the performance of polymer modified asphalts is underway at the University of Waterloo at the time of writing.

The Disk-Shaped Compact Tension (DCT) test is another cracking test that characterizes the cracking resistance in terms of the fracture energy which is calculated by the area under the load-CMOD curve normalized to ligament length. The test is performed using a similar specimen to the IDEAL-CT; however, two holes and a notch are cut into the sample. The transducer is placed over the notch and the sample is pulled apart to increase the CMOD. The test is performed at low temperatures but is worth mentioning due to their use of fracture mechanics to evaluate cracking resistance [58, 59].

The Semi-Circular Bend (SCB) test can also be evaluated using fracture mechanics at low temperatures but it has also been used at intermediate temperatures where critical strain energy release rate is measured. This value is the absolute value of the ratio between the slope of the fracture energy and the notch depth. The test is conducted on core specimens which have been cut in half and had a notch cut into the side [37]. Kim et al. [60] tested three replicates of each specimen for three different notch depths in order to compare the approach to the IDT strength test. Loading was applied with a crosshead deformation rate of 0.5 mm/min at 25°C. The critical J-integral was calculated using:

$$J_c = - \left(\frac{1}{b} \right) \frac{dU}{da} \quad (7)$$

Where b is the sample thickness, a is the notch depth and U is the strain energy to failure. The average strain energy to failure is plotted against the notch depth to compute the slope which is equivalent to $\frac{dU}{da}$. This value divided by the thickness of the samples gives the critical strain energy release rate. The researchers found that the critical strain energy release rate correlated well with the IDT toughness index. They also found that the asphalt cement grade and aging conditions did impact the fracture resistance, while the critical strain energy release rate had some correlation with field performance. The SCB test has been adapted to specifications in Illinois and Louisiana using similar set ups but different styles of data analysis [37]. The approach has also been applied to asphalt cement tests and this will be discussed later.

2.2.5 Viscoelastic Continuum Damage Model for Fatigue Characterization

The Viscoelastic Continuum Damage Model (VECD) has been applied to both asphalt cement and asphalt mixtures in order to characterize the fatigue performance. The model allows for the prediction of fatigue performance at different load amplitudes while using a single test [18]. Creating a continuum damage model usually requires the selection of damage variables, the definition of strain energy density and a damage evolution law. The model is based on a damage model originally developed by Schapery and the elastic-viscoelastic correspondence principle. When damage occurs due to external loading, some of the energy is stored as strain energy but some of it causes damage. The amount of damage produced can be expressed in terms of the internal state variables of the material. The Schapery model allows for non-linearity and coupling between the internal state variables. It also accounts for the microcrack and macrocrack growth in many different types of materials [61]. The damage growth of elastic materials using thermodynamics is defined as:

$$- \frac{dW}{dD} = \frac{\partial W_s}{\partial D} \quad (8)$$

Where W is a function for the strain energy density based on the strain and D , the internal state variables. W_s is a function of the internal state variables which describes the dissipated energy [18]. The correspondence principle allows a substitution between elastic and viscoelastic parameters through a substitution and integration process. Therefore, the stress of the system can be written as:

$$\sigma = E_R \varepsilon^R \quad (9)$$

Where E_R is the reference modulus with the same dimensions as the relaxation modulus and ε^R is the pseudo strain. The equation takes the same form as the elastic stress-strain equation, but it has become the

viscoelastic stress-strain equation [61]. The use of pseudo strain eliminates hysteresis [18]. The following evolution law was proposed for viscoelastic materials:

$$\frac{dW}{dD} = - \left(\frac{\partial W_S}{\partial D} \right)^\alpha \quad (10)$$

Equation 10, the pseudo strain energy density function, can be simplified to:

$$W^R = \frac{1}{2} C(S) (\varepsilon^R)^2 \quad (11)$$

where C is a function of the damage parameter S and ε^R is the pseudo stiffness. C is a normalized material integrity parameter related to the stress-pseudo strain curve determined experimentally. This finds the modulus dependent on the pseudo strain, but not S. The value of S is found by using an approximation procedure to equate the rate evolution law into an integrated form. Damage is derived as a function of time and this is combined with Equation 10 to give the following equation to derive the damage:

$$D(t) \cong \sum_{i=1} \left[\frac{1}{2} \varepsilon^{R^2} (C_{i-1} - C_i) \right]^{\frac{\alpha}{1+\alpha}} (t_i - t_{i-1})^{\frac{1}{1+\alpha}} \quad (12)$$

Where α is defined as either $1+1/m$ for displacement-controlled tests or $1/m$ for load-controlled tests. The parameter m comes from the slope of the logarithmic relaxation modulus versus time curve [18]. Park et al. [61] showed that the model worked well with monotonic, uniaxial loading at a single temperature. This model and methodology eventually become the basis for the Asphalt Mixture Performance Tester. This test uses tension-compression style cylindrical specimens. It is recommended that three tests are performed at different strain levels beginning with an initial value. The strain level is then increased to decreased depending on the number of cycles to failure achieved. The test was found to have good correlations with field performance but is also deemed to be complicated with regards to equipment and sample preparation [37]. Bessa et al. [62] applied this methodology in order to relate asphalt cement and asphalt mixture fatigue. The specimens were tested at three different test temperatures and modelled at seven different strain levels. They found that the VECD resulted in lower predicted fatigue lives for asphalt mixtures, but they were also able to determine fundamental properties of the mixture.

2.2.6 Asphalt Cement Testing

A time sweep test was proposed in NCHRP Report 9-10 [63] to replace the $G^* \times \sin \delta$ parameter developed for the Superpave PG system. This was because the $G^* \times \sin \delta$ parameter was not sufficient for predicting the fatigue performance of asphalt mixtures. The correlation was poor between $G^* \times \sin \delta$ and laboratory fatigue testing. The time sweep test applies a cyclic load with a constant frequency, where the strain

amplitude can be varied depending. This allows for the consideration of pavement structure and traffic loading [18]. This test has been used effectively to evaluate the fatigue resistance of asphalt cement [63, 64] and can be applied to understanding the healing mechanism of asphalt [64]. The time sweep test is lengthy [65] and therefore the Linear Amplitude Sweep test has been proposed as a surrogate.

Apostolidis et al. [66] conducted time sweep tests using an alternative geometry in order to assess the fatigue performance of a single asphalt cement. The new plates produce a ring shape sample using a concentric hollow space in the centre. Testing was carried out at 10 Hz and a temperature of 35°C. Their testing revealed that edge damage occurred earlier in the new hollow plates when compared to the traditional geometry. This also had the effect of localizing the shear stress in the periphery of the asphalt cement [67]. Shenoy [68] used time and strain sweep tests to evaluate the fatigue characteristics of several asphalt cements. The time sweep testing took place at a frequency of 10 radians/s and a strain level of 25%. The test temperature was found by using the strain sweep in order to find a complex modulus of 1 MPa. The actual testing had values between 0.9 and 1.1 MPa and the results were normalized to 1 MPa. Each asphalt cement was found to have its own response to the loading and the inflection point was taken as the failure point rather than the change in modulus. It was found that the cycles to failure were related to the loss modulus determined using the strain sweep.

2.2.7 Applying VECD to Asphalt Cement

The Linear Amplitude Sweep (LAS) test has been proposed to help characterize the fatigue resistance of asphalt cement and is meant to replace the time sweep test as an accelerated method [69]. The test consists of two parts, a frequency sweep and an amplitude sweep. The frequency sweep is used to determine the properties of the undamaged binder. The amplitude sweep applies increasing strain rates in steps up to 30%. The test was initially developed using the VECD model and calculates the estimated number of cycles to failure using the reduction in the complex modulus [18]. The model used here is derived in the same way as it is derived for use with asphalt mixture testing. The VECD model allows for the interpretation of a single set of test results for a wide variety of conditions. The number of cycles to failure is calculated using the following equation:

$$N_f = A(\gamma_{max})^B \quad (13)$$

where A is given by Equation 14 and B = -2 α .

$$A = \frac{f(Df)^k}{k(\pi \frac{I_D}{|G^*|} C_1 C_2)^\alpha} |G^*|^{-\alpha} \quad (14)$$

where I_D is the complex modulus before damage, f is the loading frequency, D is the damage and C_1 and C_2 comes from the curve fitted to the change in $G^* \times \sin \delta$. The calculation of α is completed using the frequency sweep portion of the test by plotting the log-log plot of the relaxation modulus versus time and using an approximate interconversion method. The original methodology relied on the storage modulus, but the research done by Hintz et al. comparing the two showed that there was very little difference. Failure criteria for the VECD method is defined as a 35% reduction in the complex modulus multiplied by \sin of the phase angle [69]. This value was selected because it showed the best correlation with the time sweep testing. Hintz also suggested that the test be considered a damage tolerance test, however work to compare the LAS to fatigue testing has been conducted by many researchers [18]. Bessa et al. [62] found that the LAS correlates well with the traditional time-sweep approach, but the LAS typically had values that were 4.5 times lower. Chen et al. [70] found that 100 cycles to failure after applying a 15% strain corresponds well to the Illinois Flexibility Index test specification limit of 8. Soenen et al. [71] use the time sweep test to evaluate unmodified asphalt cement with a frequency of 25 Hz in a strain-controlled mode and compared the results to the LAS. They found that the data for both tests showed similar trends but proposed using the phase angle as an indicator. It should be noted that this testing was done solely on unmodified asphalt cement.

The test is intended to be performed at intermediate temperatures if it is used to evaluate fatigue cracking. However, some research has been performed by Castorena (née Hintz) and Underwood to evaluate the effect of test temperature on the failure. If the temperature selected is too cold, the asphalt cement may not stick to the DSR plates, but if the temperature is too high flow can occur as seen in Figure 2-11. The modulus should be between 10 and 60 MPa for cohesive cracking to take place. They also found that it showed a reasonable correlation with field performance. However, the current LAS data analysis ignores the effects of nonlinear viscoelasticity [72].

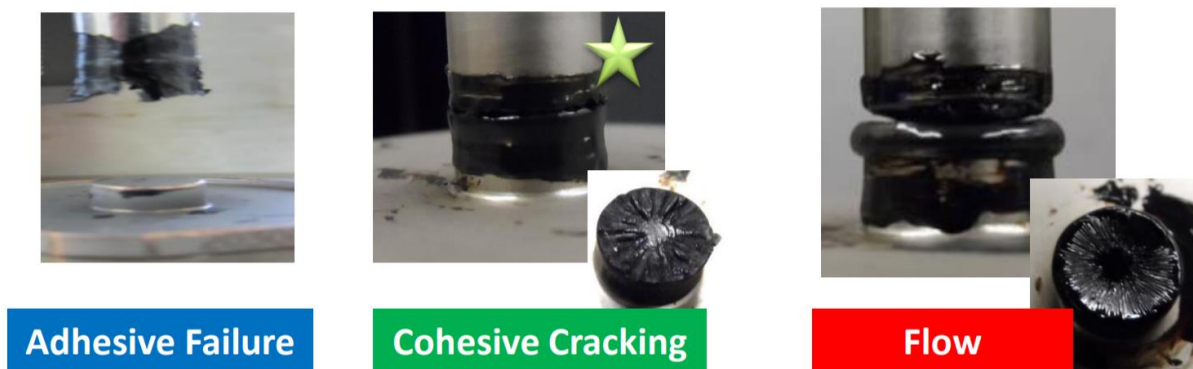


Figure 2- 11 Examples of the effect of temperature on the type of failure observed in LAS testing [72]

2.2.8 Applying Fracture Mechanics to Asphalt Cement

Zhou et al. [65] proposed deviating from the VECD model in favor of a fracture mechanics approach after discovering a weak correlation between aging and the number of cycles to failure. The new method, called the Pure LAS (PLAS) does not make use of the frequency sweep portion of the LAS and characterizes binder performance in terms of the fatigue resistance energy index (FREI) rather than the number of cycles to failure. This change has been made because the VECD model assumes the crack size is smaller than the continuum and this assumption may not be valid for heavily aged binders. FREI is defined as:

$$FREI = \frac{J_{f-\tau_{max}}}{G_{0.5\tau_{max}}} \cdot (\gamma_{0.5\tau_{max}})^2 \quad (15)$$

Where $J_{f-\tau_{max}}$ is the shear fracture energy calculated until maximum shear stress, $G_{0.5\tau_{max}}$ is the calculated shear modulus at point of half of the maximum shear stress and $\gamma_{0.5\tau_{max}}$ is the shear strain at the point of half of the maximum of the shear stress. Larger values of FREI indicated an increased fatigue cracking resistance. Large values of shear fracture energy typically indicate better cracking resistance. Larger values of shear strain are indicative of better relaxation properties and a large shear modulus would indicate the binder is more prone to cracking [65].

The results produced by Zhou et al. [65] show that there is some tendency to predict Pressure Aging Vessel (PAV) aged material as expecting to perform better than Rolling Thin Film Oven (RTFO) aged or unaged binders in terms of their number of cycles to failure. Figure 2-12 shows the result of testing a PG 64-22 at five different levels of aging. The asphalt cement performance tends to improve when aging is increased when the number of cycles to failure is calculated using an applied strain of 2.5%. The relationship is less clear when calculated using 5% strain. This result runs in opposition to the expected trend that aging would reduce fatigue life. The use of FREI improves the correlation between aging and expected fatigue performance. This can be seen in Figure 2-13. The relationship shows a much clearer trend towards decreasing as the level of aging increases. The test has also shown good correlation with two different mixture cracking tests.

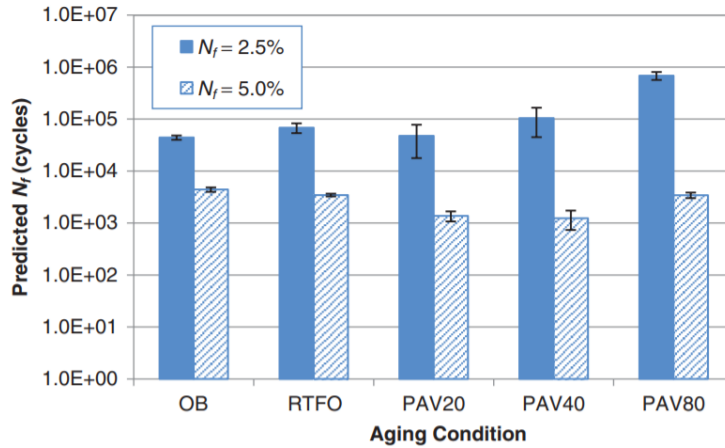


Figure 2- 12 Number of cycles to failure for a PG 64-22 [65]

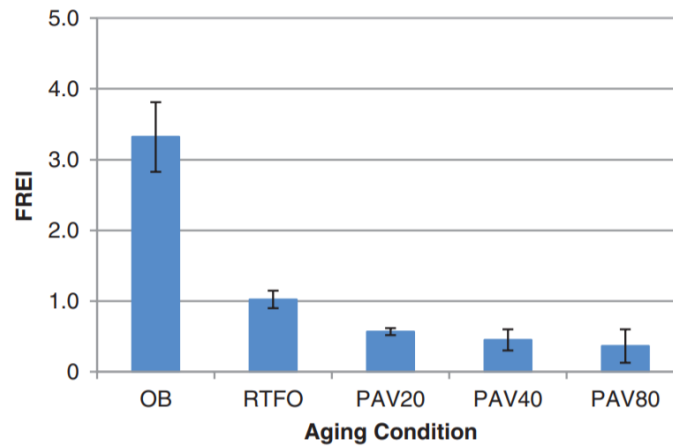


Figure 2- 13 Fatigue Resistance Energy Index for a PG 64-22 [65]

2.3 Introduction to Self-Healing Asphalt Pavements

The study of self-healing mechanisms of asphalt and the development of self-healing technologies for pavements is a very interesting field of research. The first observations of the inherent healing ability of bituminous pavements was in 1960s by Bazin and Saunier [4] and Deacon who observed rest periods improved fatigue life [39]. The proper development and characterization of self-healing asphalt cements could lead to the decrease in cost and emissions over the lifespan of the pavement [5]. Healing with respect to bituminous materials has been defined in literature previously as the recovery of material properties by reparation of the chemical structure [4] and as the ability of the material to return to an acceptable operating state through adjustments or resisting the formation of defects [73]. As a growing area of interest, it becomes important to work with a standardized set of definitions in order to ensure that the phenomenon is discussed consistently. RILEM (Réunion Internationale des Laboratoires et Experts des Matériaux) Technical

Committee on Crack-Healing of Asphalt Pavement Materials (TC 278-CHA) has proposed the following definitions with relation to self-healing asphalt materials [74]:

Damage: loss of original mechanical properties, such as the strength or the stiffness, due to the initiation, coalescence and propagation of micro-cracks within the material.

Restoration: The total amount of the change of mechanical properties that have been impaired due to the mechanical loading.

Recovery: Component of the restoration that can be attributed to changes in response resulting from cyclic loading, more specifically heating and thixotropy.

Self-healing: Component of the restoration that can be attributed to the closure and repair of (micro) cracks.

Extrinsic (Self-)healing: Aspect of the self-healing behaviour that can be attributed to an added phase or action that is specifically added to the material to improve self-healing capabilities.

Intrinsic (Self-)healing: Aspect of the self-healing behaviour that is inherent to the material used.

Not included in the definitions is the term rest period, which can be defined as a period of time where the applied stress is minimized nearly to zero [38]. A rest period is necessary for restoration of material properties to take place.

2.3.1 Intrinsic Self-Healing of Asphalt Cement

The asphalt cement used in asphalt mixtures is responsible for the self-healing properties that are achieved by the mixture. As microcracks develop, asphalt cement has shown an ability to heal those cracks when given sufficient rest periods [13]. Evidence obtained from evaluation of in service and test track pavements has shown that mechanical properties improve following a rest period. Multiple studies have shown that the stiffness of the pavement is higher following a rest period indicating that microcracking is healing within the pavement [38].

The chemical composition of asphalt cement can vary greatly between sources and as previously discussed can have an impact on the mechanical properties and performance of the mixture. The self-healing properties of asphalt cement are also influenced by the chemical composition, but it can also be affected by the temperature, length of rest period, amount of damage and if the asphalt cement is modified with any additives such as SBS [13, 39]. The magnitude of healing is also heavily dependent on the test methodology

and therefore should be examined empirically until a suitable test method is developed [75]. Healing typically begins immediately after the removal of external loading. Restoration can affect the fatigue performance even when rest periods are not applied. This can be seen when performing tension-compression testing on cylindrical samples. Under compression, the cracks are forced closed momentarily and this allows for some wetting to occur [75]. Several mechanisms can influence the rate of healing within asphalt mixtures. They are the surface free energy theory, capillary flow theory and the molecular diffusion theory [13]. It is likely that all three mechanism can occur in an asphalt mixture contributing to the overall restoration of properties. However, the surface free energy and molecular diffusion theories are more likely to represent self-healing while capillary flow represents recovery.

The self-healing of asphalt cement is similar to the process found in polymers and can be described in multiple stages. The mechanism for self-healing can be seen as the reverse of the fatigue process where each step proceeds depending on the chemical composition, rate of damage and other factors. This can be seen in Figure 2-14. The stages that are consistently described amongst researchers are wetting, molecular diffusion and randomization of the molecules [13, 38, 39]. The original mechanism proposed by Wool and O'Connor also includes surface rearrangement and surface approach [13, 76]. Strength is gained instantaneously with cohesion of the crack faces, and long-term strength is gained from the diffusion of molecules across the crack interface [75]. Wetting, or instantaneous strength gain, is related to the surface free energy while the molecular diffusion, or long-term strength gain, is related to the self-diffusion rates of the asphalt cement [77] which is controlled by the molecular weight of the components of the asphalt cement [75]. Asphalt cement with a higher asphaltene content may have a lower capacity to flow and hence stiffer asphalt cement tends to have a lower self-healing capacity [38, 39].

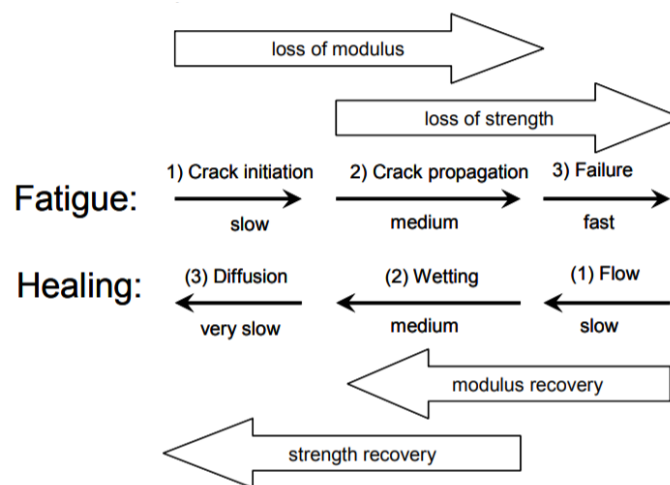


Figure 2- 14 Self-healing and fatigue cracking mechanism [13]

The amphoteric nature of asphalt cement and aromaticity also play a role in affecting the surface free energy and molecular mobility, which has been shown by Little et al. [28] to have an impact on the self-healing properties of asphalt cement. Amphoteric molecules contain acidic and basic functional groups allowing parts of the larger molecule to behave either as an acid or a base. These play a role in the chain formation within asphalt cement by allowing the molecule to interact at two different sites. The aromatic component of asphalt cement tends to form stacks due to pi-pi bond interactions. The aromatic component also tends to be smaller in size and more capable of moving freely. Higher aromatic content has been associated with improved self-healing properties [13, 28, 39]. The waxy fraction of asphalt cement can also impact the flow of molecules within asphalt cement [28]. Reducing molecular movement can affect the diffusion rates and the capillary flow of the asphalt cement.

Surface energy is thought to be highly influential towards the self-healing properties of asphalt cement and the surface energy properties are controlled by the Lifshitz-Van der Waals (LDVW) effect and acid-base interactions. The aromaticity and amphoteric nature of asphalt cement are therefore heavily influential on the surface energy of asphalt cement. It has been found that asphalt cement exhibiting low amphoteric content and high aromatic content would exhibit better self-healing properties due to the increase in acid-base surface energy and lower LDVW surface energy. The total surface energy of asphalt cements of this nature is lower and thus it has been concluded that lower surface energies are beneficial to self-healing properties [28].

2.3.2 Healing of SBS Modified Asphalt Cement

The effect of SBS modification on the self-healing properties of asphalt cement has had conflicting information published. SBS modification is a well-known technique for improving the fatigue resistance of asphalt mixtures [16, 25] and therefore is an interesting material to study with respect to the self-healing properties of asphalt cement. Lv et al. [13] also determined that SBS modified asphalt cement had a decrease in self-healing properties but found that long term laboratory aging increased the healing efficiency. As discussed previously, SBS absorbs the aromatic and saturate fraction of the asphalt cement leaving an asphaltene rich phase. This may reduce molecular mobility and reduce the ability of asphalt cement to heal damage. The researchers suggested healing properties improved in laboratory aged SBS modified asphalt cement because of the shorter chains which positively interact with the unaged chains of the remaining asphalt cement. Little et al. [28] found that two of the five sources of asphalt cement they tested had a reduced healing index with the inclusion of SBS. This was not an expected result for the researchers and may be because the SBS acts as a filler. Simulations performed by Sun et al. [75] found that SBS modified asphalt cement has a higher activation energy and pre-exponential factor in their model. This indicates that

SBS modified asphalt cement has a stronger ability to heal instantaneously but requires more energy to do so. The researchers also found that SBS modified asphalt cement exhibits greater diffusion coefficients. This information leads them to the conclusion that self-healing performance of SBS modified asphalt cement is greater above the glass transition temperature. Further research has shown that SBS can reduce the healing efficiency of the asphalt cement in asphalt cement specific testing [78] but improved the healing efficiency when tested in the asphalt mixture [79]. It is likely that the variance in chemical composition of asphalt cement due to the differences in crude source controls whether SBS modification has a positive or negative effect on the restoration of mechanical properties.

2.3.3 Approaches for Developing Self-Healing Asphalt Pavements

Although bituminous materials have an inherent ability to heal damage, there have been many attempts to improve the self-healing properties of asphalt pavements. Self-healing materials are a growing area of research with many potential applications and it would be wise to look to these materials for inspiration when developing self-healing asphalt pavements. These are materials that have been designed to fully or partially restore properties in order to return functionality. There are currently several approaches which are common in polymeric and composite materials, some of which have been attempted in asphalt pavements. Those approaches include [81]:

1. Capsule Based Self-Healing Materials
2. Vascular Self-Healing Materials
3. Intrinsic Self-Healing Materials

Capsule based and intrinsic self-healing concepts have previously been applied to asphalt pavements [73] while vascular systems have not yet appeared. In addition to this, a method called induction healing has also been used in pavements [4]. The proposed methodology in this research would fall under the category of intrinsic self-healing materials but has not been attempted previously.

2.3.4 Capsule Based Self-Healing Materials

Capsule based self-healing materials use microcapsules containing healing agent that are dispersed throughout a material matrix. When the capsules break, the healing agent is released, and this repairs the material [38]. Crack propagation and fracture energy are sufficient to open the capsules [73]. The first reported self-healing polymer composite was produced by White et al. [80]. The material matrix consisted of microcapsules containing a healing agent and a catalyst dispersed throughout. Crack formation due to damage was enough to rupture the microcapsule and release the healing agent. Through capillary action,

the healing agent was able to fill the crack and interact with the catalyst resulting in polymerization and bonding of the crack interfaces. Capsule wall thickness and relative stiffness are important attributes when considering this type of system. The capsules must be able to withstand production but be able to open during crack propagation. The researchers stated that this approach would help with issues such as microcracking and hidden damage which will increase the lifespan of the material.

It is also possible to disperse two types of capsules within the material matrix. Somewhat like the example above, the healing agent and a catalyst are then required to react to close the crack damage [81]. Producing a capsule based self-healing material this way may prove to be more difficult because it requires that capsules containing both reactants must rupture in close proximity. It is also possible to produce capsules that contain the catalyst within a separate layer of the capsule [81]. This method ensures that the healing agent and catalyst will react when the capsule ruptures. One such effort consisted of a capsule with fluidic monomer core and polymer shell which was coated by the catalyst and further contained by a protective shell. The capsules were approximately 100 μm in size and have shown to be more thermally stable when compared to single walled capsules. The researchers were also able to show that the reactivity of the constituents remained over long periods of time [82].

2.3.5 Capsule Based Self-Healing Asphalt Pavements

The ease of mass production of these capsules containing healing agent makes them a good candidate for producing self-healing asphalt pavements. Asphalt cement is known to oxidize over the service life, and this has led to the development of rejuvenating agents (or rejuvenators) that are intended to alter the chemical structure of the aged asphalt cement [4]. Rejuvenators are typically cationic emulsions containing maltenes and saturates but it has also been found that vegetable oil and waste cooking oil can behave as suitable rejuvenating agents [4, 73]. This helps to restore the original chemical structure which reduces the stiffness of the oxidized asphalt cement which increases the molecular mobility, and this heals microcracks [4, 73]. As a surface treatment, the rejuvenating agent is typically only capable of penetrating the upper 20mm of the pavement. This would not be sufficient for repairing the damage caused by fatigue [83]. Dispersing the capsules in the asphalt cement of an asphalt mixture would allow the rejuvenating agent to heal cracks throughout the pavement.

Multiple groups of researchers have successfully produced microcapsules that can be dispersed in an asphalt mixture successfully. The material of the shell and the capsule size have been the main areas of focus for these researchers. It has been found that microcapsules with a mean size below 10 μm tend to coalesce due to electrostatic attraction [73]. Capsules which are too big can possibly break during the production process.

Epoxy, poly(melamine-formaldehyde) and calcium alginate have all been used to produce self-healing asphalt materials in the laboratory. Epoxy capsules were produced using porous sand which absorbed the rejuvenator and break when a certain stress threshold is reached. The capsules contained a limited amount of rejuvenating agent which necessitated a large number of capsules. This could potentially reduce the quality of the pavement [4]. Poly(melamine-formaldehyde) capsules have shown good thermal stability but pose a potential environmental hazard through leaching.

This makes calcium alginate an interesting alternative. Calcium alginate is a biopolymer that is stored in brown algae making it an environmentally friendly option for microcapsules [4]. Xu et al. [84] optimized calcium alginate capsules and found that a ratio of 30% alginate to 70% rejuvenator is very effective. The capsules are porous with a honeycomb structure allowing for increased mechanical and thermal resistance and improved absorption of the rejuvenating agent. The calcium alginate network is visible in Figure 2-15. The Environmental Scanning Electron Microscope (ESEM) images show how the porous structure changes with different calcium alginate to rejuvenator ratios with Figure 2-15f showing the greatest ability to store rejuvenator. The mixture containing the capsules saw a 40% restoration in bending strength while the mixture without only saw a 4% restoration. Calcium alginate fibre compartments were also used but had limited rejuvenating agent contained within them and limited healing capacity [4, 84].

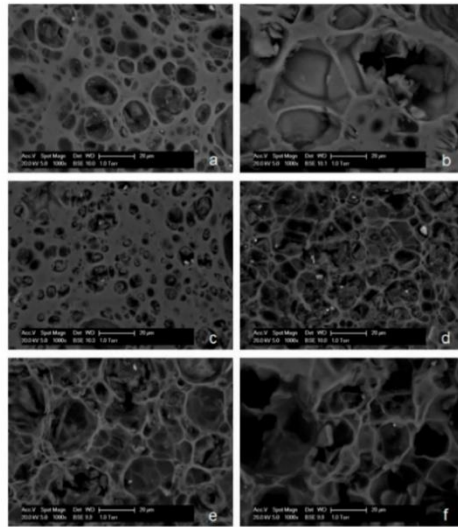


Figure 2- 15 ESEM images of calcium alginate capsules with various calcium alginate to rejuvenator ratios [84]

Although the capsule based self-healing methods have shown a good ability to improve restoration, there are some commonly cited concerns with their usage. The first issue is the fact that the capsules can only be used once because there is a limited amount of rejuvenating agent contained in the capsules [4, 38, 73].

Single use of the capsules would be beneficial to reduce the propagation of cracks, but this would only be useful for short term healing. In some cases, the capsules were found to break during compressive testing leaving voids in the mixture and increasing the rate of deformation [38, 85]. In addition to this, the capsules can also potentially release during the production phase [4]. This would have a negative impact on the permanent deformation characteristics of the pavement. The use of capsules has been promising, but the limitations are unlikely to benefit the long-term restoration capacity of an asphalt pavement.

2.3.6 Vascular Self-Healing Materials

Although not used in asphalt pavements, vascular self-healing materials may prove to be an interesting concept for the development of future asphalt pavements. Vascular systems draw inspiration from blood vessels in humans [38] and fauna [86]. For example, fig trees are known to deliver latex to damaged areas via a separate network in order to seal wounds and prevent bacterial infection [86]. Typically, a vascular self-healing material follows this concept by placing microchannels throughout the matrix of the material which can deliver a healing agent. One advantage of such a system is the ability to deliver a large amount of healing agent [81]. The system can act passively, but some researchers have developed systems with active pumps and sensors. Hamilton et al. [87] developed the use of active pumps to deliver two healing agents. This allowed the healing agents to be stored externally, which could be potentially useful for replenishing the system. The use of pumps reduced the reliance on capillary action and improved the mixing of the healing agents. In order to produce a material which repairs autonomously, Hamilton et al. discuss the importance of sensing and estimating damage size in order to apply the correct quantity of healing agent. Other researchers have published work which has included the use of a low-pressure sensor and both have found high degrees of healing efficiency [81].

Such a system could potentially be used to deliver rejuvenating agents throughout as asphalt pavement, which would act to restore some of the original material properties. There are potentially drawbacks to the use of rejuvenating agents, as previously discussed, which could cause deterioration of performance if the system is not developed properly. The correct dosage and timing of the dosage would need to be considered carefully. Construction of a vascular self-healing pavement could possibly be quite difficult and would require deviation from standard practice.

2.3.7 Induction Healing of Asphalt Pavements

Induction healing is the self-healing pavement technology that is furthest along in its development. This method takes advantage of the viscoelastic properties of asphalt cement by increasing the temperature which improves molecular movement and capillary flow. Increasing the temperature of neat asphalt cement

is known to improve the restoration of properties [4, 13, 73]. Induction heating requires blending of electromagnetically sensitive materials such as steel fibres, carbon fibres, graphite, steel wool or conductive polymers into the asphalt cement. An induction source capable of producing an electromagnetic field is applied producing an eddy current in the conductive materials which produces heat [4, 73]. This is an interesting choice for improving the restoration of material properties in asphalt pavements and one that has already been used to pave test sections. A schematic of the induction heating process can be seen in Figure 2-16.

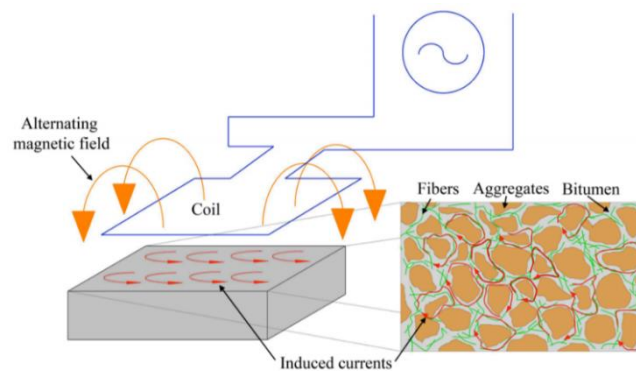


Figure 2- 16 Schematic overview of induction heating process [88]

Schlangen et al. [88] designed the first self-healing asphalt pavement road in the Netherlands. The first test section using induction heating was paved in 2010 with the first induction treatment applied in 2014. This trial was produced using steel fibres which were approximately 1 cm in length [73]. The steel fibres were added at 4% of the weight of the asphalt cement. Early indications were that the test section was performing well, however information regarding the long-term performance has been difficult to find [88]. HEALROAD was second attempt to produce an induction healing pavement was funded by the European Research Area Network. Steel wool with a diameter of 40 μm and a length of 2 mm was determined to be the optimal material for this project as they were able to be added to the asphalt mixture with no changes to the production process. Healing levels in both projects were determined to be quite good achieving approximately 80% recovery in the laboratory specimens [4].

The Schlangen research group and HEALROAD project found that restoration was optimized at elevated temperatures (85°C and 90°C respectively), however the restoration decreased when the temperature exceeded this value. This was likely due to the due to swelling of the asphalt cement and possibly drainage [4, 73]. HEALROAD reported that there was no detectable increase in aging during the induction process [4], but this may still be a potential issue. Another potential issue is the loss of conductivity of the steel fibres through corrosion [4, 73], however some researchers have shown that carbon-based additives would

also work suitably for this application [73, 89]. The steel fibre orientation can also affect the amount of heat generated from the eddy currents and the induction source may not produce a homogenous electromagnetic field [4, 90]. These can reduce the healing efficiency by producing temperature gradients within the material. The induction treatment also requires that the pavement be closed for 4 hours in order to maximize the effectiveness of the treatment [73]. This could make the solution impractical for heavily trafficked roads.

2.3.8 Intrinsic Self-Healing Materials

Materials which can heal damage intrinsically appear to be a fascinating option for producing self-healing asphalt pavements although little research has been produced in this area. This class of self-healing material would not require any external stimulus in order to repair the damage and instead relies on the reversible nature of chemical bonds. These systems would theoretically be able to heal themselves an infinite number of times [81]. Synthesis of a self-healing polymer could be simpler than the capsule-based methods mentioned previously [76] and the addition to an asphalt cement could follow similar steps to SBS modification. The Diels-Alder reaction [81] and metal-ligand coordination chemistry [91] are just two of the options that have been explored by researchers to produce self-healing polymers. The self-healing mechanism of neat asphalt cement has been based on the research on self-healing polymers [75] and therefore the mechanism of healing is similar between these materials. The stages of healing in polymeric materials can be described as surface approach, wetting, diffusion and random molecular movement [76].

The Diels-Alder reaction is a [4+2] cycloaddition reaction between a conjugated diene and an alkene to produce a cyclic product. The reaction is thermally reversible meaning that at an elevated temperature the product can break and form into the two initial constituents. Once the heat is removed, the bonds can reform, and the material regains some of its initial properties. The first self-healing polymer developed using this chemistry showed an average healing efficiency of approximately 50%. The authors were able to improve the healing efficiency to 80% by choosing low melting point monomers [76]. Self-healing epoxies have been developed and Diels-Alder chemistry has been combined with memory shape polymers to produce a wide range of self-healing polymers. These polymers have been heated to temperatures that would not be typical to pavements in Canadian climates (above 50°C) [76, 81] and therefore may not be suitable for Canadian asphalt pavements.

Polydimethylsiloxane (PDMS) is an interesting material that has been explored with respect to self-healing polymers. PDMS based self-healing polymers have used a mix of reversible covalent and non-covalent bonds to produce films with tuneable mechanical properties [81]. Li et al. [91] demonstrated that this could be accomplished by crosslinking the PDMS chains with iron-based coordination complexes. The resulting

material was highly stretchable and demonstrated an ability to heal at temperatures as low as -20°C . The material receives its elasticity and self-healing properties from the use of bonds of varying degrees of strength. This can be seen in the chemical structure in Figure 2-17. The ratio of coordination complex to PDMS chain has also been shown to produce polymers of varying tensile strengths. The healing efficiency has been measured as high as 90% and 68% at -20°C following a 72-hour rest period. The elastomeric nature of the polymer and the ability for restoration to take place at temperatures as low as -20°C make this an interesting material for potentially producing a self-healing asphalt pavement.

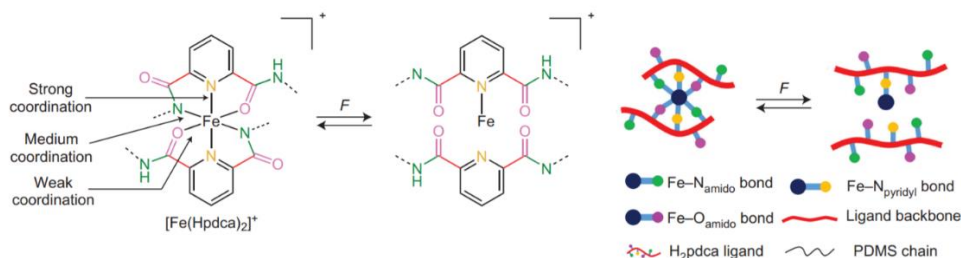


Figure 2- 17 Chemical structure and overview of self-healing mechanism of iron-based metal coordination PDMS self-healing polymer [91]

Wang et al. [92] have also provided evidence that it is possible to produce a self-healing elastomer using PDMS and zinc-based coordination complexes. This material was also able to achieve a healing efficiency of approximately 90% at room temperature. Figure 2-18 shows chemical structure and final thin film produced by Wang et al. Both PDMS based polymers produced have a similar reddish-brown and transparent appearance [91, 92]. When comparing this chemical structure to the structure of the polymer produced by Li et al. it can be seen that they are quite similar. The use of PDMS and coordination complexes to produce self-healing polymers is certainly a viable area of research because these materials have not been used to produce self-healing asphalt pavements as of yet.

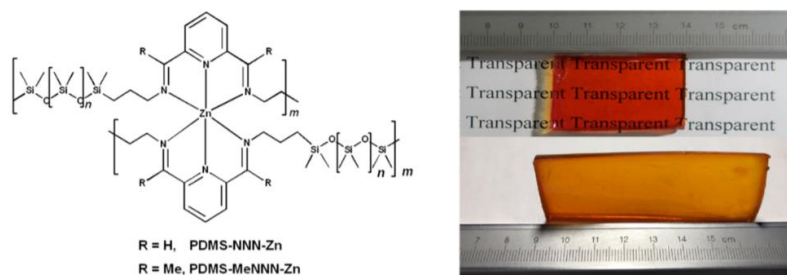


Figure 2- 18 Chemical structure and appearance of final product of zinc-based metal coordination PDMS self-healing polymer [92]

2.3.9 Nanoparticles

Nanoparticles have been used to improve the ageing and rheological properties of asphalt mixtures [73] but have also been shown to improve the healing of microcracking. Nanoparticles have been shown to reduce the stress concentration at the tip of the crack. In polymers, this causes the chains near the crack to stretch and reduce crack propagation [38, 73]. Nanoclays and nanorubbers have both been explored for use in asphalt mixtures. Nanoclay has been shown to improve fatigue performance [73, 93], and part of this is thought to be related to the improvement in healing characteristics. Research in this area is limited.

2.4 Characterizing the Self-Healing Properties of Asphalt Cement and Mixtures

Like the efforts to characterize fatigue performance of asphalt mixtures, there is a fair number of different methods that have been employed to characterize the self-healing properties of asphalt cement. Different binder and mixture tests have been developed that may look at particular aspects of the healing process. Tests are typically limited to adaptations of fatigue tests with the inclusion of a rest period. The rest period decreases the rate of modulus drop in the sample over the entirety of the test. Some of the recovery in modulus can be attributed to thixotropy and not the actual chemo-mechanical healing process [5]. This is also why the differentiation of restoration and self-healing becomes necessary. Most literature describes both forms of recovery in modulus as the healing of asphalt. This could be accurate in the context of asphalt mixtures but not asphalt cement.

2.4.1 Self-Healing Properties of Asphalt Mixtures

Testing of the asphalt mixture is good practice for understanding the fatigue performance of the material because it is representative of the final product placed on the road. As mentioned earlier, mixture performance testing is used in different ways in different countries and as a result, there is a multitude of different test methods to choose from in order to develop a test to evaluate the self-healing properties of an asphalt mixture even though all of the healing takes place within the asphalt cement portion. The aggregate skeleton and film thickness of the mixture has been shown to impact the healing efficiency [94]. Indirect tensile testing, 3-Point Bending Beam and uniaxial tension-compression testing have all been used in order to evaluate the self-healing capabilities of asphalt mixtures. Some researchers have also attempted to develop novel approaches to evaluate healing, such as the Beam-on-elastic-foundation (BOEF) test set up by researchers at Delft University [95].

The BOEF set up presents an interesting methodology because it deviates from the traditional test methods listed above. An asphalt mixture beam is prepared with a small notch and glued to a piece of neoprene

rubber which was also glued to a steel plate. The researchers make use of a remote-control camera in order to monitor the crack propagation, while linear variable differential transducers are used to monitor the crack opening displacement (COD). Monotonic loading was applied at a rate of 0.001 mm/s until the COD reached a target value. Dynamic loading was also used with 300 N of force being applied for 5 seconds at a frequency of 5 Hz. After the external load was removed, the samples were allowed to heal at either 5°C or 40°C and for 1, 3 or 24 hours in order to determine the effects of temperature and rest period time on healing. The rubber foundation confines the sample and prevents abrupt failure from occurring. The researchers measured the healing in terms of the apparent stiffness of the beam by determining it before and after the rest period. Figure 2-19 shows an example of the test set up used.

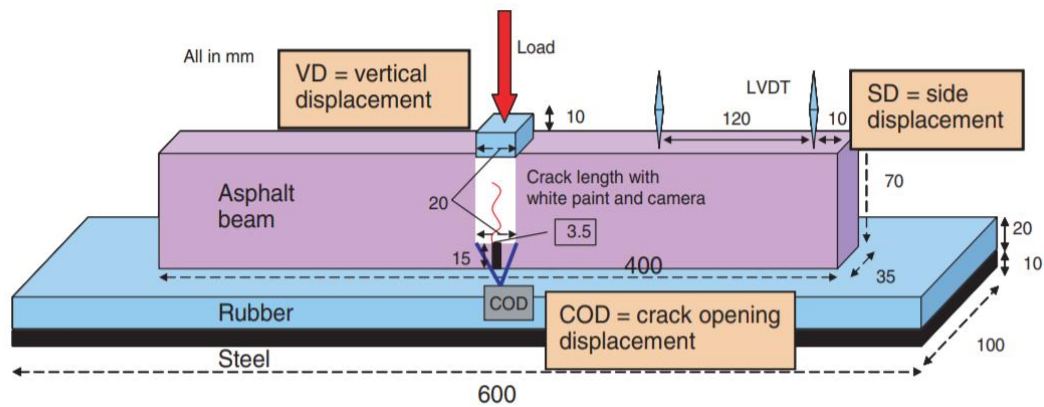


Figure 2- 19 Schematic of Beam-on-elastic-foundation set up developed by Delft University [38]

The test is capable of highlighting three distinct phases of the cracking. By analysing the changes in the COD, it was determined that there is a viscoelastic, macrocrack and microcrack zone. In the viscoelastic zone, no damage occurs. The macrocrack zone corresponds to the phase of visible crack growth while the microcrack zone corresponds to the nonlinear behaviour while no cracking is visible. In addition to being able to evaluate different crack phases, the test method offers a few more advantages over other methods. The confinement from the rubber-steel plate allows for the full closure of the crack and the method is easily transferable to other rest periods and temperatures. Using this test, the researchers observed that the healing temperature was more important than the healing time and that under dynamic conditions most of the healing occurred immediately and slowed with time. The authors also determined that monotonic loading was measuring strength gain which they stated depends on the viscosity of the asphalt cement and the recovery under dynamic loading was due to crack closure [95]. The role of temperature and healing rate under dynamic loading seems consistent with the proposed mechanisms of the healing process. It should also be noted that the properties measured here are likely highly system dependent rather than material dependent [38].

Indirect tensile testing (IDT) has the advantage of being a relatively quick test which allows for the determination of the resilient modulus. Grant [96] used two different test set ups involving the use of rest periods. The first involved testing the sample for 1000 cycles at 15°C, stopping the test, cooling it down to 10°C and resuming the test after one hour. The second method applied 1000 cycles to the specimen and measured the resilient modulus at five points within an hour of removing the loading. The initial intention of the first method was to prevent a change in properties, but a small recovery in the resilient modulus was observed. Healing was observed to be a non-linear process occurring quickly initially followed by a decrease in rate. Steric hardening was also noted as the primary reasoning for the initial large drop in modulus. Sun et al. [94] used a different approach with IDT. Intermittent rest periods were applied following each application of a load with resilient modulus testing performed at four different times following the final loading cycle. The testing took place on three different mix types: stone mastic asphalt (SMA) and two Marshall designs standard to Sweden. The testing revealed that the gradation type and rest time have a significant impact on the healing efficiency of the asphalt. Increasing the intermittent loading time increased the resistance to fatigue. The SMA proved to have the highest healing potential due to the increased film thickness provided by the design despite having the lowest asphalt cement content. In addition to the IDT, the researchers also made use of computed tomography (CT) scanning in order to monitor crack healing which can be seen in Figure 2-20. Three and two-dimensional imaging confirmed that the cracks were becoming smaller with time.

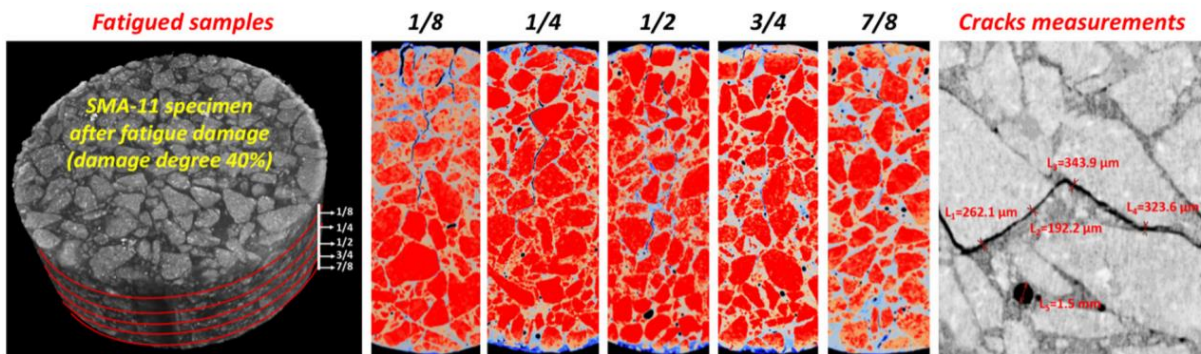


Figure 2- 20 Computed Tomography (CT) images of crack healing for an SMA-11 mixture [94]

The 3-Point Bending Beam (3PB) test is a classic example of an asphalt mixture fatigue test. Variations of the test exist using 2 and 4-point set ups, with the 4-Point Bending Beam becoming the most widely used method. 3PB is also a popular test for examining the mechanical and healing properties of materials in other industries. Several researchers have used this method and versions where the beam contains a notch to test a diglycidyl ether of bisphenol A epoxy by measuring the load recovery of the sample [81]. The

HEALROAD project also made use of 3PB in order to test the healing efficiency of their induction heating asphalt mixture. The researchers used two different methods. The first measured the 3PB strength before and after applying the induction source, and the second measured the increase in fatigue resistance resulting from the application of the induction heating. The researchers found that approximately 80% of the strength was recovered at -20°C under conditions used in the first method [4]. Daniel and Kim [97] applied 3PB testing to evaluate the role of temperature and rest period on the healing properties of asphalt cement. First the resonant frequencies were determined at 20°C , followed by 3000 cycles of load at 1.7 Hz. The beams were removed once loading was completed and allowed to rest for 4 hours at 20°C or 60°C . Following the rest period, the beams were conditioned at 20°C and 10,000 cycles were applied. They continued to alternate rest periods and loading cycles until a 50% reduction on modulus was measured. The life span of each beam increased, and the modulus recovered following the addition of rest periods. The evolution of dynamic modulus with respect to the number of cycles is shown in Figure 2-21. The amount recovered decreased following subsequent rest periods. The authors concluded that crack healing was the primary reasons for the recovery in the modulus after determining that no viscoelastic relaxation had taken place after analysing impact resonance measurements.

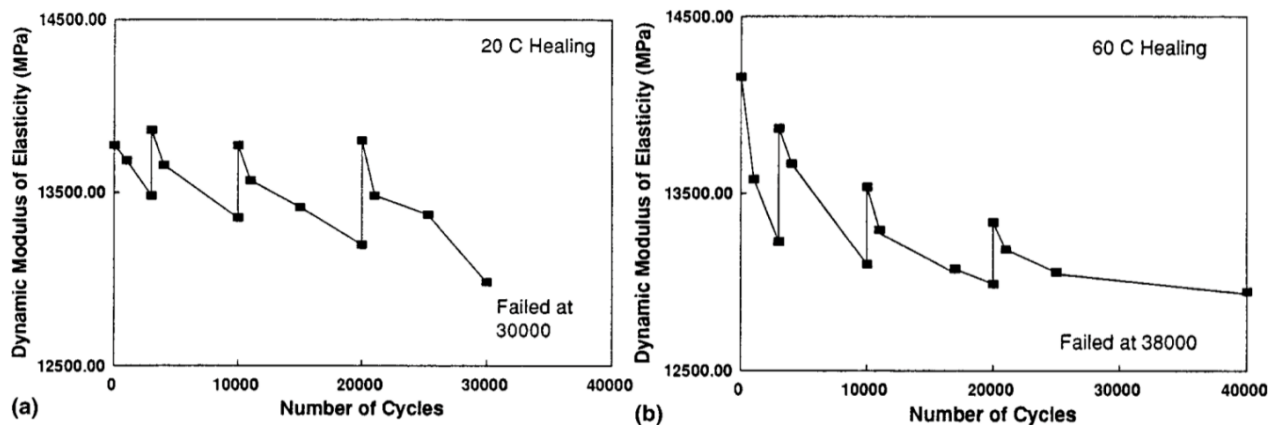


Figure 2- 21 Evolution of dynamic modulus versus the number of cycles at 20°C (left) and 60°C (right) [97]

Shirzad et al. [98] also used a 3PB set up to test the influence of recycled asphalt materials and a self-healing polymer on the self-healing properties of an asphalt mixture. Temperature and exposure to UV light were varied for the rest period while the healing properties were evaluated by using the strain energy recovery ratio. The researchers determined that the self-healing polymer improved healing and cracking resistance following exposure to UV light. They also confirmed the role of temperature in effecting the healing abilities of asphalt mixtures. The addition of recycled materials reduced the crack healing abilities

as expected. The addition of aged asphalt cement may have decreased the molecular mobility of the virgin asphalt cement once blending occurred.

Narambuena-Contreras et al. [99] used a modified 3PB set up to test the healing efficiency of their calcium alginate capsules containing sunflower oil as a rejuvenating agent. The beams were conditioned at -20°C for 4-hours before being broken into two pieces with the 3PB set up. A plastic membrane was applied to the crack face and the pieces were placed back together inside a steel mould. A compressive load was applied at a rate of $2\text{mm}/\text{min}$ until a vertical displacement of 5mm was reached in order to break the capsules. The plastic sheet was removed, and the pieces were placed back in the mould. The beam inside the mould was placed in a temperature-controlled chamber for the rest period of 120-hours with a temperature of 20°C . Following the rest period, the loading step was repeated again (Figure 2-22). The healing index was measured in terms of the maximum load applied before and after the healing process. CT scans were used to evaluate the distribution and integrity of the capsules within the asphalt mixture. They were found to be intact and well mixed in within the cylinders imaged. The researchers found that the healing efficiency was negatively impacted by the aging process due to the increase in viscosity (poorer molecular mobility). The researchers were also able to confirm that the presence of capsules improved the healing properties of the asphalt mixture regardless if it had been aged. The temperature and stage when the capsules were added to the mixture impacted the performance causing some deterioration to occur and the authors recommend adding the capsules at the end of the mixture process.

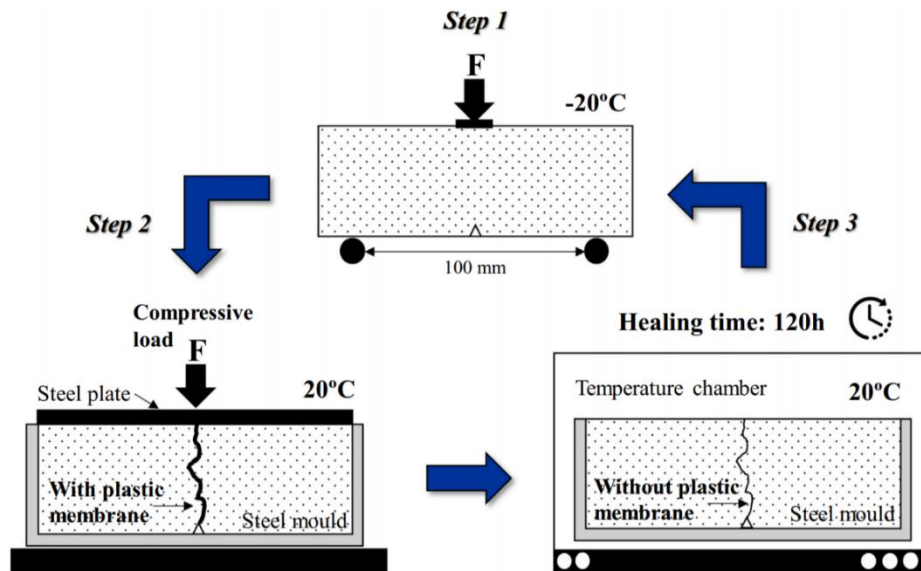


Figure 2- 22 Diagram of test set up and procedure used to evaluate calcium alginate capsules containing rejuvenator [99]

Uniaxial tension-compression testing provides more homogenous stress conditions than beam testing and improves on fatigue characterization of asphalt mixes [50]. The test has also been used to evaluate the healing of damage. Little et al. [28] developed a healing index using based on the dissipated pseudo strain energy before and after rest periods. Cylindrical samples were tested using an intermittent loading pattern where they used a 0.5 second rest period between haversine loads. The load was converted into a pseudo strain in order to eliminate time dependant effects. They found that the pseudo strain energy consistently increased following a rest period. They noted that the recovery was mostly due to a change in stiffness and claimed that the healing index is not a fundamental material property due to the influence of molecular structuring and hysteresis.

Baaj et al. [79] used tension-compression to characterize the healing properties of several French mixtures including one containing SBS. The test set up used a sinusoidal loading frequency of 10 Hz and measured the strain with transducers placed triaxially around the cylindrical sample. The test consisted of alternating loading and rest periods. The evolution of the complex modulus can be seen in Figure 2-23. Each loading periods consisted of either 300,000 or 150,000 cycles followed by a 24-hour rest period. Temperature was held constant during loading but was varied during the rest periods. In addition to change in modulus, the set up was also able to measure the change in phase angle and the change in dissipated energy was calculated for each cycle (Figure 2-24). The researchers found that the fatigue life increased greatly through the addition of the rest periods when the temperature was kept at 10°C or above. A minimum temperature is required to ensure sufficient molecular mobility to allow rearrangement of the molecular structure. It can be observed in Figure 2-24 that the change in complex modulus observed here is similar to the observed change in dynamic modulus observed by Daniel and Kim [97].

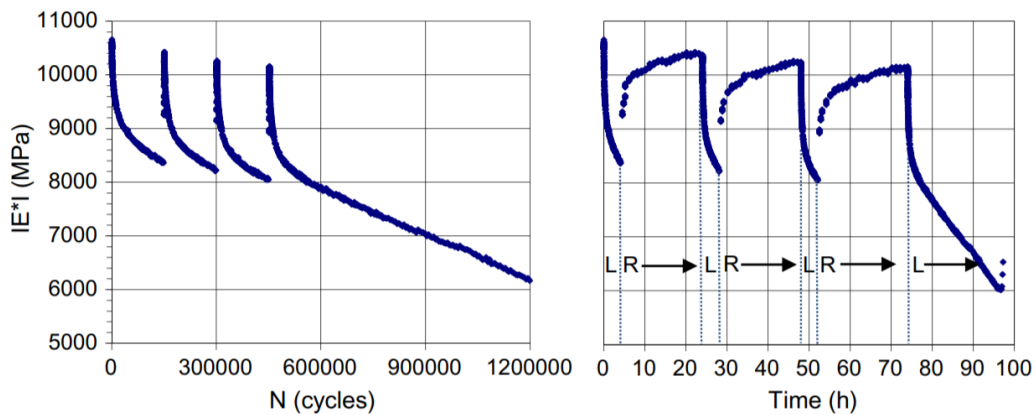


Figure 2- 23 Evolution of complex modulus versus the number of cycles (left) and the loading time (right) [79]

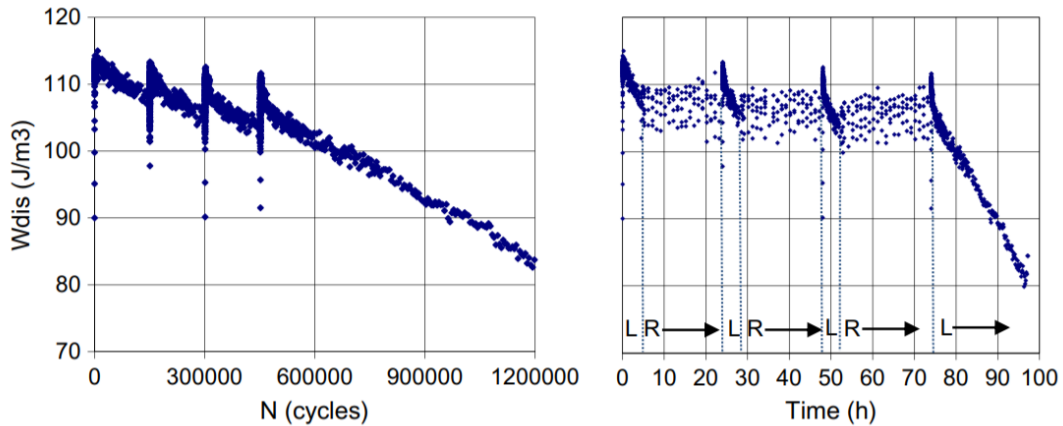


Figure 2- 24 Evolution of dissipated energy versus the number of cycles (left) and the loading time (right) [79]

The obvious similarity between the tests discussed here is the addition of a rest period to a traditional fatigue test set up. The difficulty is in ensuring that sufficient damage has occurred within the sample in order to prompt healing. These researchers have confirmed that the temperature and rest period play a significant role in improving the fatigue performance of asphalt mixtures. Some authors have made attempts to distinguish between thixotropic recovery in modulus and crack healing, but it still remains a difficult task.

2.4.2 Characterizing the Self-Healing Properties of Asphalt Cement

The healing properties of asphalt mixtures and pavements is controlled by the chemical composition and structure of the asphalt cement. Efforts to characterize the healing potential of asphalt cement is conducted using the DSR or Dynamic Mechanical Analyzer because of the high precision and control these devices have. Methods have been proposed that induce damage, measure the wetting properties and rates of molecular diffusion. The methods designed to induce damage have been derived from time-sweep tests that are used to evaluate the fatigue resistance of asphalt cements. Other tests have been designed to exam the performance of the mastic, which will be discussed in this section despite technically being a mixture.

Two of the methodologies being evaluated by RILEM [74] are the PoliTO protocol based on a time-sweep technique and the Linear Amplitude Sweep Test with Healing (LASH) developed at the Beijing University of Technology which is based on the LAS test described in the asphalt cement fatigue section. The PoliTO protocol performs a time sweep at 10 Hz and a standard temperature of 20°C. The time-sweeps are most effective when performed outside of the linear viscoelastic region of asphalt cement and this is done by selecting a larger strain value. This also has the benefit of shortening the test time by inducing damage and failure sooner. PoliTO selected a strain level of 3%. A 2-hour rest period is applied after a certain amount

of damage is induced and healing is determined by evaluating the number of cycles it takes to reach the corresponding decrease in the dissipated energy. The damage is initially applied and following the rest period the asphalt cement is tested to failure. A strain rate of 0.01% is applied during the rest period to monitor the changes in rheological properties necessary to calculate the dissipated energy. This process can be seen in the plot of the complex shear modulus versus the number of cycles in Figure 2-25. The figure depicts the preliminary conditions phase, followed by a loading phase then the rest period and a second loading phase which runs until failure. The kinetics of the recovery process can be evaluated by examining the changes in dissipated energy. An abrupt increase is observed, followed by a decrease in the rate and an asymptotic behaviour. The authors also used the change in dissipated energy to predict the time in hours it would take to achieve 99% of the asymptotic value. This value increases as the amount of damage induced increases. The testing revealed that the healing index was higher for the lower penetration grades asphalt cement [100].

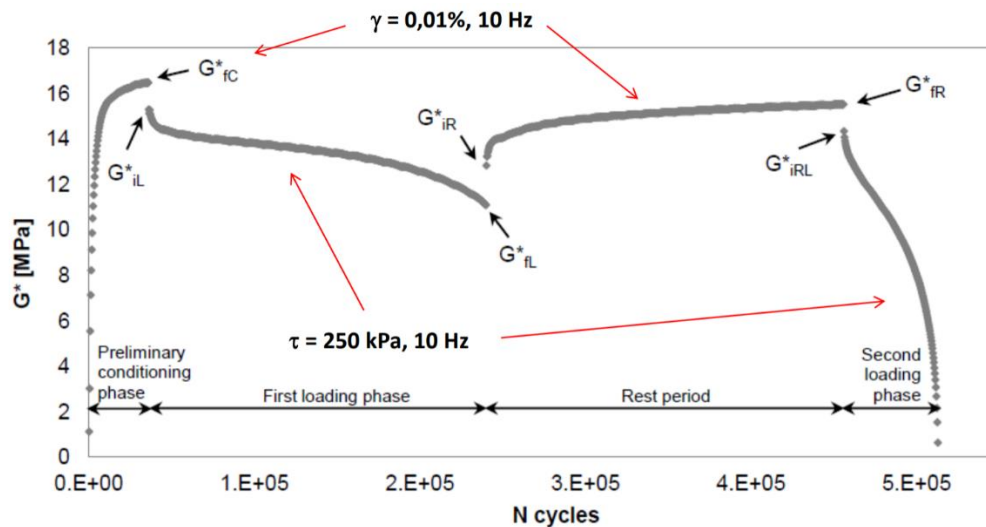


Figure 2- 25 Example of the data collected using the PoliTO protocol including test parameters [100]

The LASH test uses the same basic framework that is outlined in AASHTO TP 101. Prior to adding a rest period to the procedure, the continuous LAS test is run in order to determine the failure occurrence value ($\%S_f$) which corresponds to a certain strain level. A second sample is then prepared, and the strain is applied continuously until the strain value determined from the calculation of $\%S_f$ is reached. The rest period is then applied followed by the test resuming to reach the final strain level designated in the LAS procedure [78]. Xie et al. [78] used $\%S_f$ values of 25, 50, 75 and 100% S_f with rest periods ranging from 1 to 30 minutes. The healing index was calculated using the change in damage intensity that is calculated using the S-VECD methodology employed by the LAS. There is evidence that the pseudo stiffness also shows some

recovery following the rest period. The researchers also plotted “healing master curves” by plotting the percent healing versus the time of the rest periods. Figure 2-26 compares the damage intensity versus the pseudo stiffness for different rest periods at 50 and 75 % S_f . The increase in rest period clearly indicates in higher recovery of pseudo stiffness and lower values of damage intensity following the rest period. The use of the LASH test found that the neat asphalt cement had a better self-healing capability than the SBS modified asphalt tested.

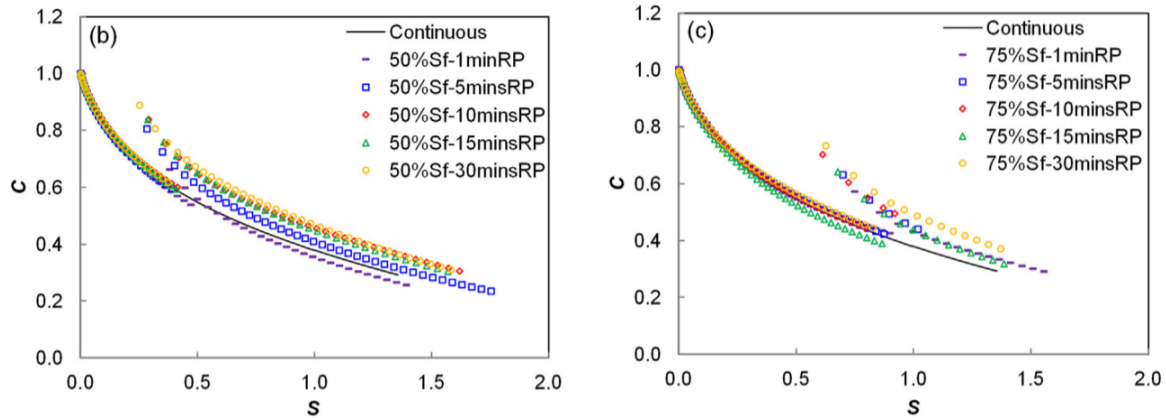


Figure 2- 26 Damage intensity versus pseudo stiffness curves for 50 % S_f (left) and 75 % S_f (right) for rest periods of 1, 5, 10, 15 and 30 minutes [78]

Canestrani et al. [101] used a novel time sweep approach incorporating multiple rest periods rather than a single rest period like the methods mentioned above. Multiple, intermittent rest periods were inserted when the sample reached specific damage levels. The asphalt cements were first characterized by analysing their master curves produced using a frequency sweep finding little difference between the asphalts despite increasing SBS concentration. The researchers incorporated reclaimed asphalt intended to simulate aging and this did have an impact on the rheological properties. Multiple rest periods were selected in order to give adequate time to allow intermolecular diffusion to take place. These conditions also better simulate field conditions of the asphalt cement would experience in the pavement. A strain amplitude of 5% was applied with a frequency of 10 Hz and alternated with 30-minute rest periods. The researchers applied 12 load-rest cycles. The temperature applied during the test varied with sample in order to start the test at the same iso-stiffness value of 3 MPa. This could possible remove stiffness depend effects from influencing the results. The researchers found that increasing the SBS concentration increased the self-healing capacity of the asphalt cement. Non-reversible damage was reduced, and thixotropic characteristics were enhanced. The long-term aging of asphalt cement was found to improve the fatigue resistance of the asphalt cements, which resembles observations made by Zhou et al. with respect to the LAS test [65]. This could be due to

the fact that the addition of reclaimed asphalt to each blend increased the polymer concentration of the blend. The aging process shortens the length of the SBS chains which are then able to interact more favourably with the virgin asphalt cement.

Pang et al. [102] performed a stress-controlled time sweep targeting 40, 60 and 80% damage with rest periods of 0.5, 1 and 3 hours. The test method measured the decrease in the complex modulus in order to determine damage. The healing index was calculated as a ratio of damaged before and after the rest period. Their findings suggested a potential reduction in healing potential due to the addition of SBS due to a decrease in the viscous component. The researchers also concluded that a larger degree of damage would weaken the self-healing capacity. Sun et al. [39] used a simple fatigue-rest-fatigue set up with a constant strain rate of 3% followed by an hour-long rest period at 25°C. The healing index was determined using a damage ratio comparing the change in complex shear modulus during the loading and rest phases. This method was combined with analytical techniques such as FTIR and Nuclear Magnetic Resonance (NMR) to understand the role of the chemical structure in healing. The researchers found that the increase in large molecule size particles lead to a lower self-healing capability. It was also determined that the methylene to methane ratio was a good indicator of healing potential. The amount of hydrogen atoms located close to aromatics, determined using NMR, was also a good indicator of healing potential. These two parameters are indicative of the degree of chain branching. A lower degree of branching will improve the molecular mobility and the self-healing ability of the asphalt cement.

Leegwater et al. [103] proposed a technique for exploring the role of normal force on the self-healing properties of asphalt cement. The main mechanisms of healing involve wetting and strength gain from interdiffusion between two surfaces in contact. This test method was designed to replicate the coming together of two different crack faces. The testing was conducted on the DSR using a direct tensile loading. One piece of asphalt cement was applied to each plate and the samples were then brought into contact. Following a rest period, the tensile strength was tested. The asphalt cement was poured into a small steel ring to improve handling while a piece of silicon paper was used in order to control the contact area. The test schematic showing the test preparation is in Figure 2-27. Samples were exposed to single rest period of one hour at 13°C while five different loads were applied. As the load increased, the maximum tensile strength increased thus showing that the load level has a direct impact on the healing efficiency of the asphalt cement.

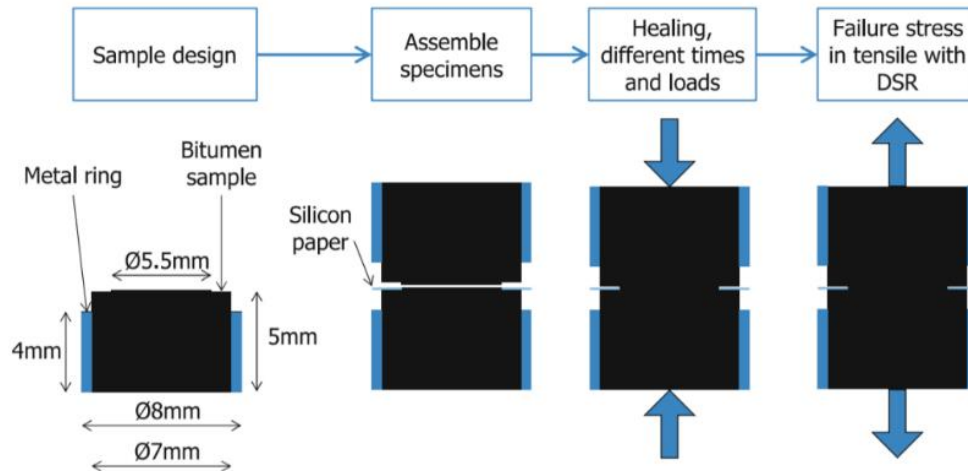


Figure 2- 27 Illustration of the sample preparation and test set up for analysing the effect of normal force on self-healing properties [103]

Bhasin et al. [75] used the Wilhelmy Plate test to evaluate the cohesion of asphalt cement in order to understand the role of wetting and instantaneous healing. The Wilhelmy Plate test measures the angles of wetting and dewetting [28]. The measurements were combined with the acid-base theory of surface free energy components in order to determine the surface free energy and work of cohesion for the asphalt cements selected. The results of the Wilhelmy Plate test were compared to two different healing tests, one using the DSR and one using the dynamic mechanical analyser (DMA). The DSR test involved bringing two pieces of asphalt in contact and applying a few loads in order to determine the shear modulus which was normalized by comparison to a similarly sized single piece of asphalt cement. Following the initial contact, the DSR was programmed to measure the dynamic shear modulus periodically for one hour. The measurement was conducted using 50 cycles at a strain rate of 0.001% and a frequency of 10 Hz. The healing index was determined to be a ratio between the initial the dynamic shear modulus and any point taken during the data collection phase. This test method tests for the instantaneous wetting and interdiffusion. The DMA has been shown to be an effective tool for evaluating the fatigue cracking properties of the fine aggregate matrix (passing the 1.18mm sieve) and hence was used here to evaluate healing. The mixture was short-term aged for two hours and compacted using a gyratory compactor. The test specimens were cored from the mixture and the air void content was maintained at approximately 13%. Cyclic torsion loading was applied with a strain amplitude of 0.2% and a frequency of 10 Hz. Rest periods were introduced after certain numbers of cycles corresponding to a percentage of the original fatigue life.

The three asphalt cements examined were found to have different initial and long-term healing rates. The surface free energy is related to the molecular weight of the asphalt cement and testing determined that the

asphalt cement with the lowest molecular weight had the lowest cohesive strength of the three studied. This corresponded well with their results that showed this asphalt cement had the poorest initial healing but the best for long term healing because of the improved molecular mobility. This suggests that the instantaneous healing rate is related to the work of cohesion. Little et al. [28] pointed out that having high Lifshitz-VDW forces inhibits initial healing and this would be related to the molecular weight.

Qiu et al. [104] used a direct tension test (DTT) machine in order to evaluate the healing potential of mastics. Test specimens were conditioned for 24-hours at -18°C prior to being placed in the DTT chamber for 2 hours at 0°C . Cracks were developed by applying a load in direct tension of 10mm/min. The machine was programmed to stop at designated elongation levels following peak load. The specimens were removed and allowed to rest for 5 minutes, 30 minutes and 3 hours at 20°C . The researchers noted that it was possible to obtain multiple cracks under these conditions. Healing was largely dependent on the duration of the rest period; crack phases present and material types. Smaller cracks and long rest periods lead to better healing. SBS modified mastics showed a better strength healing at small crack distances but were worse than the neat mastics when larger cracks were produced.

Lv et al. [13] used the binder bond strength (BBS) in order to evaluate the healing properties of SBS modified asphalt cement. Specimens were prepared according to AASHTO TP91. A silicon mould with a hole in the centre had asphalt cement poured into it and a stub was placed on top. Samples were cured under ambient conditions before being placed in a water bath for 24-hours [112]. The stubs were marked and the initial pull-off tensile strength test was performed. In order to test the healing, the stubs are replaced without applying pressure to the sample. The specimen is placed back in the water bath for 24-hours and the pull-off tensile strength is measured again following the rest period. In addition to the healing index, CT scanning was performed to visually inspect the changes to crack size. The researchers found that water had a negative effect on the instantaneous healing properties of the asphalt cement but unexpectedly played a positive role in long-term healing. The water may interact favourably with the hydrogen bonds at the surface of the asphalt cement. Once the healing reaches its maximum level however, the water begins to exert a negative influence again. The researchers also confirmed that the increase in temperature led to an improvement in the healing capacity. It was also observed in the healing test and CT scans that SBS had a negative influence on the healing potential of the asphalt cement. The unaged neat asphalt cement showed better healing after repeated cycles than the methods that were laboratory aged. The SBS modified asphalt cement showed better healing properties with laboratory aging with the PAV aged material having the best healing efficiency. This may be due to the fact that when SBS oxidizes, the chain length decreases which becomes favourable for healing even though the non-polymer portion increases in particle size with aging.

2.5 Gaps in Current Research

Current research on the self-healing properties of asphalt cement can be divided into two main areas of study. The first is understanding how to characterize the healing properties of asphalt cement and the second is developing techniques for improving crack healing in pavements. This thesis largely focuses on the latter but does discuss issues regarding the evaluation of healing on asphalt cement.

2.5.1 Limitations to Healing Characterization

Current methods in healing characterization are derived from standard fatigue cracking tests developed for asphalt mixtures and asphalt cement. Fatigue cracking tests are far more developed for asphalt mixtures than for asphalt cement. Characterization of the intrinsic healing properties of asphalt cement as a stand-alone material requires further research. Current methods attempt to induce damage in the samples, but it is difficult to reproduce the cracking that occurs in the pavement. Methods such as the LAS test have been shown to characterize fatigue resistance well, but the test is affected by the stiffness of the asphalt cement. While increasing the stiffness is a proven way to improve fatigue resistance, the LAS test has difficulty differentiating the various levels of laboratory aging. As a result, it is possible that a healing test derived from this method could be prone to the same shortcomings. The adhesive style tests that combine two pieces of asphalt cement together are also artificial attempts to produce cracks. These do not accurately represent what occurs in the pavement. Asphalt mixture testing does a better job of simulating the crack formation that occurs in pavements and likely presents a better avenue for healing characterization.

Although simulating crack growth is difficult, it may be more difficult to separate recovery and self-healing. Restoration is a relatively easy value to measure, but it can be induced by test methods. For example, internal heating and thixotropy during the initial phase of cyclic asphalt mixture fatigue tests. Minimizing the role of bias effects is crucial for an improved understanding of the healing characteristics of asphalt cement. The PoliTO method evaluates the damage using dissipated energy. The energy can be dissipated through internal heating which is a bias effect that can influence the stiffness of the asphalt cement.

As characterization techniques are still in development, it should also be noted that many different types asphalt cement modifiers have not yet been examined extensively with respect to their effect on the healing properties of pavements. SBS is one of these additives which is known to improve cracking resistance. It may be difficult to fully understand the role of SBS in healing until a proper characterization technique is developed. Other modifiers that influence chemistry or viscosity, such as warm mix additives, anti-stripping agents and rejuvenators also warrant study. It is possible that these additives provide additional benefits through healing that are currently unknown.

2.5.2 Limitations to Extrinsic Self-Healing Pavements

The ideal self-healing pavement is one that can repair damage continuously and indefinitely without external stimuli being required. This would result in the ability to repair damage at all moments when traffic loading is removed. Current research efforts in this area present techniques with potential shortcomings. Induction healing pavements require the application of magnetic fields over the pavement which renders the pavement unusable for some time. The elevated temperatures required to induce healing would leave the pavement susceptible to rutting if opened to traffic too soon. The effects on aging in the field are also not fully known at this time. Capsule based pavements would only have the capability to heal damage once by depleting the rejuvenating agent after a single use. It is also possible that the capsules can burst during mixing at the hot mix plant. This could result in softening of the asphalt cement prior to paving which could also leave it prone to rutting. These techniques may also require specific characterization methods in order to be evaluated. These methods must be produced with an understanding of the current limitations with characterizing healing properties.

Some self-healing polymers are designed to work without external stimuli and are often based on reversible bond chemistry which allows them to have multiple healing cycles. The use of a self-healing polymer to modify asphalt cement is a technique has been explored infrequently. The exploration of a self-healing elastomer to modify asphalt cement does not seem to have been attempted. The use of a self-healing elastomer is meant to help overcome the shortcomings of previous self-healing pavement technologies. The potential for improved pavement life may be similar but excess road closures can be avoided while the healing can occur multiple times potentially over the life of the pavement. The elastomeric nature of this polymer could also have the potential to reduce cracking in the pavement. The difficulty of this solution lies in finding a polymer that shows good compatibility in asphalt cement and is stable through oxidative aging used in laboratory testing.

Chapter 3: PRELIMINARY TESTING OF A SELF-HEALING ASPHALT CEMENT

The following section is adapted from two conference papers that have been accepted for publication in the “Proceedings of ISBM Lyon 2020” by Springer in RILEM Series:

- Aurilio, R. M., M. Aurilio, and H. Baaj. The Effect of a Chemical Warm Mix Additive on the Self-Healing Capability of Bitumen. *Proceedings, RILEM International Symposium on Bituminous Materials*, 2020.
- Aurilio, M. and H. Baaj. Examining the effects of a Self-Healing Elastomer on the Properties of Bitumen. *Proceedings, RILEM International Symposium on Bituminous Materials*, 2020.

3.1 Material Preparation

A self-healing elastomer was synthesized by a commercial laboratory in accordance with the supplemental information provided by Li et al [91]. The self-healing elastomer produced for this study was treated differently compared to the original research [91]. The commercial laboratory dissolved the material into ethyl acetate and purified using sodium bicarbonate and brine. The synthesis was upscaled to generate approximately 100g of self-healing elastomer. The authors selected an iron (Fe^{3+}) to ligand-PDMS molar ratio of 1:2 because this ratio had the most desirable properties for asphalt cement as reported in the original research. This ratio can be altered to change the elastomeric properties of the material in future research [91]. The product received is shown in Figure 3-1. The final product achieved a similar reddish-brown colour to the material described by the original researchers. When compared to SBS in terms of solubility with asphalt cement, PDMS and the resulting polymer should have good compatibility. The maltene fraction and SBS typically fall between 7.8 and 8.8 $(\text{cal}/\text{cm}^3)^{1/2}$ in terms of their Hildebrand solubility parameter [35] while PDMS has an expected value of 7.3 $(\text{cal}/\text{cm}^3)^{1/2}$ [105].



Figure 3- 1 Self-healing elastomer as received from the commercial laboratory

As a result of having a much larger sample to dry, the commercial laboratory was unable to produce a thin film by following the procedure outlined in the original research. As a result, the self-healing elastomer was still dissolved in solvent when it was acquired, which is observable in Figure 3-1. Several attempts were made to evaporate the solvent and the successful attempts are outlined here. Approximately 1g of self-healing elastomer was poured into a tin and left in the oven for 20-24 hours at $70 \pm 5^\circ\text{C}$. This was followed by using a vacuum degassing oven, which was operated at 170°C for 40 minutes for Method A and B. Method C did not use the vacuum degassing oven after the initial curing time. Method B was sealed during the initial curing time while Method A and C were left exposed to air. After the curing time was complete, 9g of PG 58-28 which was heated to 155°C was added to the tin and mixed by hand. The methodology for each curing process is summarized in Table 3-1.

The methods discussed here represent the most successful attempts to recreate the thin film observed in the original research. The other methods used were based on higher temperatures and shorter curing times. The results from these samples were highly inconsistent. Figure 3-2 shows the material after the curing process was completed. Figure 3-2a shows the material produced using Method B and Figure 3-2b shows the material following Method C. The solvent was removed successfully from the self-healing elastomer although the appearance response to agitation did not indicate it had fully achieved the elastomer nature cited by the original researchers. The elastomeric nature was observed in testing outlined in the remaining portion of this section. It is possible that the changes made by the commercial laboratory influenced the difficulty in creating the thin film. Samples of 1g were selected in order to more closely replicate the curing procedure outlined in the original research.

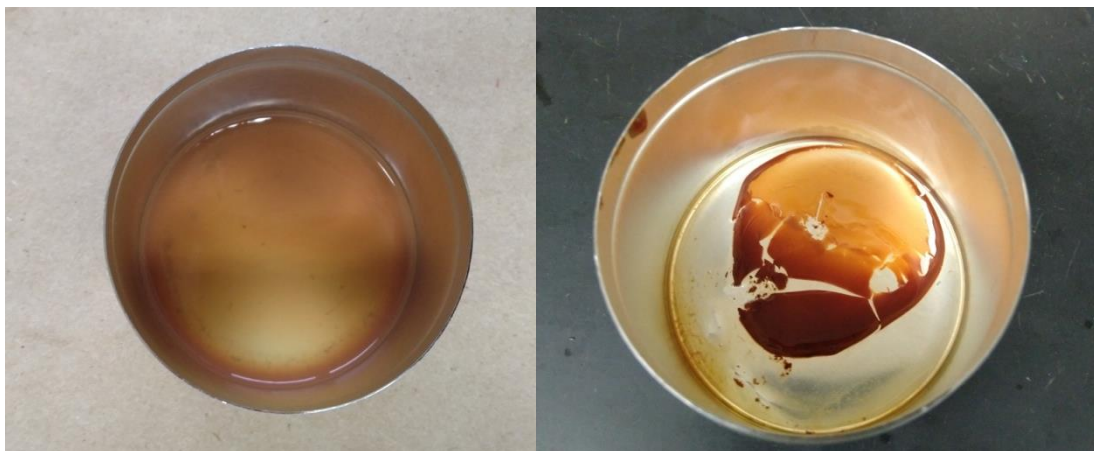


Figure 3- 2 Self-healing elastomer following a) curing Method B and b) curing Method C

Table 3- 1 Curing times and temperatures for the Self-Healing Elastomer

Sample	Concentration (wt.%)	Time (hr)	Temperature (°C)	Vacuum Degassing Oven
Method A	10	20	65	Yes
Method B	10	20	65	Yes
Method C	10	24	75	No

The SBS modified asphalt contains 2% linear SBS with 31.1% styrene content and a proprietary cross-linking agent. The process was completed using a Silverson high shear mixer and heating mantle. After preheating the asphalt cement to 170°C, polymer was added and milled for one hour. A crosslinking agent was added at the end of the hour and allowed to mill for a further 30 minutes. The crosslinking agent was added at 10 percent by weight of the polymer. After milling the crosslink and polymer, the high shear mill speed was reduced, and the sample milled for another hour. The final hour was used as a curing time. Temperatures were monitored and maintained at 180°C +/- 5°C. This method produces PMA that compares well with production trials.

3.2 Testing Methodology

Intermediate temperature properties and fatigue performance were evaluated by calculating the cycles to failure (N_f) from the LAS test and the percent healing from the SLASH test at 19°C which was modified from the LASH test protocol. LAS N_f was calculated using the spreadsheet available on the Modified Asphalt Research Center (MARC) website. In the original LASH Test, strain levels are determined using the cohesive failure damage level (S_f). The failure strain amplitude is determined by finding the maximum pseudo strain energy of the continuous LAS (cLAS) Test as shown in Figure 3-3a [78]. During the LASH Test, samples are loaded to a percentage of the failure damage level ($\%S_f$). Upon loading to $\%S_f$, the sample is unloaded for single rest period. The rest period is followed by a second loading phase resuming at the strain value at the end of the first loading phase. The percent healing ($\%H_s$) is calculated as follows,

$$\%H_s = \frac{S_1 - S_2}{S_1} \quad (1)$$

Where S_1 is the damage parameter at the end of the first loading phase, and S_2 is the damage parameter corresponding to the beginning of the second loading phase [78/]. In the SLASH test developed by the

University of Waterloo, the sample experiences a linear sweep to a pre-selected strain amplitude and the degree of self-healing is determined as seen in Figure 3-3b without calibrating S_f from a cLAS test. Samples were loaded to 10% strain level and a 15-minute rest period was used before the second loading phase which continued to a strain level of 30%. Calculation of $\%S_f$ for the SLASH data suggests that the stopping the test at 10% strain corresponds to an $\%S_f$ value in the 76-80% range for the PG 58-28. 75 $\%S_f$ was one of the chosen values in the original LASH testing [78]. This would indicate that 10% strain a suitable place to begin the rest period. The cLAS number of cycles to failure (N_f) was calculated using 50% damage level and this was selected based on previous research which has not yet been published. The use of percent restoration will replace the term percent healing which can still be calculated using Equation 1 without any modification [106]. It is likely that this method quantifies restoration which includes the self-healing ability and the recovery of reversible phenomena rather than the chemo-mechanical changes of the asphalt cement.

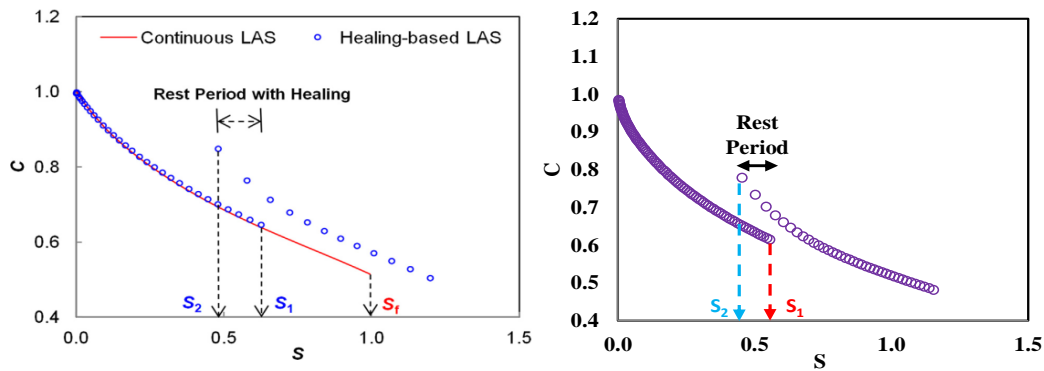


Figure 3- 3 Pseudo-stiffness (C) vs damage parameter (S) for (a) the original LASH Test incorporating the cohesive failure damage level, S_f , from [78] and (b) the Simplified-LASH Test [106]

High temperature properties (46 to 64°C) were evaluated using temperature-frequency sweeps and the data was shifted using the Time-Temperature Superposition Principal (TTSP) and the Williams-Landel-Ferry equation. This data was used to generate master curves and black space diagrams. Fourier Transmission Spectroscopy (FTIR) was performed in Attenuated Total Reflectance mode (ATR) to analyze the materials before and after mixing. ATR was selected a RILEM round robin study noted it was the most commonly used technique of the participating laboratories [107]. This was completed to verify the persistence of the self-healing elastomer structure following mixing.

3.3 Results and Discussion

The SHAC properties have shown some promise with regards to improving the self-healing properties of asphalt cement. Method A and C both show a marginal increase in the restoration when compared to the unmodified asphalt cement. It is possible that although the restoration is similar, the self-healing capacity

of the SHAC is improved. The SBS modified asphalt cement also shows an increase in percent restoration. Some previous research notes that noted SBS reduced the self-healing ability of asphalt [108], while other researchers have found the opposite [79]. This could be explained by differences in the chemical composition of the base asphalt cement that were studied or the addition of a cross-linking agent which was used here. The LAS N_f indicate that the SHAC in Method B and C improved the fatigue performance when compared to the unmodified asphalt cement. This increase was not as large as the increase observed with the addition of SBS. Slight improvements in the cycles to failure and restoration may indicate that the self-healing elastomer is having a positive impact on the properties of the asphalt cement. These results can be seen in Table 3-2.

When examining the master curves in Figure 3-4a, the SHAC samples perform similarly to the unmodified asphalt whereas with the SBS modified sample there is a clear increase in complex modulus. The SHAC tends to have lower complex modulus values when compared to the unmodified asphalt cement. Some of the SHAC samples exhibit an inflection point where the complex modulus increases relative to the unmodified asphalt cement at higher frequencies. The black space diagrams, Figure 3-4b, reveal a more interesting behaviour. The phase angle tends to be much lower for the SHAC when compared to the unmodified asphalt cement. The SBS modified asphalt cement and SHACs appear to have an inflection point at higher modulus values. The black space diagram of the SHACs compare well to the SBS modified asphalt cement indicating that SHACs have a more elastomeric behaviour.

Table 3- 2 LAS number of cycles to failure and percent restoration for unmodified, SHACs and SBS modified asphalt cement

Sample	LAS $N_{f 50\%}$	% R_s
Unmodified	4166	20.4%
Method A	3613	20.9%
Method B	4789	19.5%
Method C	4792	20.8%
SBS Modified	6073	23.3%

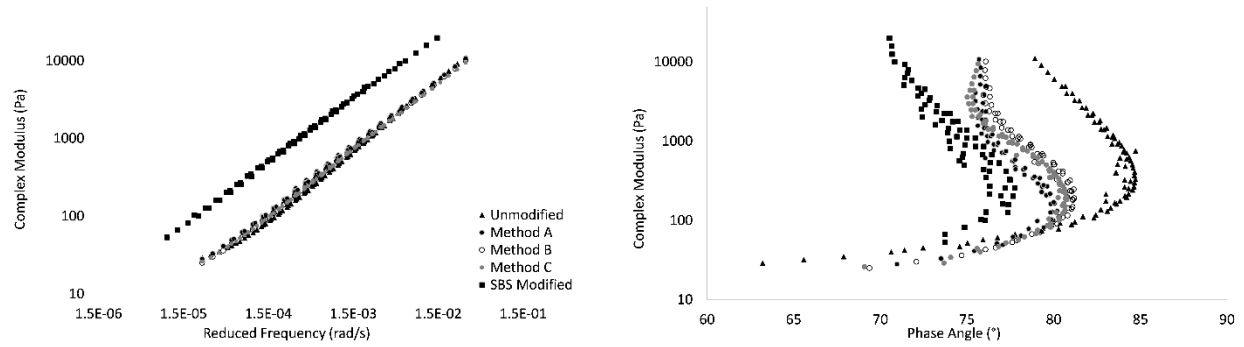


Figure 3- 4 Temperature-frequency sweep master curves (left) and temperature-frequency sweep black space diagrams (right)

The data thus far indicates that the self-healing elastomer is modifying the properties of the asphalt cement in a desirable way. With conflicting information about the ability of SBS modification to improve self-healing properties of asphalt, it is a positive to see that the SHACs at least maintain the restoration properties of the asphalt cement. It is possible that the LAS based self-healing tests do not properly capture the self-healing performance of SHACs and asphalt mixture performance testing is planned for further evaluation of the material. Although it does not increase the complex modulus in a similar fashion to SBS, the SHACs show a considerably decrease in the measured phase angle indicating a shift towards a more elastomeric behaviour. This behavior is similar to the increase in the elastomeric nature of asphalt cement with the addition of SBS [6]. Likewise, the properties of the SHAC compare favorably to the SBS modified asphalt cement. Upscaling the curing procedure and further characterization of the SHAC is planned for future work.

Figure 3-5 and 3-6 present the infrared reflectance spectra for the self-healing elastomer, unmodified asphalt cement and the SHAC samples. When examining the spectra of the self-healing elastomer, peaks were observed at 1012 and 1078 cm^{-1} which correspond well to the Si-O-Si bonds in the PDMS chains. The peaks at 1257 and 1413 cm^{-1} correspond to the deformations of the C-H bonds in the $\text{Si}(\text{CH}_3)_2$ groups while the peaks at 786 cm^{-1} are due to the presence of Si-C bond stretching [109]. These peaks are also visible in the SHAC spectra with varying degrees of intensity. The differences in intensity are likely due to the non-homogenous nature of the SHAC samples. It is interesting to note that the addition of the self-healing elastomer causes a noticeable increase in the peak at 3270 cm^{-1} which may be due to N-H bond stretching. This peak is not significant in either the unmodified asphalt cement or self-healing elastomer spectra and may be due to interactions between the materials. The similarity in SHAC spectra likely indicates the use of the high temperature of the vacuum degassing oven did not have a detrimental effect on the self-healing elastomer.

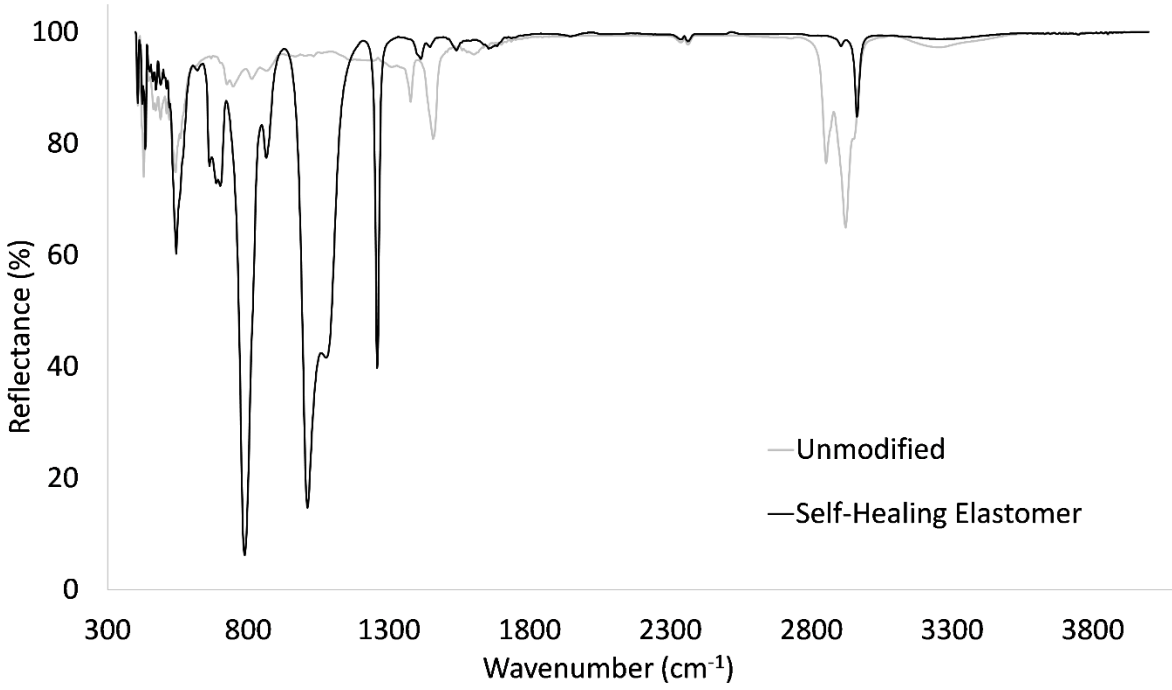


Figure 3- 5 Fourier Transmission Infrared Spectroscopy (ATR-FTIR) reflectance spectra for the self-healing elastomer and unmodified asphalt cement

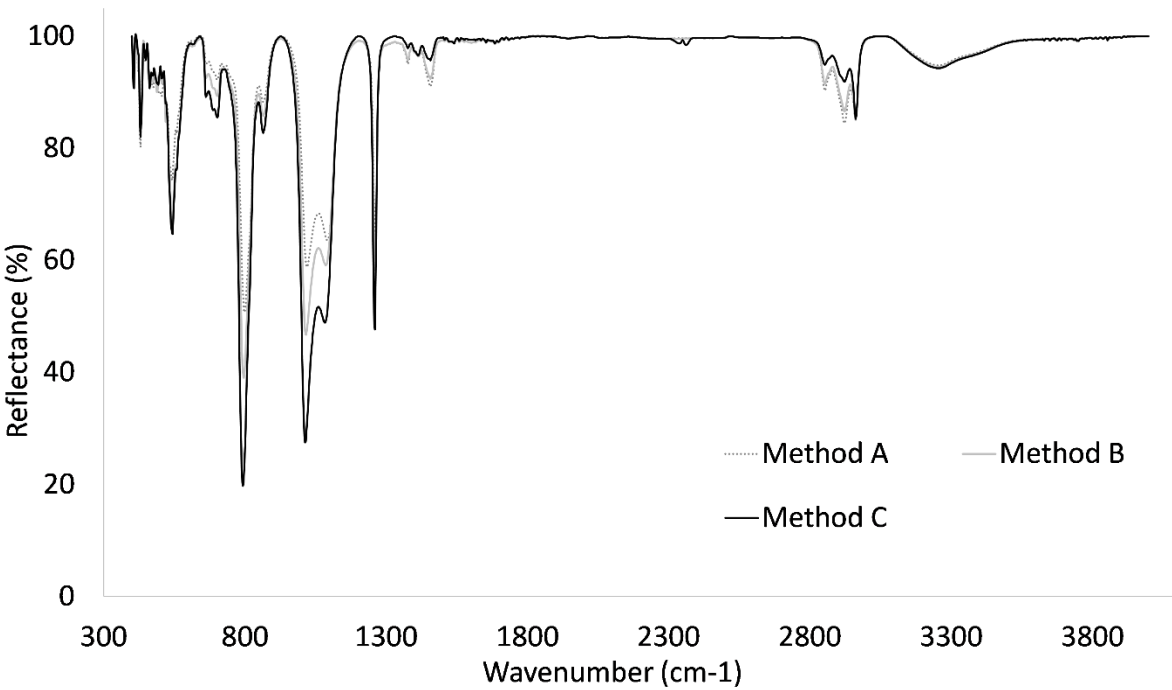


Figure 3- 6 Fourier Transmission Infrared Spectroscopy (ATR-FTIR) reflectance spectra for Method A, Method B and Method C

Although the increase in restoration is slight in two of the samples, the change in elastomeric properties indicate that the self-healing elastomer may be having a positive effect on the properties of the asphalt cement. It is difficult to understand what role the self-healing elastomer has in the restoration of properties and how much it is contributing to self-healing. Although restoration in properties is similar, it is possible the self-healing behaviour is different when compared to the unmodified asphalt cement. The LAS N_f also increased showing a potential improvement in fatigue performance. The improvement in these properties is similar to the improvement seen in SBS modified asphalt cement. Based on some previous research, it was expected that SBS might have a negative impact on self-healing properties but that was not observed here. On this basis, it was decided to further explore the role of SBS in the restoration properties of asphalt cement by testing the same asphalt cement at a second concentration (4%).

The interesting behavior of the SHAC has warranted further study and based on these preliminary results, two further samples were produced with the remaining self-healing elastomer using Method C. Subsequent material preparation made use of a mechanical mixer in order to improve the homogeneity of the sample. The two samples were produced were; one of approximately 100g in weight and a second approximately 400g in weight using a concentration of 9% self-healing elastomer by weight of the asphalt cement. The second sample is intended for use in mixture testing, but due to time restrictions it was not possible to include them in this thesis. The 100g sample was used to continue testing on the percent restoration as well as understanding the evolution of predicted fatigue life by adding rest periods to the LAS test. These methods will be outlined in the following section. Standard MGAC testing was also conducted in order to view the material from a traditional asphalt cement perspective. The samples blended here had a more gel-like consistency following the curing method as shown in Figure 3-7 as opposed to the slightly more brittle appearance shown earlier in Figure 3-2. It is possible that less solvent was removed from the larger samples but also possible that the gel is more likely to exhibit the viscoelastic properties that are expected.



Figure 3- 7 Self-healing elastomer following the second and third attempts using curing Method C

3.4 Chapter Summary

The key findings in Chapter 3 are as follows:

- SLASH testing indicated that the restoration of the self-healing asphalt cement was similar or slightly improved compared to the unmodified asphalt cement. This warrants further study.
- SBS showed a larger increase than expected in percent restoration. This also warrants further study.
- The addition of self-healing elastomer did not have a significant impact on the complex modulus of the asphalt cement. A shift in phase angle was observed indicating a more elastomeric response.
- FTIR results confirmed the presence of the self-healing elastomer in the asphalt cement. A notable peak was observed at 3270 cm^{-1} which was not significant in either the unmodified asphalt cement or self-healing elastomer spectra.

Chapter 4: ENHANCED HEALING CHARACTERIZATION OF SBS MODIFIED AND SELF-HEALING ASPHALT CEMENT

4.1 Performance Grade Asphalt Cement Testing

When examining the effect of the self-healing elastomer on the physical properties of the asphalt cement, it was observed that the unaged asphalt cement saw a marginal increase in the complex modulus and the critical temperature. This is similar to the observations made during preliminary testing where the master curves showed that their modulus did not change significantly when the self-healing elastomer was added. There is also a decrease in the phase angle when adding the self-healing elastomer, which was also observed in the preliminary testing. This decrease in the phase angle is likely responsible for the increase in the critical temperature. A decrease in the phase angle also suggests a move to a more elastic material, which is similar to change in properties observed with the addition of SBS [2]. These results are summarized in Table 1. The results become more interesting when laboratory aging methods are applied. The self-healing asphalt cement shows a larger increase in the complex modulus and critical temperature when RTFO aged but the change in phase angle is similar between the two asphalts. The bigger change in stiffness may indicate that the self-healing asphalt cement is more prone to oxidation than the unmodified 58-28. This may be due to the PDMS chains that make up the self-healing elastomer or the reactivity of the crosslinking components. When compared to SBS, the self-healing asphalt cement does not increase the complex modulus to the same degree. SBS is known to increase the complex modulus and decrease the phase angle of asphalt cement [2].

The Multiple Stress Creep Recovery (MSCR) test also reveals that the stiffness of the RTFO aged self-healing asphalt cement was higher than the unmodified 58-28. The MSCR has been shown to be a much better evaluator of rutting performance in asphalt cement [23]. This difference is noticeable despite having the similar stiffness when the materials are unaged. The percent recovery gives an indication of the elastomeric response of the material and the increase is a positive for the self-healing asphalt cement. This increase would be similar to the addition of 1-1.5% SBS, depending on the stiffness of the base asphalt [25]. The large increase in relative stiffness after RTFO aging would suggest that the self-healing elastomer is not increasing the stiffness, but this change is result of oxidation.

Table 4- 1 High temperature test properties measured for the 58-28 and self-healing asphalt cement

Test Property	Test Temperature	Specimens	
		Unmodified 58-28	Self-Healing Asphalt Cement
Unaged Asphalt Cement			
Complex Modulus ($G^* / \sin \delta$)	58°C	1.86	1.84
Phase Angle (°)	58°C	83.3	78.0
Critical Temperature (°C)		63.0	63.5
RTFO Aged Asphalt Cement			
Complex Modulus ($G^* / \sin \delta$)	58°C	4.18	6.38
Phase Angle (°)	58°C	79.8	73.6
Critical Temperature (°C)		63.2	67.1
Multiple Stress Creep Recovery			
J_{nr}	58°C	2.12	1.26
Percent Recovery (%)	58°C	3.7	15.6

The low temperature properties measured using the BBR are also quite interesting. The addition of the self-healing elastomer causes a decrease in the creep stiffness, but also a dramatic change in the m-Value. The m-Value is a measure of the relaxation rate of the asphalt cement [6], and the decrease means that the self-healing asphalt cement is likely to have a more brittle response to loading despite the decrease in creep stiffness. For reference, the relationship between the m-Value and addition of SBS has been shown to be asphalt cement dependent while the creep stiffness tends to decrease [2]. The BBR data can also be used to calculate the cracking parameter ΔT_c . This is calculated using the difference between the critical temperatures with the m-Value critical temperature being subtracted from the critical temperature of the creep stiffness. A limit of -5°C has become common for both 20 Hour and 40 Hour PAV aging methods [19]. There is a dramatic decrease in the ΔT_c when the self-healing elastomer is added. This was not expected because PDMS has a very low glass transition temperature ($T_g = -125^\circ\text{C}$) and the claims from the original developers of the self-healing elastomer that the material had healing properties as low as -20°C [91]. This may be explained by the aging process which seems to affect the self-healing asphalt cement to a greater degree. It should be noted that the ΔT_c parameter is designed for non-load associated cracking, but due to the relationship between response to loading and temperature attempts have been made to evaluate fatigue cracking performance as well. Researchers have also recently learned that the parameter does not characterize the cracking performance of elastomeric modifiers well [19].

Table 4- 2 Bending Beam Rheometer test properties measured for the 58-28 and the self-healing asphalt cement

Test Property	Test Temperature	Specimens	
		Unmodified 58-28	Self-Healing Asphalt Cement
m-Value	-12°C	-	0.306
Creep Stiffness (MPa)	-12°C	-	73.5
m-Value	-18°C	0.358	0.232
Creep Stiffness (MPa)	-18°C	187	140
m-Value	-24°C	0.281	-
Creep Stiffness (MPa)	-24°C	431	-
Critical Temperature, T_m , (°C)	-	-32.5	-22.5
Critical Temperature, T_s , (°C)	-	-31.4	-35.1
ΔT_c , $T_s - T_m$, (°C)	-	1.1	-12.6

4.2 Master Curves and Black Space Diagrams

Temperature-Frequency sweeps were performed on the DSR. The unaged specimens were tested in a temperature range of 20 to 70°C, while the PAV aged specimens were tested in the -18 to 70°C. Frequencies used ranged from 0.1 to 15 Hz. RTFO aged asphalt was not tested due to limited quantities available for the self-healing asphalt cement. The raw data was shifted using the Williams-Landel-Ferry equation and fitted into the 2S2P1D model which is used to predict viscoelastic properties at different temperatures and loading frequencies. This model is based on the combination of two springs, two parabolic elements and one dashpot in series. To generate a single curve, the complex modulus is shifted to the reduced frequency using the temperature. The 2S2P1D model is then fitted to the data to produce a master curve. The 2S2P1D model can be defined by Eq. (1):

$$G^*(\omega) = G_0 + \frac{G_g - G_0}{1 + \alpha(i\omega\tau)^{-k} + (i\omega\tau)^{-h} + (i\omega\beta\tau)^{-1}} \quad (1)$$

where G_g is the glassy modulus as the reduced frequency, ω , reaches infinity and is approximated to be 1×10^9 Pa. G_0 is assumed to be zero for asphalt binders, the exponents k and h are defined by $0 < k < h < 1$, α is a constant, β is related to the Newtonian viscosity and τ is the characteristic time [21]. BBR data was used in the curves by taking the creep stiffness measurement at different times. The time is converted into

a frequency and the creep stiffness is converted into the modulus using Eq. (2) [21] as discussed in the literature review:

$$G^*(\omega) \approx \frac{S(t)}{3} \quad (2)$$

Where ω is the reduced frequency and $S(t)$ is the creep stiffness measured by the BBR.

The master curves in Figure 4-1 seem to confirm the issues with aging that were discussed previously. Both asphalt cements have a “flatter” shape (lower complex modulus at high frequencies and higher complex modulus as low frequencies) when PAV aged indicating that the oxidation process reduces the ability to relax stresses as expected. However, this difference is greater for the self-healing asphalt cement indicating that it may be more susceptible to oxidative aging. Although it has been observed that an elastomer, like SBS, can also cause the master curve to flatten, it is more likely here that the change in shape is related to a reduction in the relaxation properties associated with oxidative aging. Further evidence of this is presented in the black space diagrams in Figure 4-2. The unaged self-healing asphalt cement exhibits a plateau region in a similar fashion to SBS modified asphalt, but this plateau no longer exists when the material is PAV aged. This plateau is typically indicative of elastomeric behaviour and good compatibility between the polymer and asphalt. SBS modified asphalt cement does exhibit this plateau when PAV aged [2]. It is clear that the aging process has a larger impact on the self-healing asphalt cement than the unmodified 58-28. This will also be reflected in the testing discussed in the following sections.

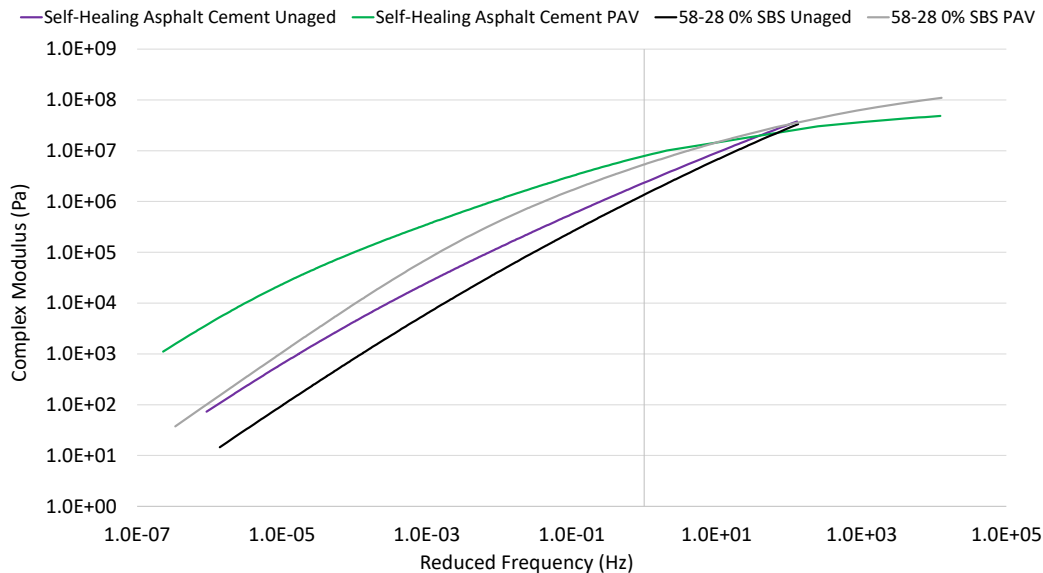


Figure 4- 1 Master curves modeled using 2S2P1D for the unaged and PAV aged 58-28 and self-healing asphalt cement

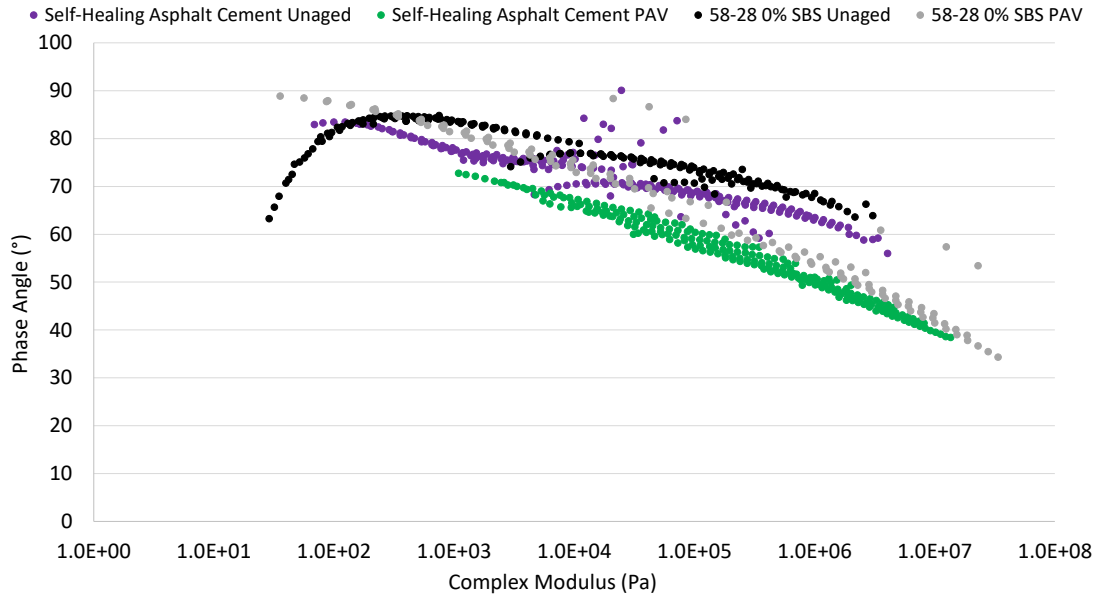


Figure 4- 2 Black space diagrams for the unaged and PAV aged 58-28 and self-healing asphalt cement

4.3 DSR Based Cracking Resistance

Cracking resistance can be measured using the LAS and analyzed using either the VECD or the fracture mechanics approaches outlined in the literature review. The number of cycles to failure predicted by the VECD method are a good indicator of cracking resistance and have been shown to have a good indication of fatigue cracking resistance [110]. It can be seen from Figure 4-3 that the increase in SBS concentration does correspond with an increase in the number of cycles to failure as expected. This can be seen with the unaged, RTFO and PAV aged materials. The addition of the self-healing elastomer to the asphalt cement improves the cracking resistance when unaged but there is a significant decrease in the number of cycles to failure for RTFO and PAV aged material. This is likely due to the increased susceptibility to oxidative aging that the self-healing elastomer appears to impart on the asphalt cement. The decrease in cracking resistance when the self-healing asphalt cement is aged corresponds well with PG testing and master curve analysis discussed in the previous sections.

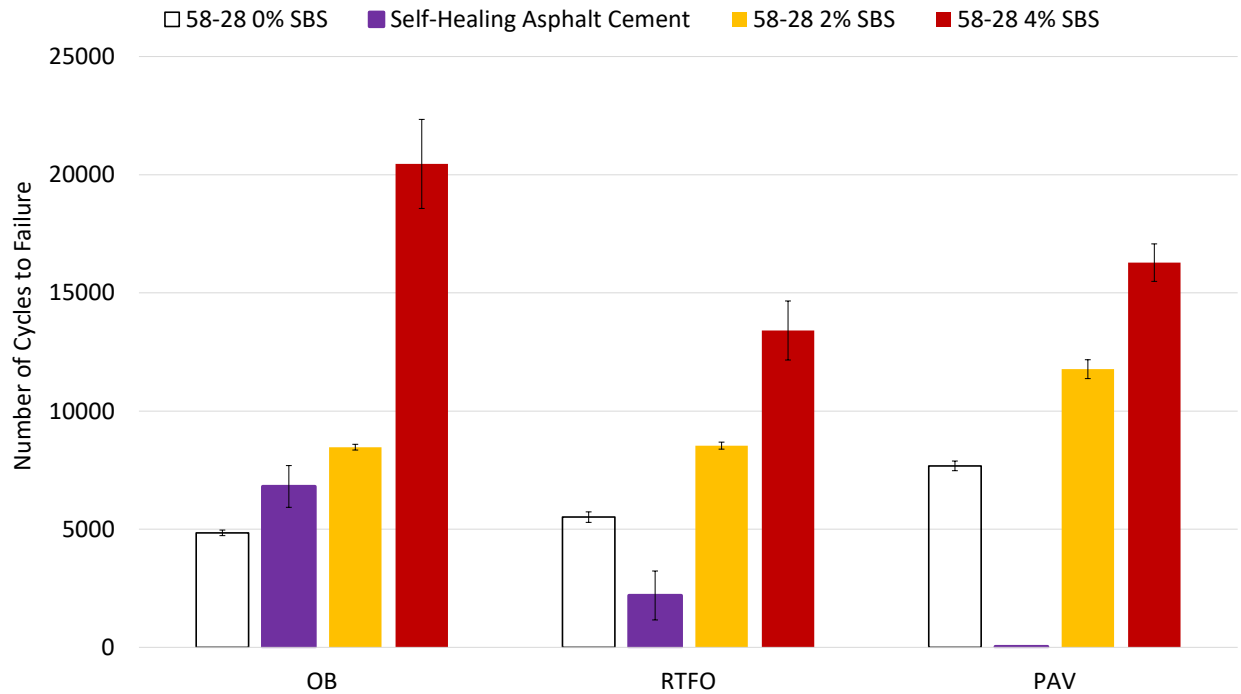


Figure 4- 3 Linear Amplitude Sweep data analyzed using the VECD model

As noted by Zhou et al. [65], the VECD model does not correlate well with the expected performance of laboratory aging. This can be seen here when examining Figure 4-3, and thus the FREI analysis has been included for the same data. The FREI data shows a smaller difference between the asphalt cements with 0% SBS, 2% SBS and the self-healing elastomer. The difference increases as the level of aging increase which can be seen in Figure 4-4. The FREI also seems able to differentiate the laboratory aging more clearly than the VECD with the cracking resistance decreasing as the level of aging increases. It should be noted that the self-healing asphalt cement still performs poorly when this type of analysis is performed. The LAS test method exhibits good repeatability as observed in the error bars presented in the figures. The unmodified and SBS modified asphalt cements tend to have better variability than the self-healing asphalt cement. The exception to this is the 58-28 with 4% SBS when it is unaged. Testing was conducted in duplicate or triplicate except when an error bar is absent. Overall, it appears as though the self-healing elastomer is detrimental to the cracking resistance of the asphalt cement and it would be expected to be detrimental to the mixture performance. This assertion requires verification with mixture testing.

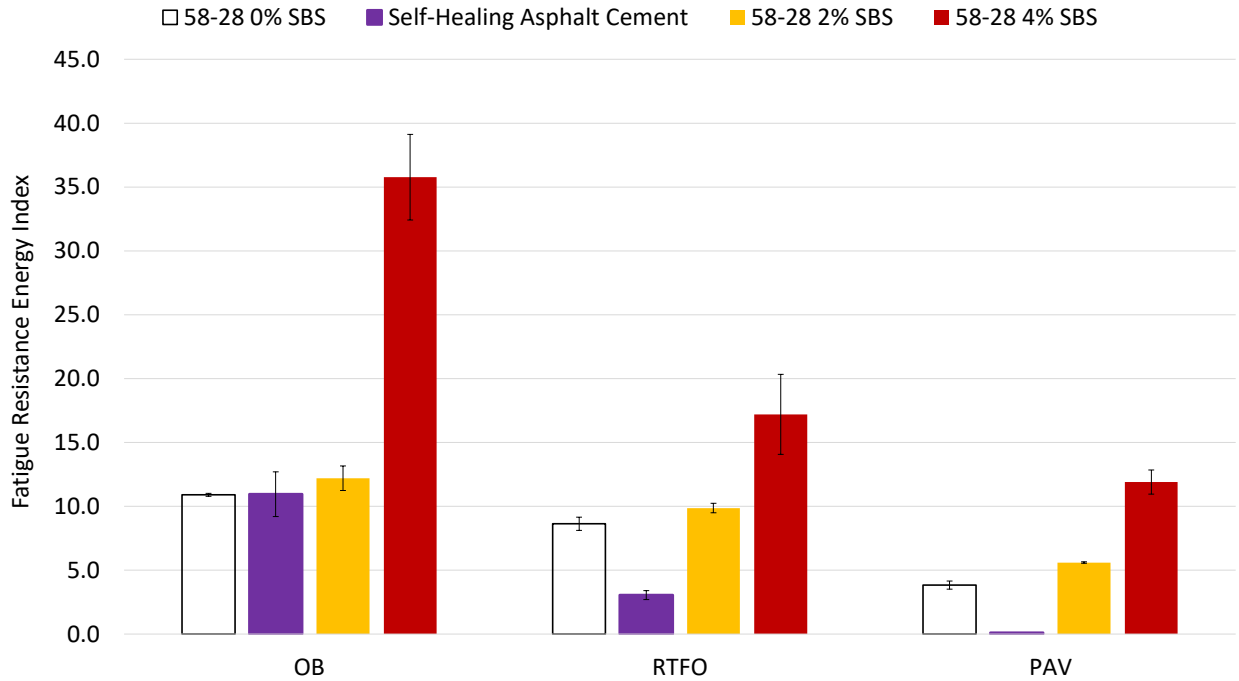


Figure 4- 4 Linear Amplitude Sweep data analyzed using fracture mechanics approach

4.4 Healing and Restoration Properties- SLASH Percent Restoration

The restoration properties determined using the SLASH test of the different unaged asphalt cements can be seen in Figure 4-5. The most notable trend is the dramatic drop off in percent restoration for the self-healing asphalt cement at 16°C. As the temperature decreases, the stiffness increases, and the molecular mobility also decreases. The negative values of percent restoration indicate that the amount of damage is increasing during the rest period despite no loading being applied. This may be because the damage is far beyond what is recoverable by the specimen. When the loading begins again, the sample’s modulus is lower. These values are not observed for the traditionally modified asphalt cements. The self-healing asphalt cement has slightly lower percent restorations than the unmodified asphalt cement at 25°C and 19°C. At 25°C the percent restoration of the self-healing asphalt cement is similar to the 58-28 with 2% SBS.

The percent restoration of the virgin asphalt cement tends to decrease between 25°C and 16°C before there is a slight increase at 13°C. This may be because as the asphalt cement becomes stiffer, it is more resistant to deformation here making recovery easier. This is also similar to the issues seen with the LAS-VECD analysis where the laboratory aged material, which is stiffer, may have a higher predicted cracking resistance. Since the SLASH is based on the LAS-VECD analysis, it is possible they have similar shortcomings. The percent restoration of the 58-28 with 2% SBS does not show an observable relationship with temperature. This may also be due shortcomings of the LAS-VECD analysis. It was expected based

on the literature review performed that the decrease in temperature would lead to a decrease in the healing efficiency of the asphalt cement. This is generally observed with the exceptions noted above. The 58-28 with 4% SBS was not tested at 13°C because it suffered from adhesion issues with the DSR plates.

The SBS modified asphalts also tend to have higher percent restorations than the unmodified and self-healing asphalt cement. This may again be due to the increase in stiffness decreasing the deformation or it may be due to the elastomeric properties provided by the SBS. Some of the deformation may be recovered elastically as the load is removed. The percent restoration values here are also higher than the results shown in Chapter 3 despite being poured from the same sample tin. This occurred for both the 58-28 0% SBS and with 2% SBS. The original testing was conducted several months prior to the testing displayed in Figure 4-5. It is possible that reheating the material allowed for rearrangement of the molecules within the samples leading to a positive effect on the percent restoration. Three replicates of the 58-28 and two replicates of the 58-28 2% SBS were included below and showed very good repeatability due to the more similar thermal history of the specimens tested. Two replicates of each sample were originally tested during the preliminary work and showed excellent reproducibility with each other.

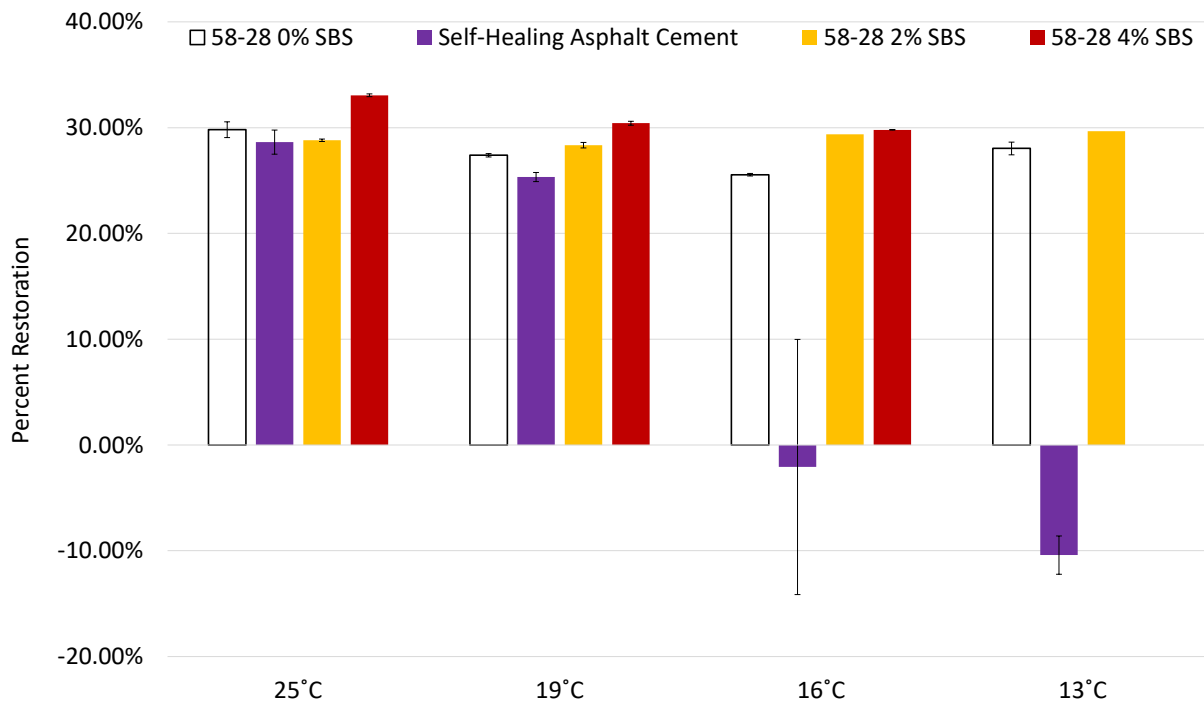


Figure 4- 5 Percent Restoration determined by the SLASH test at different test temperatures

Two separate research groups cited in the literature review noted that the increase in oxidative aging improved the healing efficiency of SBS modified asphalt cement relative to unmodified specimens due to the decrease in SBS chain length which occurs through oxidation. These shorter chains are then able to

interact more favorably with the virgin asphalt cement. Figure 4-6 shows that percent restoration for different levels of laboratory aging tested at 19°C. Since the SBS modified asphalt cements already have higher percent restoration when unaged in some cases, the trend discussed above is observed for RTFO aging but not PAV aging. The aging induced by the PAV results in larger asphalt cement molecules which decreases the molecular mobility. The 58-28 with 4% SBS has a lower percent restoration with PAV aging than the virgin and 58-28 with 2% SBS. This contrasts with the trend seen with unaged testing where the 58-28 with 4% SBS generally had better percent restorations. This may also contradict the assertions made by the previous researchers. The 58-28 with 2% SBS also has a very similar percent restoration to the unmodified asphalt cement when PAV aged. This may suggest that there is an optimum concentration for SBS with respect to healing efficiency but the 58-28 with 4% SBS still has superior cracking resistance and the decrease in percent restoration may not be significant. Interestingly, the percent restoration tends to increase for the unmodified and SBS modified asphalt cements as the level of aging increases. This may be due to the increase in stiffness as discussed previously.

The self-healing asphalt cement displays a negative percent restoration when aged. This supports the claims that the self-healing elastomer is greatly accelerating the aging process in the asphalt cement. Where the increase in stiffness does not impact the SBS modified asphalt cements negatively, it does so with the self-healing elastomer. The self-healing asphalt cement becomes very brittle and susceptible to damage. It is expected that the increase in aging should be detrimental to the healing efficiency of asphalt, but this is only observed with the self-healing asphalt cement. This may be related to the issues with predicting differences in laboratory aging discussed earlier for the VECD model.

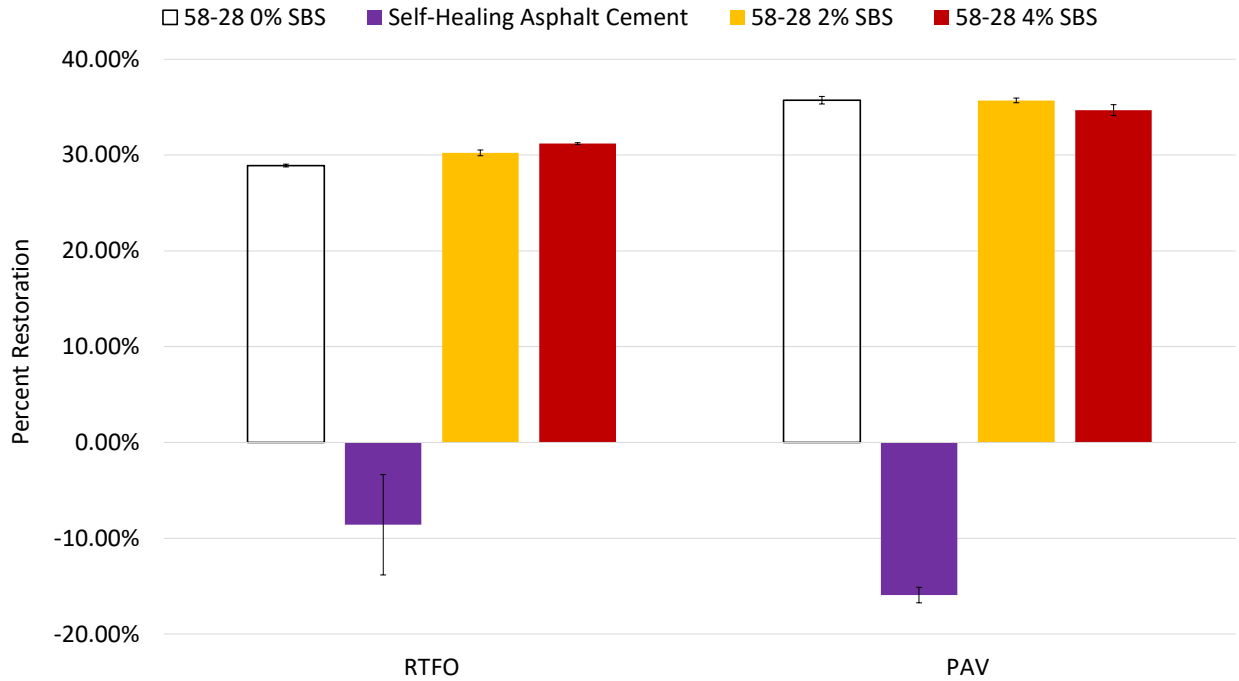


Figure 4- 6 Percent Restoration determined by the SLASH test at different levels of laboratory aging

In order to evaluate if the damage induced by 10% strain was excessive for the self-healing asphalt cement, the test was also conducted using 5% strain as the cut off point before the rest period at 19°C (Figure 4-7) and 13°C (Figure 4-8). Based on the literature review, it is expected that decreasing the amount of damage induced will have a positive impact on the healing efficiency of asphalt cement and this should be reflected in the percent restoration. In Figure 4-7, it can be observed that this trend did not hold true for the 58-28 but did hold true for the self-healing asphalt cement at 19°C. This is also observed in Figure 4-8 although to a lesser degree for the 58-28 where the difference may be negligible at 13°C. There is a significant improvement for the self-healing asphalt cement which saw a negative percent restoration when 10% strain was applied before the rest period. It is unknown why the 58-28 trends in the opposite direction as to what would be expected. This was also attempted for the PAV aged self-healing asphalt cement, but a negative percent restoration was still found. There RTFO aged material was not tested due to a limited quantity remaining being preserved for other testing.

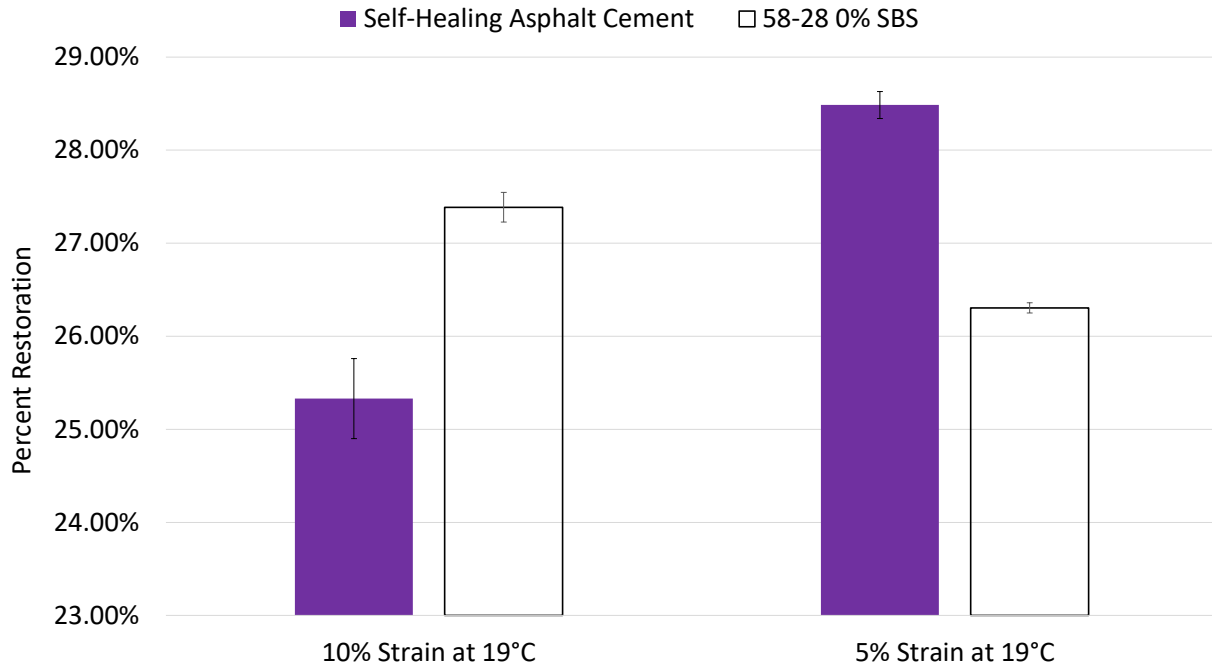


Figure 4- 7 Percent restoration determined by the SLASH with different strain levels applied before the rest period at 19°C

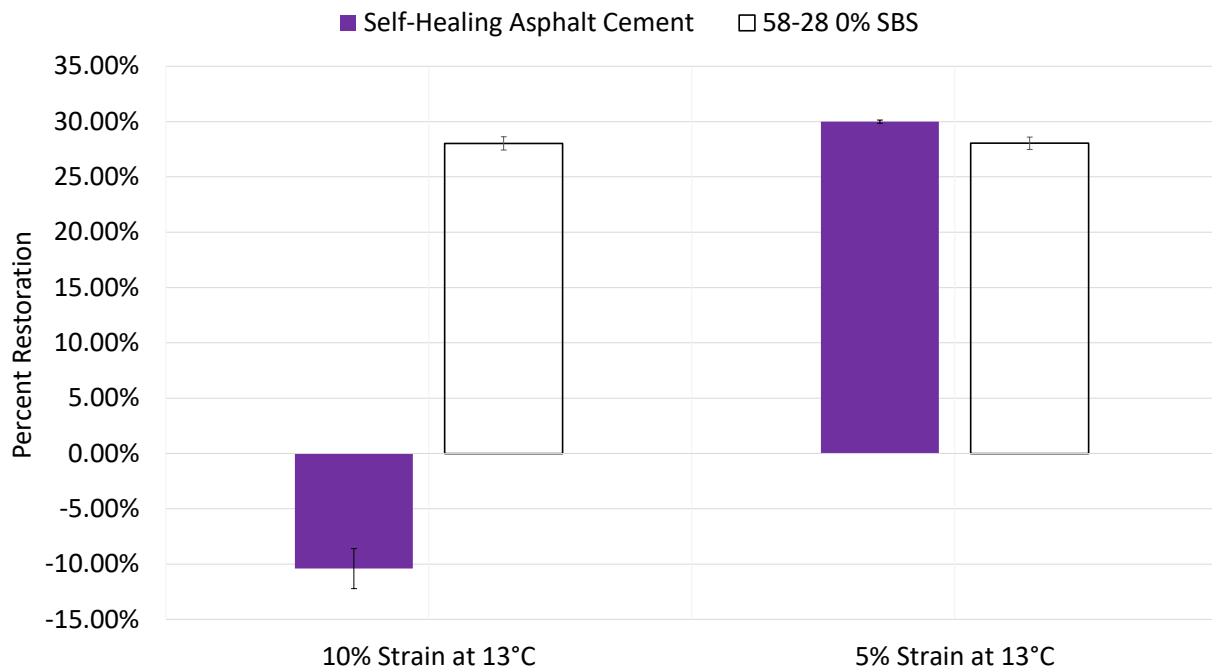


Figure 4- 8 Percent restoration determined by the SLASH with different strain levels applied before the rest period at 13°C

4.5 Healing and Restoration Properties- Healing Ratios

Many tests evaluating the healing process compare the fatigue life of the asphalt cement or mixture with and without a rest period. With way the data is analyzed, it is also possible to do this using the LAS in order to calculate the healing ratio. This is done by using the following equation:

$$HR = \frac{F_{Rest\ Period} - F_{Initial}}{F_{Initial}} \quad (3)$$

where HR denotes Healing Ratio and F represents the fatigue life or cracking resistance as determined by the different types of analysis. The Healing Ratio represents a percentage change in the fatigue life of the asphalt cement. Since the LAS fatigue resistance can be determined in terms of number of cycles to failure and the fatigue resistance energy index, either of these values can be substituted into the equation. It should be noted that these models were not necessarily developed to quantify the healing process and as a result may not be suited to this task, nevertheless it presents an opportunity to further probe the data collected.

The number of cycles to failure as determined by the LAS-VECD including the rest period can be seen in Figure 4-9. There is an increase in the cracking resistance that can be seen when comparing the values to Figure 4-3 for the 58-28 and the SBS modified asphalt cements. The self-healing asphalt cement did not see an increase in the cracking resistance when a rest period was added for the RTFO and PAV aged materials. This may be due to the issues discussed earlier with excessive damage not being repairable when the material becomes stiffer through oxidation. It was expected that including a rest period would improve the fatigue performance and this is seen through the increase in cycles to failure calculated using the VECD model. The data here still shows that increasing the concentration of SBS will have a positive impact on the fatigue life or cracking resistance of an asphalt mixture.

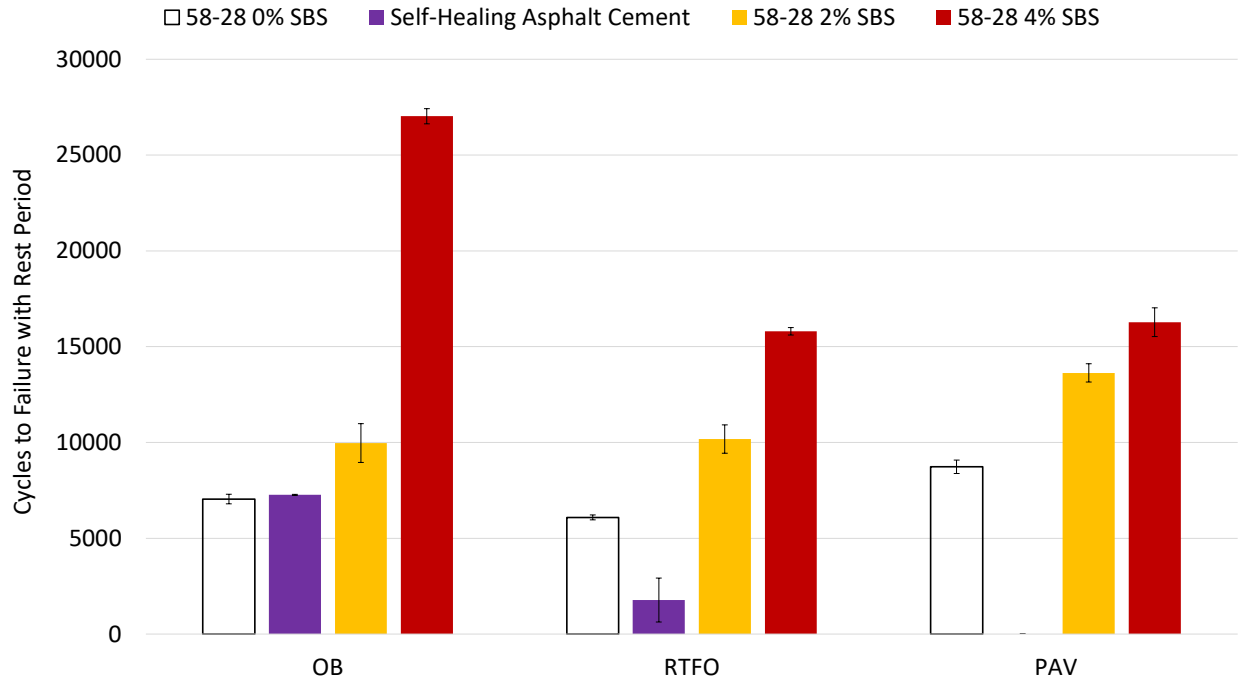


Figure 4- 9 Linear Amplitude Sweep data analyzed using the VECD model including the rest period

The VECD healing ratio for each material and level of laboratory aging can be seen in Figure 4-10. The most obvious trend in the data is the decrease observed in the VECD healing ratio as the level of aging increases. Generally, PAV aged material has the lowest VECD healing ratio for each asphalt cement tested. The self-healing asphalt displays the most negative decline in VECD healing ratio as expected based on the discussion above. According to the VECD, the self-healing asphalt cement would have a dramatic decrease in the healing ratio as the aging increases. The data also indicates that the unmodified 58-28 also has the best VECD healing ratio for unaged material, but the ranking changes for RTFO and PAV aged material. The VECD healing ratio for the 58-28 is relatively similar for the RTFO and PAV aged material, although it is expected that oxidation reduces the healing efficiency of asphalt cement. The VECD healing ratio of the 58-28 with 2% SBS remains the most consistent which may indicate that relative low concentrations of SBS do interact favorably with the virgin asphalt cement when oxidation occurs. The 58-28 with 4% SBS has a higher VECD healing ratio initially than the 58-28 with 2% SBS when unaged, but it decreases in a more linear fashion as the aging increases. This may indicate there is an optimal concentration of SBS for healing for this specific asphalt cement. It may also be possible that the effect of SBS on the healing abilities of asphalt is controlled by the specific chemical composition of each asphalt cement in practice.

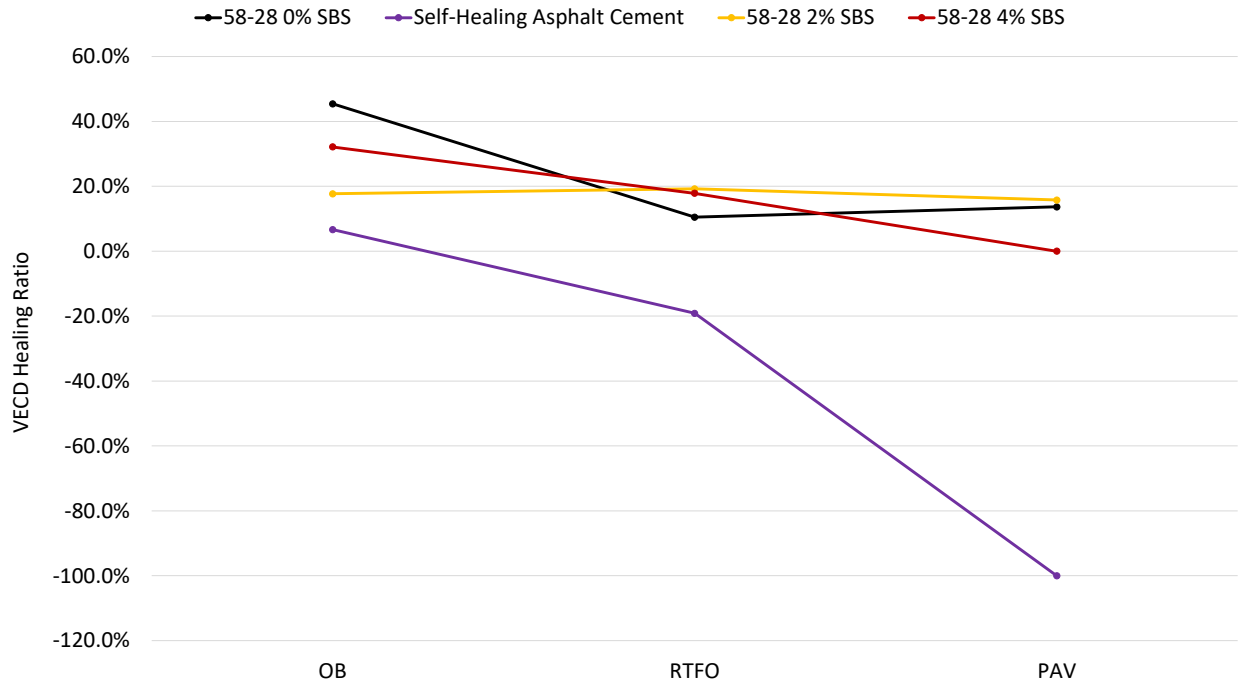


Figure 4- 10 Healing ratios calculated using the VECD number of cycles to failure

The FREI with the inclusion of a rest period is presented in Figure 4-11. When comparing to Figure 4-4, an increase in the cracking and fatigue resistance can be seen, which is again to be expected. The self-healing asphalt cement continues the trend of performing the most poorly of the asphalt cements tested. Interestingly, there is less separation between the asphalt cements as the level of aging increases. This contrasts with the calculated FREI values that did not include a rest period. The unmodified 58-28 even appears to have a slightly better performance than both polymer modified asphalt cements when the rest periods are applied. This also contrasts the relationship seen above in the VECD analysis and the expectation that SBS modified asphalt would continue to have the best fatigue cracking resistance when a rest period is applied. The FREI healing ratio can be seen in Figure 4-12 (Figure 4-12a is presented with what appears to be an outlier removed to enhance clarity). In contrast with the VECD healing ratios presented in Figure 4-4, the FREI healing ratio increases as the level of aging increases. This does not correspond well with expectations that healing efficiency of asphalt decreases as the material becomes more oxidized. The self-healing asphalt cement sees comparable healing ratios to the other materials here. When it is PAV aged, it shows a dramatic increase in terms of percentage. Practically speaking, this is because the FREI without a rest period is incredibly small and any increase would result in a significant percentage gain. The performance is still predicted to be much worse than the other asphalt cements. When excluding this outlier, the largest increase is seen by the PAV aged unmodified 58-28 which also has the highest FREI healing ratio under RTFO aged and unaged conditions as well.

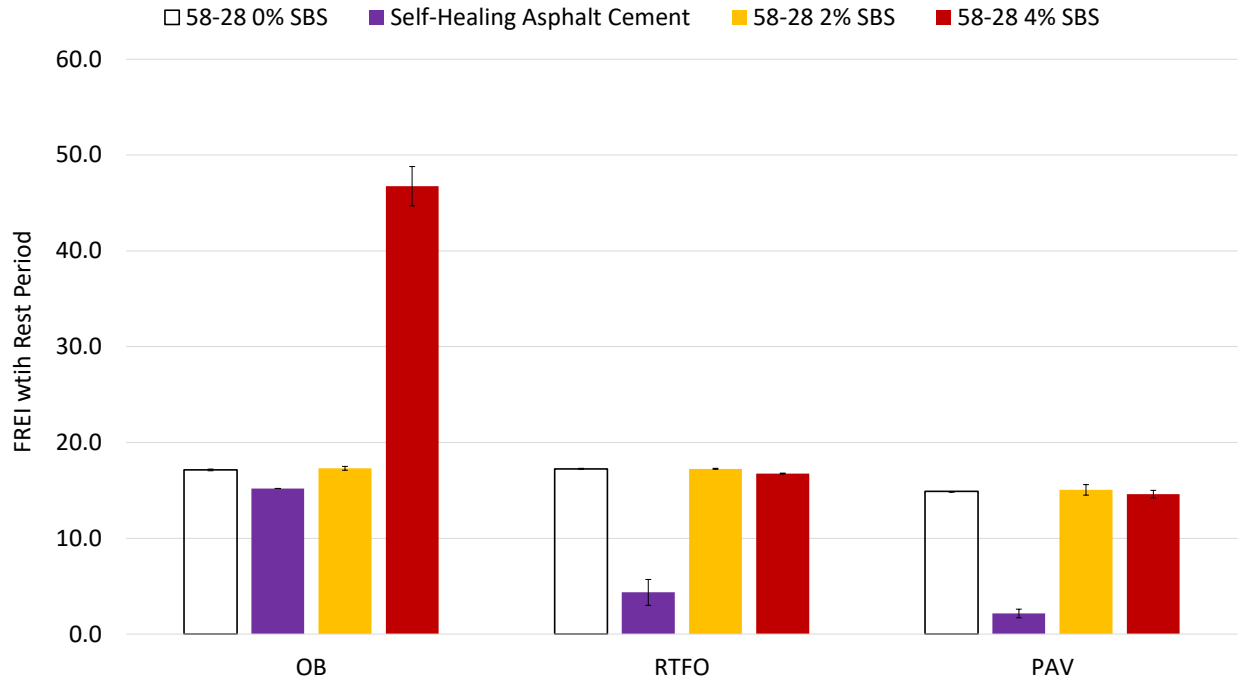


Figure 4- 11 Linear Amplitude Sweep data analyzed using the fracture mechanics approach including the rest period

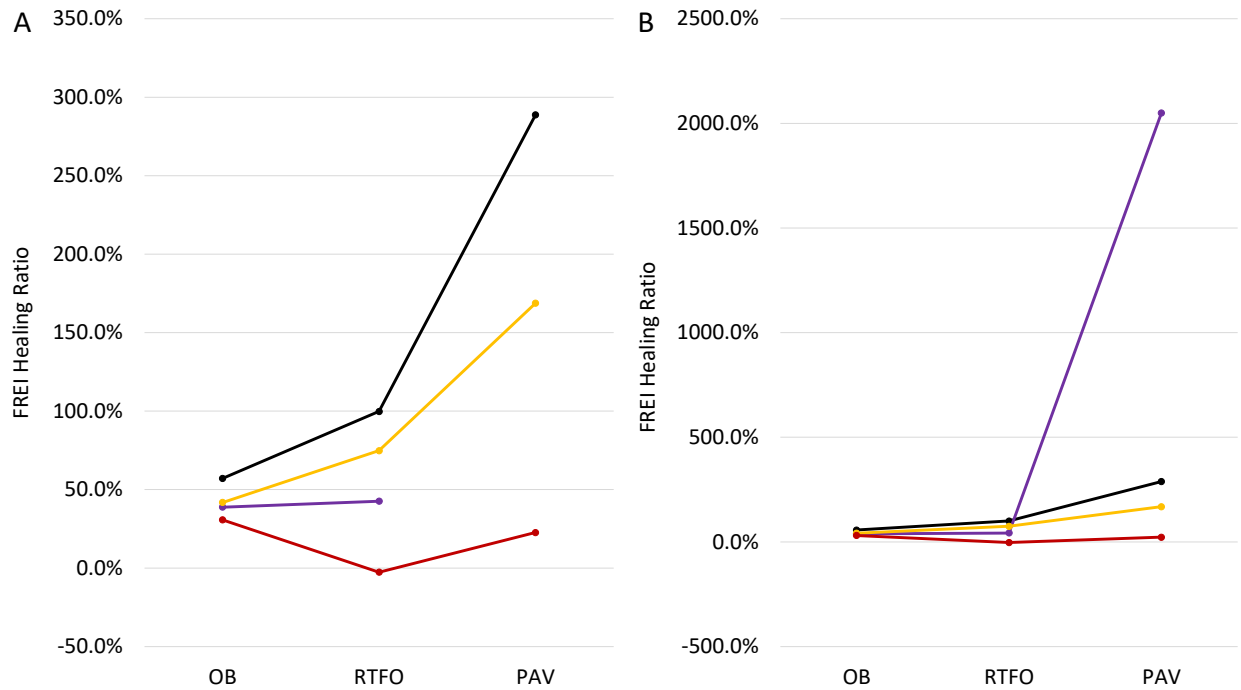


Figure 4- 12 Healing ratios calculated using the fatigue resistance energy index (A: outlier removed for clarity, B: all the data points)

Based on the data above, it is not expected that the two methods have a good relationship when a rest period is included in the test. Removing the rest period may improve the correlation between the FREI and VECD number of cycles to failure. The relationship between the VECD and FREI healing ratios is shown in Figure 4-13. Despite a high R^2 value, there appears to be little relationship between the two methodologies. Removing the outlier discussed earlier causes a large decrease in the R^2 value. This poor relationship is to be expected. Figure 4-14 and 4-15 show the relationship between the percent restoration and the VECD healing ratio and the percent restoration and the FREI healing ratios respectively. The R^2 values here are also inflated by the outliers and the data overall suggests little relationship between the three parameters. It may be possible that the methods discussed here are analyzing different aspects of the data, they could be capturing different aspects of the healing process, different aspects of the restoration process or simply giving no indication of the healing efficiency at all. It could be necessary to perform a different type of test (tensile rather than cyclic) or compare the results with mixture testing in order to learn more.

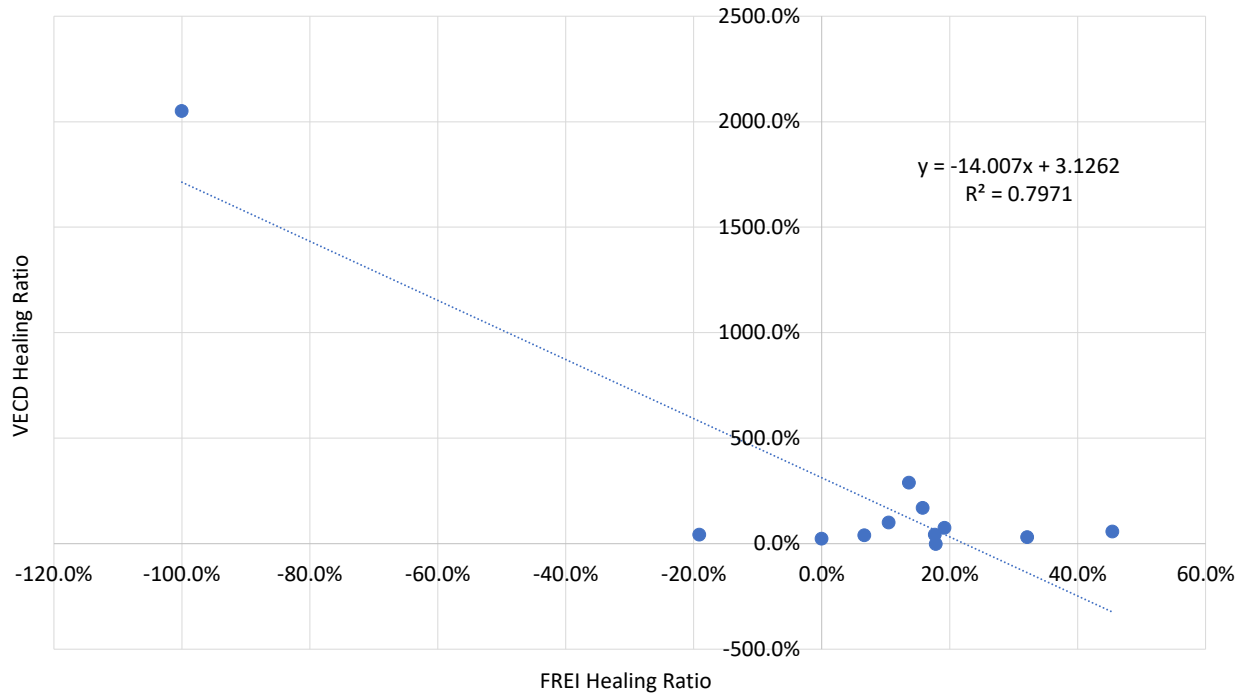


Figure 4- 13 Relationship between VECD number of cycles to failure and FREI healing ratios

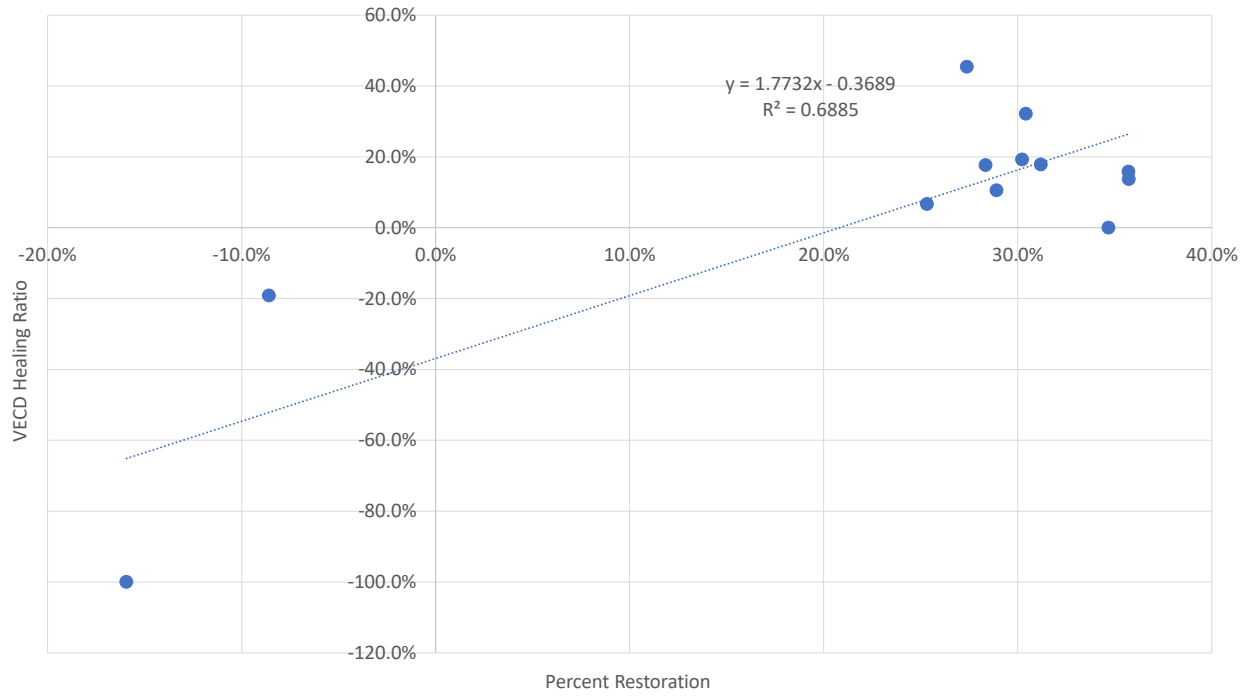


Figure 4- 14 Relationship between VECD number of cycles to failure healing ratio and percent restoration

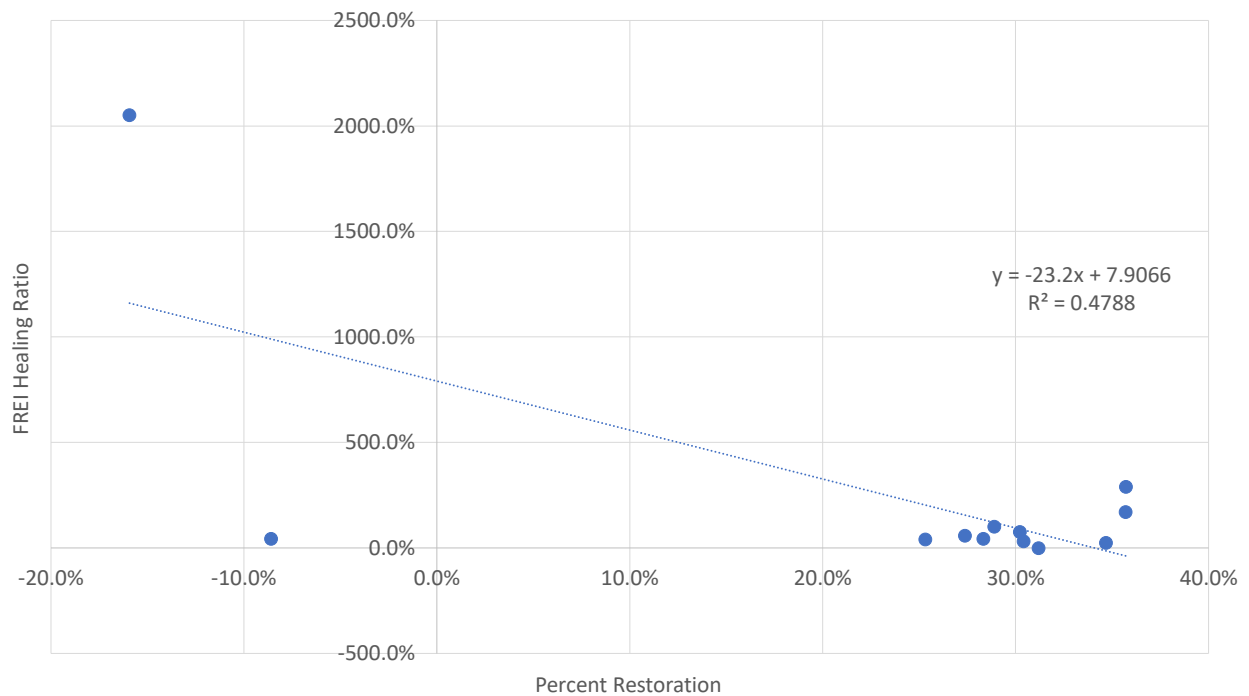


Figure 4- 15 Relationship between FREI healing ratio to failure and percent restoration

4.6 Healing and Restoration Properties- PoliTO Healing Index

In addition to the LAS-style healing tests, the PoliTO method discussed in the literature review was also used to examine the healing properties of the self-healing asphalt cement when compared to the 58-28. Due to the shortage of available testing material, the 35% targeted loss in dissipated energy was skipped at the test was performed with 15% and 50% targets only. Due to the non-homogenous nature of the self-healing asphalt cement blend, the damage periods were based on the number of cycles rather than a precise drop in the dissipated energy that would come from the calibration tests where damage was imparted on the material before the rest period. The calibration tests had similar drops in dissipated energy to each other, but when the self-healing asphalt cement was reheated and tested again, there was a noticeable change in the behaviour and as a result, the number of cycles required to induce the correct dissipated energy loss was under predicted. This may be due to the fact the material ages more quickly as evidenced by the PG testing and LAS healing efficiency data. The healing index values calculated using the PoliTO spreadsheet can be seen in Table 3 and 4, along with the damage level achieved in each test. Replicates were taken for each damage point and are presented here along with the average.

Table 4- 3 Healing index and dissipated energy loss data for 58-28 replicates

Specimen	Target Percent Loss in Dissipated Energy (%)	Healing Index (%)
58-28 0% SBS- R1	15	19.5
58-28 0% SBS- R2	15	18.5
58-28 0% SBS- R1	50	24.8
58-28 0% SBS- R2	50	24.8

Table 4- 4 Healing index and dissipated energy loss data for self-healing asphalt cement replicates

Specimen	Target Percent Loss in Dissipated Energy (%)	Measured Percent Loss in Dissipated Energy (%)	Healing Index (%)
Self-Healing Asphalt Cement- R1	15	12.7	8.1
Self-Healing Asphalt Cement- R2	15	11.8	3.7
Self-Healing Asphalt Cement- R1	50	53.9	10.8
Self-Healing Asphalt Cement- R2	50	39.3	9.5

The testing conducted using the PoliTO method ranks the healing abilities in a similar way to the percent restoration, VECD healing ratio and the FREI healing ratio. The self-healing asphalt cement has a lower healing index according to this method. All four of these healing and restoration parameters indicate that the self-healing elastomer does not transfer any of its self-healing properties and reduces the natural ability of the unaged asphalt cement. Although the rankings are similar, the magnitude of the change depends on the method being used. It is possible that the mechanism of healing within the self-healing elastomer is not characterized by the test methods chosen here. It is also interesting to note that the healing index of both asphalt cements tested using the PoliTO method saw an increase in the healing index when the loss in dissipated energy increased (implying a more damaged sample). This would contrast with the expectation that the increase in damage to asphalt typically decreases the healing efficiency. This may indicate that a cyclic test may not best be able to capture the healing process.

The plots of the complex modulus versus the test time are also interesting to examine. Figures 4-16, 4-17 and 4-18 show the calibration test data, 15% dissipated energy loss test data and the 50% dissipated energy loss test data. The increase in variability between the data sets for the self-healing asphalt cement can be clearly seen here. The 58-28 shows good repeatability between the two specimens. In the calibration test data (Figure 4-16), the self-healing asphalt cement is observed to have a less sharp decline in the complex modulus in the damage phase of the test. This is also observed in Figure 4-17 for the 15% loss in dissipated energy, but not when examining the 50% loss in dissipated energy data (Figure 4-18). A qualitative look at the data also reveals that the recovery in complex modulus is not as great for the self-healing asphalt cement

than it is for the 58-28. This is reflected in the healing index. The increase in rest period time would be expected to increase the healing efficiency of the asphalt cement.

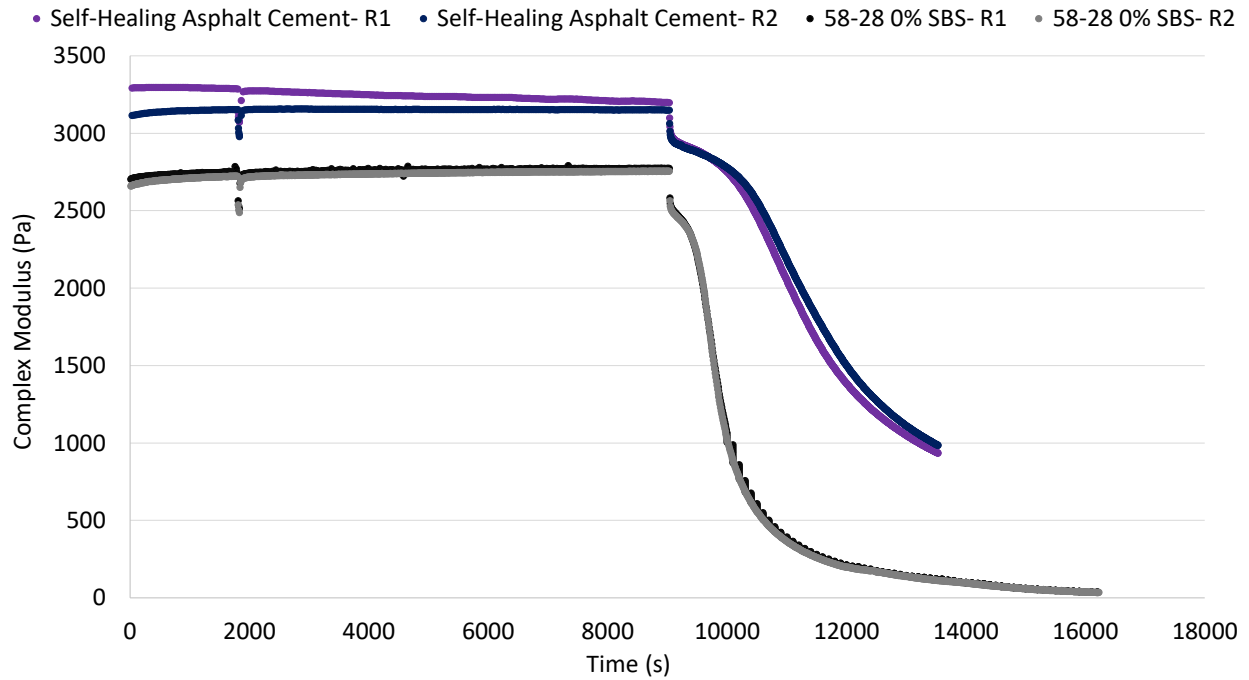


Figure 4- 16 Complex modulus versus time for the calibration test data

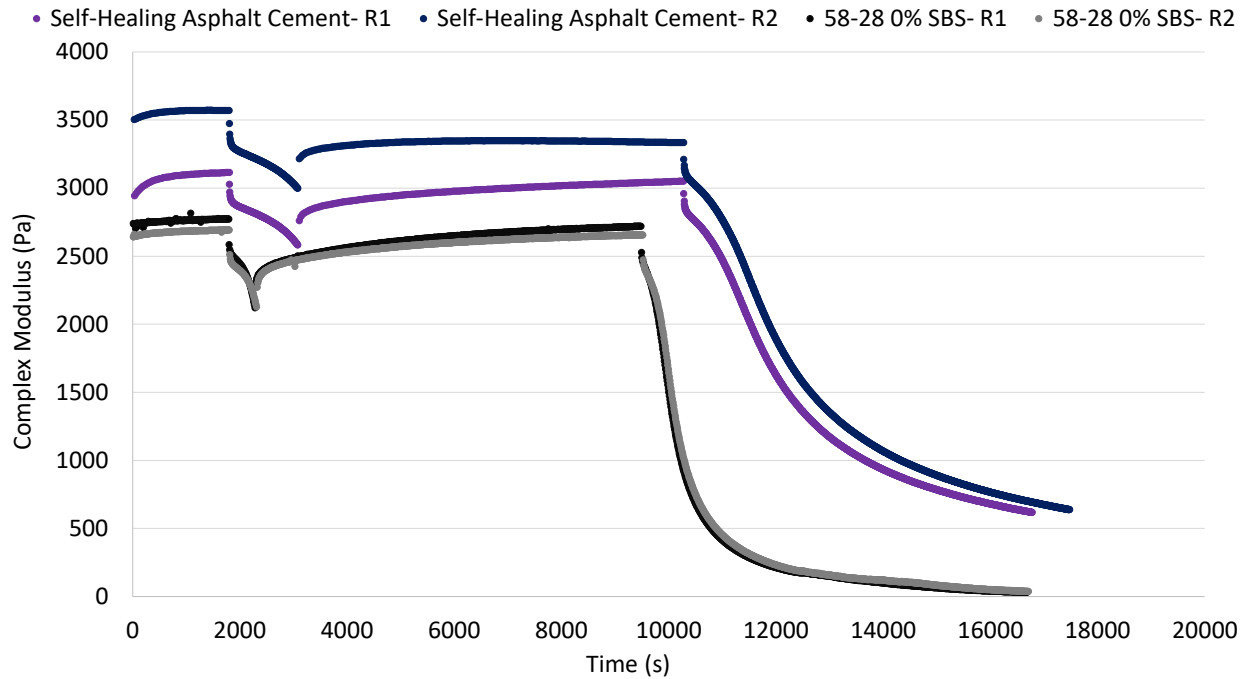


Figure 4- 17 Complex modulus versus time for the 15% loss in dissipated energy test data

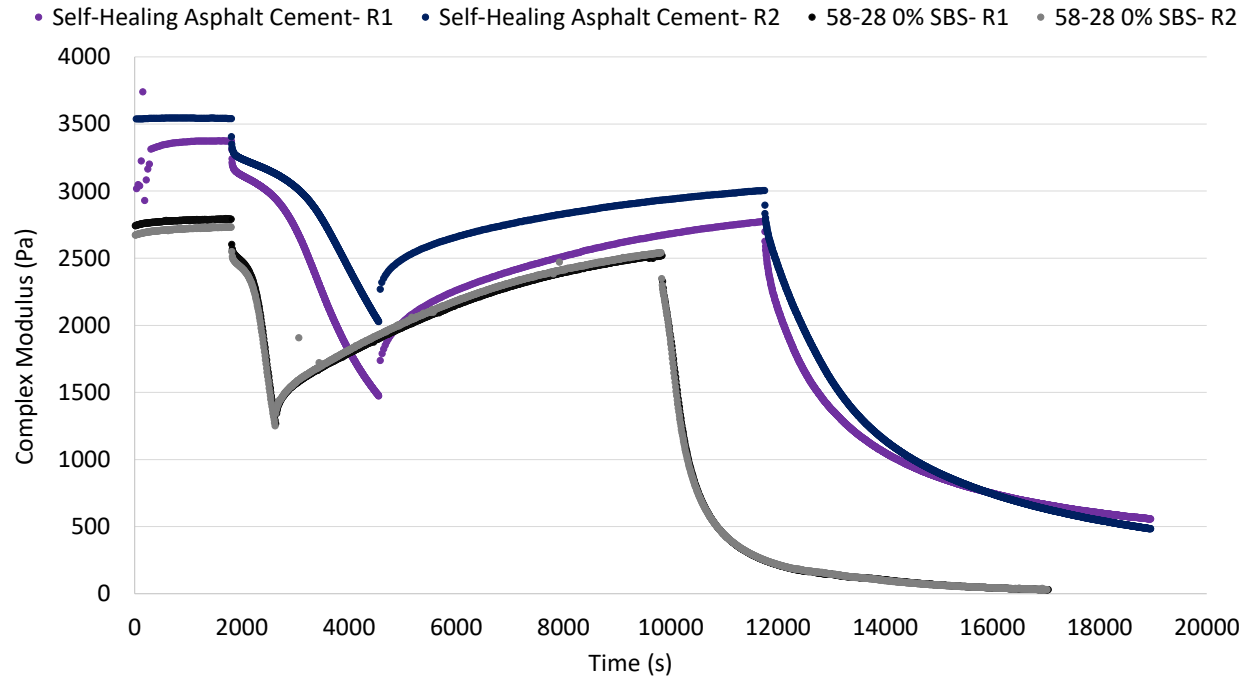


Figure 4- 18 Complex modulus versus time for the 50% loss in dissipated energy test data

4.7 Chapter Summary

The key findings in Chapter 4 are as follows:

- The self-healing asphalt cement is more susceptible to oxidative aging. The modulus increased more quickly after RTFO aging and there was a significant decrease in the m-Value following PAV aging. The BBR results indicate that the self-healing asphalt will be more prone to thermal cracking than the unmodified asphalt.
- Master curves and black spaces diagrams confirmed this increase in aging. The relative gap between the unaged and PAV aged curves for the self-healing asphalt is larger than that of the unmodified asphalt. In terms of aging, this flatter shape indicates a decrease in relaxation properties. This was also observed with the BBR m-Value. Black space diagrams confirm the elastomeric properties degrade with oxidative aging.
- A decrease in cracking resistance would be expected based on the above observations. This is confirmed for RTFO and PAV aged self-healing asphalt. SBS improved cracking resistance as expected.
- The restoration properties of the self-healing asphalt are typically lower than the unmodified asphalt cement for a strain value of 10%. Negative values observed here indicate that the damage was too extensive to repair. Decreasing the strain to 5% allowed the self-healing asphalt cement to have a

similar restoration to the unmodified asphalt. This trend only occurred for the unaged binder, but it also suggests the self-healing asphalt cement is more susceptible to damage.

- SBS seemed to improve the percent restoration but this is likely due to the increase in stiffness and changes to the rate of deformation.
- The use of healing ratios does not improve the characterization of the healing properties tested here. It is possible the addition of a rest period to these standard methods needs to be evaluated.
- The PoliTO method ranked the self-healing asphalt cement as performing more poorly than the unmodified asphalt cement. However, an unexpected trend was observed where the samples with larger amounts of induced damage had higher healing indices.

Chapter 5: ADHESIVE HEALING PULL OFF TEST

5.1 Background

The LAS healing tests outlined in the previous chapter may be ineffective for evaluating the healing potential of asphalt cement. Thus, it was decided to develop a test that would better replicate the crack closing that is expected within a pavement. If the crack is growing along the aggregate it is considered adhesive failure and if it is in the asphalt cement it is considered cohesive failure [28]. Leegwater et al. [103] originally developed a methodology that follows this vein by bringing to pieces of asphalt cement together and allowing them to bond. This type of test is also similar to test developed to evaluate the tackiness of asphalt cement. The tackiness is related to the adhesive qualities of the asphalt cement, which affects the initial transfer of load after first contact. Strength is gained instantaneously when the two crack faces are brought together through wetting. This is related to the surface free energy of the asphalt cement [75]. Softer asphalt cements have been shown to have better healing abilities, and they also tend to have better adhesion. It is important to keep the sample thickness to improve reproducibility in a tackiness test and this should be take into consideration here [111]. Gorsuch et al. [111] showed that their methodology, which uses a pull rate of 15 $\mu\text{m/s}$ on the DSR, could differentiate tacky and non-tacky asphalt cements. The tackiness test involves a controlled compression of the samples. Tackiness is proportional to the area of contact during the bonding step. Therefore it is important to control the size of the contact area. Cohesive failure is said to be related to the rheological properties of the asphalt cement. Several researchers have attempted to relate adhesive bond strength to the healing properties of asphalt cement [13, 112].

5.2 Methodology

The methodology discussed here is based on the the test method developed by Leegwater et al. [103] and ASTM D8189 – 19 “Standard Test Method for Tackiness of Asphalt Binders and Emulsified Asphalt Residue Using the Dynamic Shear Rheometer (DSR).” Samples of the self-healing asphalt cement and 58-28 were poured into the standard 8mm DSR mold for specimens and allowed to cool for 10 minutes. The top and bottom 8mm plate of the DSR were preheated to 45°C in order to ensure good adhesion between the plates and the specimen. Once the specimen reached the desired test temperature of 19°C, it was allowed to sit for 10 minutes prior to the pulling action of the DSR. A pull rate of 15 $\mu\text{m/s}$ was used and the test was terminated at a gap of 15mm. Baseline testing was conducted on a single piece, poured and then trimmed like a standard 8mm DSR test specimen. This result represents the material in state where no damage has occurred. In order to simulate the coming together of two crack faces, two specimens were poured. One of

the specimens had a piece of parchment paper applied to it while still hot. This piece of parchment paper contained a hole, slightly smaller than the diameter of the specimen. It was used in order to control the contact between the two specimens. Figure 5-1 shows a the sample after demolding prior to application to the DSR.

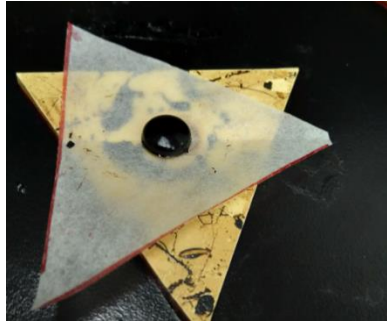


Figure 5- 1 Example of demolded specimen attached to parchment paper prior to testing

The level of contact between the two specimens was controlled by changing the gap used. The 4mm gap allowed for some force to be applied, while the 6mm gap represents a state where the samples have just come into contact. The rest period was approximately 15 minutes and was the time it took for the samples to reach 19°C and the 10 minute equilibrium time. Examples of the specimens before and after testing can be seen in Figure 5-2 and 5-3. It can be observed that there is some compression of the sample when the gap is set to 4mm. The parchment paper was trimmed in order to reduce interactions with the temperature control hood. Specimens were tested multiple times with a minimum of two replicates for each. Data was normalized to normal force of zero and analyzed by finding the work energy from the area above the cruce in the plot of the normal force versus time. Normal force was recorded as negative by the DSR because the plate was moving in the tension rather than compression. In order to verify the results, self-healing asphalt cement samples using 10% and 8% of the self-healing elastomer were tested.

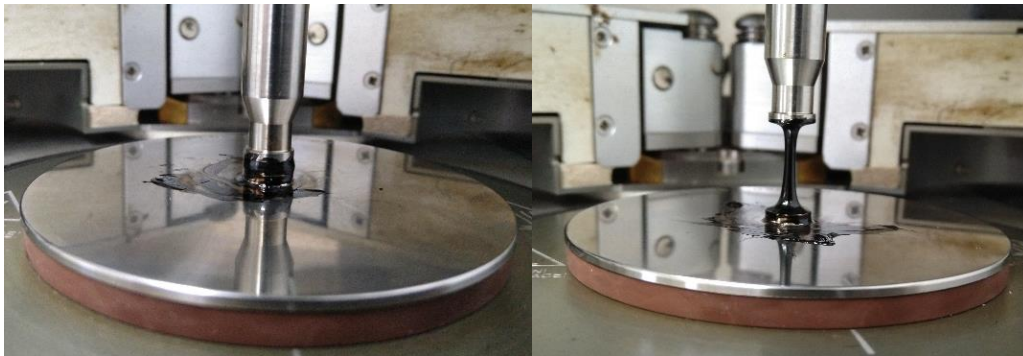


Figure 5- 2 Single specimen testing before and following test completion

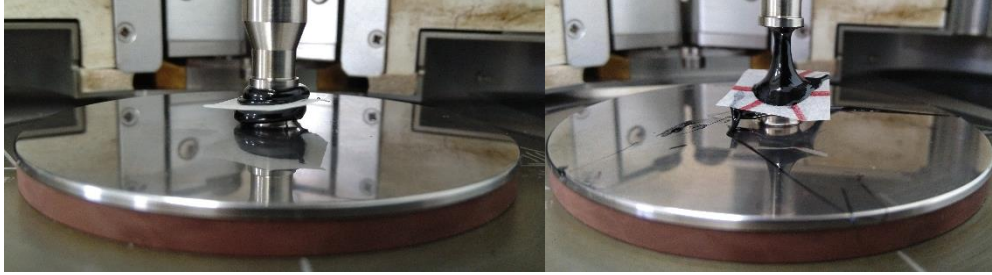


Figure 5- 3 Healing specimen prior to and following test completion

5.3 Results and Discussion

The peak normal force is an indication of the force needed to pull the specimen apart. A larger normal force may indicate the specimen has a stronger level of internal bonding and an increased level of tackiness. The self-healing asphalt cement has a higher peak normal force than the unmodified 58-28 indicating that the self-healing asphalt with 10% self-healing elastomer is having a positive impact on the tackiness of the asphalt as seen in Figure 5-4. This trend did not continue for the 58-28 modified with 8% self-healing elastomer where the curves had very similar normal force peaks when compared to the unmodified 58-28. The SBS modified asphalts predictably had much higher peak forces at 2% SBS, but the peak was lower with 4% SBS. The 58-28 with 4% SBS maintained a much higher force load following the peak as observed in Figure 5-5. The remaining individual curves can be found in Appendix A.

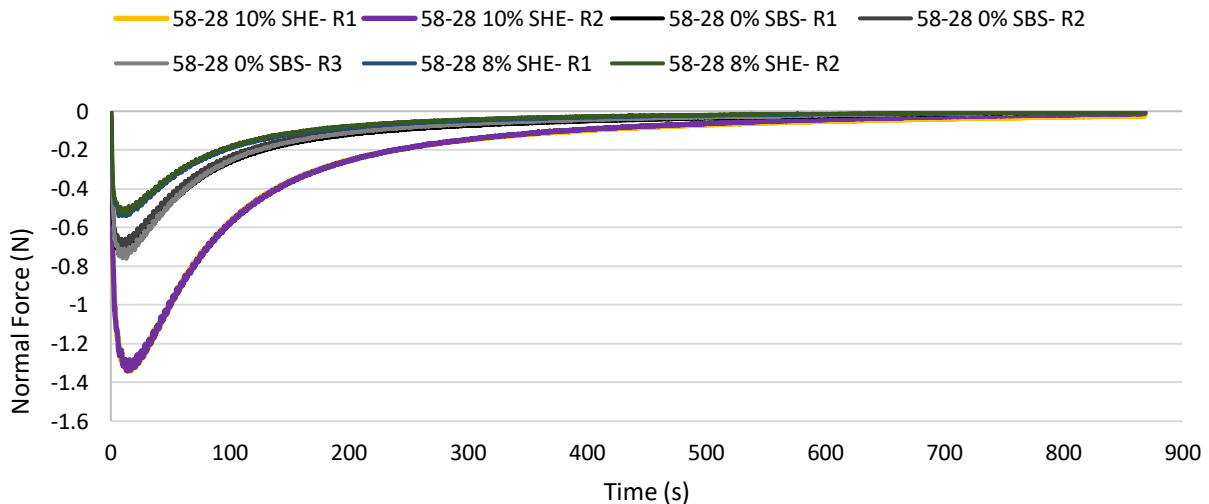


Figure 5- 4 Normal force versus time for the baseline testing of the self-healing asphalt cement (10% SHE and 8% SHE) and unmodified 58-28

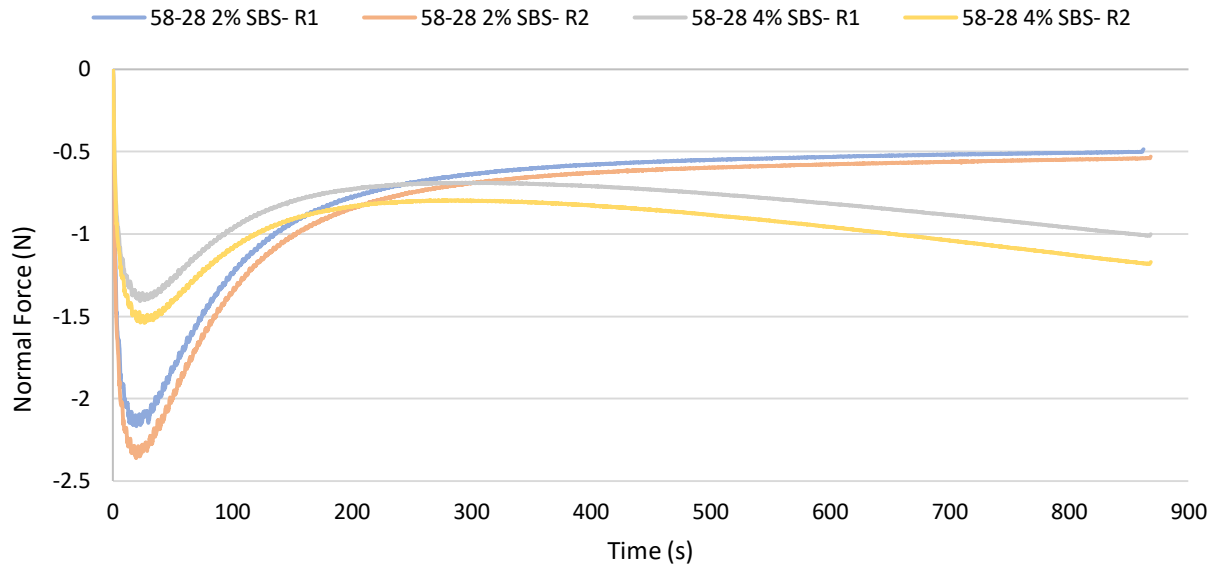


Figure 5- 5 Normal force versus time for the baseline testing of the 58-28 with 2% SBS and 4% SBS

It is expected that as the level of contact decreases, the peak normal force of the sample would also decrease due to the discontinuity between the two specimens. When the gap is set to 4mm, the peak normal force is approximately half of the baseline specimen. The normal force is also slightly higher following the peak which should be reflected in the calculation of the work. When the 6mm gap is applied, the peak normal force is approximately 15% of the single specimen. The repeatability of the single piece and 58-28 specimens is good. The repeatability is much lower again for the self-healing asphalt cement and this may be because the sample is not mixed homogeneously. The trend in peak force is also different in the self-healing asphalt specimens. When the 4mm gap is applied the peak force is nearly the same and sometimes higher than the peak force observed in the single specimen. The post peak behaviour of the healing specimens is similar, but the force observed in the self-healing asphalt cement post-peak is much higher. When the 6mm gap is applied to the self-healing asphalt, the peak force relative to the single specimen is approximately the same when compared to the 58-28 6mm gap specimens. However, the increased force following the peak indicates that the work required to pull the specimen is higher.

These differences in behaviour are reflected in the calculation of the work which was conducted using the Matlab cumulative trapezoidal numerical integration function. The percent restoration was calculated as the ratio of work for a single piece to the work required for the multiple specimen test data. The work required to pull the sample follows the observed trend in the peak normal force for the single specimen tests. The self-healing asphalt has a much higher work required for the different gap levels as well. Figure 5-6 shows the work required to pull apart the specimens for the various gap sizes. The SBS modified asphalt has much higher work required than the unmodified asphalt and self-healing asphalt cement. This is to be

expected and continues for all gap sizes. When using 10% of the self-healing elastomer, the work is much higher than the unmodified asphalt. The work for 8% self-healing elastomer and the unmodified asphalt are very similar. It is possible that 10% is required to increase the adhesion, however it appears as though the results could be outliers with the cause for increase in work unknown.

When examining the percent restoration in Figure 5-7, it can be observed that the self-healing asphalt cement with 10% self-healing elastomer tends to recover more of the work following the rest period. However, the percent restoration of the self-healing asphalt cement with 8% of the self-healing elastomer has very similar restoration to the unmodified asphalt. Despite having higher values of work overall, the SBS modified asphalt tends to have a lower percent restoration. This may not reflect the true increase in adhesion observed when analyzing the work required to pull the samples apart.

The 58-28 with 10% self-healing elastomer and the unmodified 58-28 have similar stiffnesses as discussed in the previous chapter, however they require different amounts of work to pull apart. Stiffness is a parameter that can affect adhesion and the healing properties. The additional testing of the self-healing asphalt cement with 8% of the self-healing elastomer has added uncertainty to the results. It is possible that the self-healing elastomer may improve the adhesion of the asphalt cement by containing more reversible bonds due to the nature of the crosslinking sites. The PDMS back bone has a relatively low molecular weight and may have better molecular mobility as a result. The healing process in this test also takes place between the temperatures of 19 and 45°C, where under the LAS healing tests it took place entirely at 19°C. This increase in temperature should have improved the healing abilities of both asphalts, but it is possible it was more beneficial to the self-healing asphalt cement with 10% self-healing elastomer.

The 58-28 with 4% SBS shows a higher work initially but is comparable to the 58-28 with 2% SBS when gaps are introduced. The ability for the SBS chains to interact may improve the adhesion of the two interfaces, but the large polymer chain size may inhibit molecular movement. This may mean that there is an optimal concentration for this type of adhesion, or the two mechanisms are roughly in balance. Increasing the concentration to 4% SBS certainly improves the adhesion and fatigue performance as previously discussed but could be detrimental to the healing capabilities of asphalt. It is possible that the large increase in performance would offset the small decrease in healing efficiency and thus a decrease in cohesive healing efficiency is not detrimental to the overall life of the pavement.

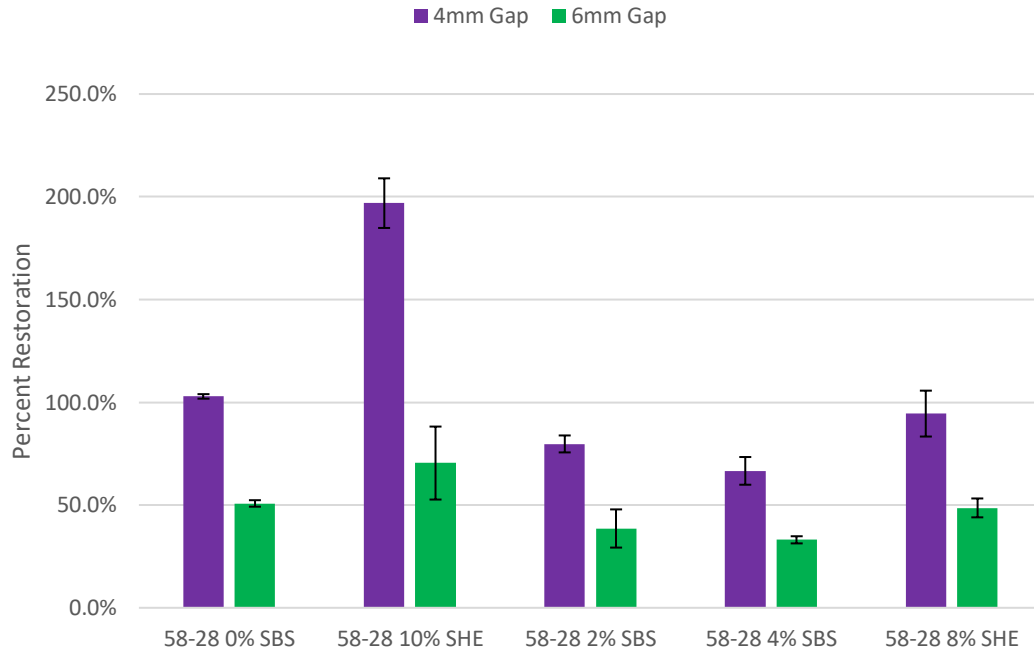


Figure 5- 6 Work required to pull the samples to a gap of 15mm

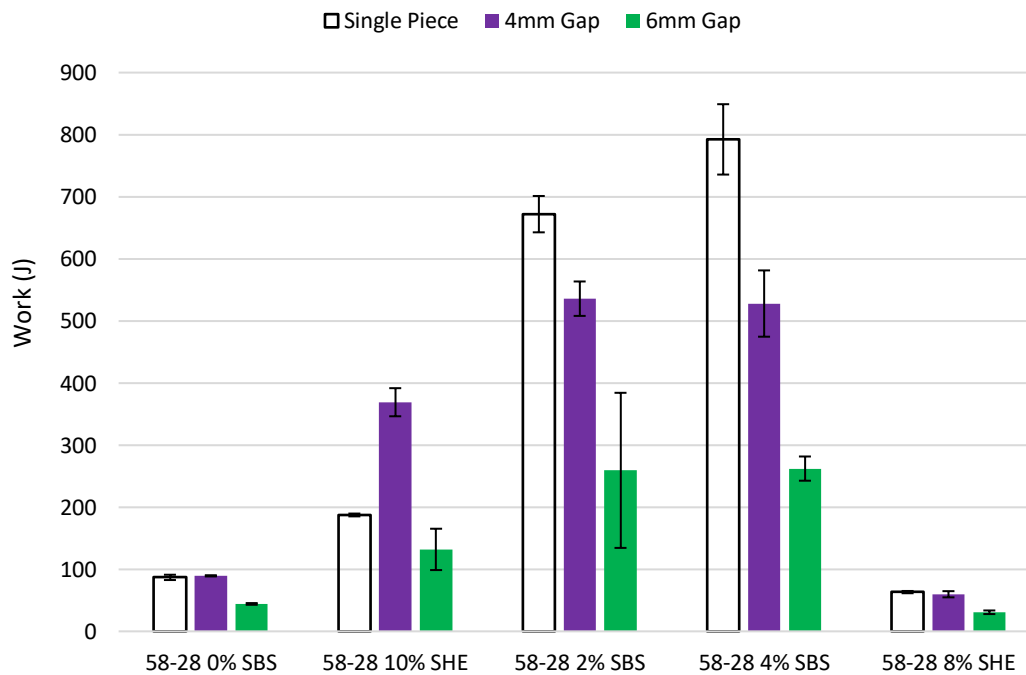


Figure 5- 7 Percent restoration for the unmodified 58-28 and self-healing asphalt cement for each gap size tested

5.4 Chapter Summary

The key findings in Chapter 5 are as follows:

- The adhesive qualities of the self-healing asphalt cement require further study. The use of 8% self-healing elastomer was unable to confirm that the presence of the self-healing elastomer was the cause of the increase in work seen with 10% of the additive. It seems unlikely that the results indicate an improvement.
- The addition of SBS is known to improve the adhesive qualities of asphalt cement and this is observed here. The magnitude of work required is much higher with SBS than the unmodified asphalt despite having a smaller percent restoration. The magnitude of change is more indicative here of the effects of the SBS. The similarities when gaps are introduced between the two SBS concentrations may indicate that there is some impairment of molecular mobility as the concentration increases.

Chapter 6: SUMMARY OF WORK AND FUTURE RECOMMENDATIONS

6.1 Conclusions

The presence of the self-healing elastomer has been shown to produce a more elastomeric binder in a similar fashion to the addition of SBS. However, the evidence presented here does not appear to indicate that the self-healing elastomer had a positive influence on the healing characteristics of the asphalt cement. This may be due to the final product received differing slightly from the intended final product produced by the original researchers. It is also possible that the test methods used here do not capture the healing process appropriately and cannot detect the positive influence of the self-healing elastomer. In addition to this, the following conclusions can also be drawn from this thesis:

- The addition of the self-healing elastomer resulted in excessive aging of the asphalt cement. The standard PGAC tests and rheological characterization confirmed that the self-healing asphalt cement aged more quickly under PAV conditions. This would also suggest that despite an improvement in elastomeric properties that the self-healing elastomer could be detrimental to cracking resistance overall. This is observed in the LAS testing without rest periods.
- Some of the data suggests that the addition of SBS improves the healing efficiency of asphalt cement. The large number of interactions between the polymer chains may increase the adhesive qualities and ability of the asphalt cement to bond at an interface. However, the large chain size may also decrease molecular mobility. Previous evidence has also been inconsistent, and it is possible that the interaction between the asphalt and SBS is important. This requires further research to confirm.
- The inconsistency of the rankings between the test methods chosen here may indicate that they are ineffective for evaluating healing or it is possible that they are evaluating different aspects of the healing process. The LAS style test may not induce damage in the necessary way to evaluate healing although it characterizes cracking performance well. It is likely that the evaluation of healing would be improved when testing asphalt mixtures.
- The pull off test is meant to simulate the interaction of two crack interfaces and has shown that the addition of SBS has a great level of adhesion than unmodified asphalt and the self-healing asphalt cement. Good adhesion would indicate that there are strong interactions between the two interfaces and suggests that healing efficiency may improve. Some of the test results show that the self-healing elastomer improved the adhesive qualities of the asphalt cement. However, at a lower

concentration the adhesion was shown to be worse than the unmodified asphalt. These results are inconclusive.

6.2 Future Work

The concept of using a self-healing elastomer is likely still an interesting avenue to explore, however it appears that alternative polymers should be explored. PDMS based polymers have shown to exhibit good healing properties and PDMS has a similar Hildebrand parameter to SBS and the maltene fraction of asphalt cement. Tuning the properties of the self-healing elastomer could allow for better use within asphalt cement. It may also be possible to produce co-block polymers incorporating butadiene, styrene and dimethylsiloxane to produce a healing polymer that has a stronger elastomeric component. More advanced chemical synthesis which is beyond the capabilities of a traditional PGAC laboratory are needed to perform these steps.

Chemical analysis of the materials was planned prior to COVID-19 laboratory restrictions were put in place and would be necessary for understanding the role oxidative aging has played in the performance of the self-healing asphalt cement. It would also provide important insights into understanding the role of SBS in the healing process for this specific combination. FTIR, SAR-AD and chromatography would all be necessary for an in-depth analysis here. Flash point testing would also be advisable to evaluate the presence of remaining solvent within the asphalt cement.

Asphalt mixture testing would also prove to be a necessary addition to the evaluation of healing in asphalt. The healing process largely occurs in the asphalt cement, but cracking is difficult to replicate in this material alone. The cracking process is much easier to characterize in asphalt mixtures and therefore healing likely would be too. Uniaxial tension compression testing represents an interesting choice because of its fundamentally improved ability to characterize fatigue damage in asphalt mixtures. A modified procedure which produces a large degree of damage and examines the performance before and after rest periods could be ideal.

References

- [1] Ontario Asphalt Pavement Council. Why Asphalt is the Better Way to Pave Fact Sheet. 2017.
- [2] Aurilio, M., P. Mikhailenko, H. Baaj, and L. D. Poulikakos. Properties of Asphalt Binders with Increasing SBS Polymer Modification. *Lecture Notes in Civil Engineering*, Vol. 48, 2019, pp. 55-66.
- [3] Padhan, R. K., A. A. Gupta, R. P. Badoni, and A. K. Bhatnagar. Improved Performance of a Reactive Polymer-Based Bituminous Mixes – Effect of Cross-Linking Agent. *Road Materials and Pavement Design*, Vol. 16, No. 2, 2015, pp. 300–315.
- [4] Xu, S., A. García, J. J. Su, Q. Liu, A. Tabaković, E. Schlangen, Á. García, J. J. Su, Q. Liu, A. Tabaković, and E. Schlangen. Self-Healing Asphalt Review: From Idea to Practice. *Advanced Materials Interfaces*, Vol. 1800536, No. 17, 2018, pp. 1–21.
- [5] Butt, A. A., B. Birgisson, and N. Kringos. Optimizing the Highway Lifetime by Improving the Self Healing Capacity of Asphalt. *Procedia - Social and Behavioral Sciences*, Vol. 48, 2012, pp. 2190–2200.
- [6] Asphalt Institute. The Asphalt Handbook. Manual Series No. 4, 7th Edition, Lexington, Kentucky, 2008.
- [7] Corbett, L. W. Refinery Processing of Asphalt Cement. *Transportation Research Record*, 1984, pp. 1–6.
- [8] Almadary, Y. Investigation of Different Factors Affecting Asphalt Binder Ageing and Durability. *University of Waterloo*. 2019.
- [9] Kriz, P. Refining Company Perspective & Approach to High Quality Asphalts. Presented at Canadian Technical Asphalt Association. Montreal, Canada, 2019.
- [10] Petersen, J. C., R. E. Robertson, J. F. Branthaver, P. M. Harnsberger, J. J. Duvall, S. S. Kim, D. Anderson, D. W. Christiansen, and H. U. Bahia. Binder Characterization and Evaluation. *Volume 1. No SHRP-A-367*. 1994.
- [11] Planche, J. P., D. Christensen, G. King, and C. Rodezno. NCHRP 9-60 Update Experimental Work-Plan. 2016.
- [12] Corbett, L. W. Composition of Asphalt Based on Generic Fractionation, Using Solvent Deasphalting, Elution-Adsorption Chromatography, and Densimetric Characterization. *Analytical Chemistry*, Vol. 41, No. 4, 1969.
- [13] Lv, Q., W. Huang, X. Zhu, and F. Xiao. On the Investigation of Self-Healing Behavior of Bitumen and Its Influencing Factors. *Materials & Design*, Vol. 117, 2017, pp. 7–17.
- [14] Read, J. and D. Whiteoak, The Shell Bitumen Handbook, Fifth Edition. Thomas Telford, 2003.

-
- [15] Amin, J. S., Enikoee, M. H. Ghatee, S. Ayatollahi, A. Alamdari, and T. Sedghamiz. Investigating the Effect of Different Asphaltene Structures on Surface Topography and Wettability Alteration. *Applied Surface Science*, Vol. 257, No. 20, 2011.
- [16] Baaj, H., H. di Benedetto, and P. Chaverot. Effect of Binder Characteristics on Fatigue of Asphalt Pavement Using an Intrinsic Damage Approach. *Road Materials and Pavement Design*, Vol. 6, No. 2, 2005, pp. 147–174.
- [17] Wakefield, A. and S. Tighe. Evaluation of Oxidative Aging with SAR- AD™ in Asphalt Recovered from Plant Produced Asphalt Mix. *Proceedings, Canadian Technical Asphalt Association*, Vol. 64, 2019, pp. 388–400.
- [18] Hintz, C. Understanding Mechanisms Leading to Asphalt Binder Fatigue. *University of Wisconsin-Madison*. 2012.
- [19] Asphalt Institute. *Use of the Delta Tc Parameter to Characterize Asphalt Binder Behavior*. 2019.
- [20] Rowe, G. M. Advanced Rheological Analysis. Presented at The Association of Modified Asphalt Producers, February 2, 2019.
- [21] Booshehrian, A., W. S. Mogawer, and R. Bonaquist. How to Construct an Asphalt Binder Master Curve and Assess the Degree of Blending between RAP and Virgin Binders. *Journal of Materials in Civil Engineering*, Vol. 25, No. 12, 2013.
- [22] Kaloush, K. E., B. S. Underwood, R. Salim, and A. Gundla. Evaluation of MSCR Testing for Adoption in ADOT Asphalt Binder Specifications. No. August, 2019.
- [23] Bukowski, J., J. Youtcheff, and T. Harman. THE Multiple Stress Creep Recovery (MSCR) Procedure. *Office of Pavement Technology - FHWA-HIF-11-038*, No. April, 2011, pp. 1–9.
- [24] Bonaquist, R. NCHRP Project 9-61 Update Short- and Long-Term Binder Aging Methods to Accurately Reflect Aging in Asphalt Mixtures. Presented at 99th Annual Meeting of the Transportation Research Board, Washington, D.C., 2020.
- [25] Aurilio, M., A. Qabur, P. Mikhailenko, and H. Baaj. Comparing the Fatigue Performance of HMA Samples with PMA to Their Multiple Stress Creep Recovery and Double Notched Tension Test Properties. *Proceedings, Canadian Technical Asphalt Association*, Vol. 63, 2018, pp. 385–410.
- [26] Quintus, H. L. von, J. Mallela, and M. Buncher. Quantification of Effect of Polymer-Modified Asphalt on Flexible Pavement Performance. *Transportation Research Record*, Vol. 2001, No. 1, 2007, pp. 141–154.
- [27] Dong, F., W. Zhao, Y. Zhang, J. Wei, W. Fan, Y. Yu, and Z. Wang. Influence of SBS and Asphalt on SBS Dispersion and the Performance of Modified Asphalt. *Construction and Building Materials*, Vol. 62, 2014, pp. 1–7.
- [28] Little, D. N., R. L. Lytton, D. Williams, and R. Y. Kim. An Analysis of the Mechanism of Microdamage Healing Based on the Application of Micromechanics First Principles of Fracture and Healing. *Proceedings of the Association of Asphalt Paving Technologists*, Vol. 68, 1999, pp. 501–542.

-
- [29] Zhu, J., R. Balieu, and H. Wang. The Use of Solubility Parameters and Free Energy Theory for Phase Behaviour of Polymer-Modified Bitumen: A Review. *Road Materials and Pavement Design*, Vol. 0, No. 0, 2019, pp. 1–22.
- [30] Huang, W., and N. Tang. Characterizing SBS Modified Asphalt with Sulfur Using Multiple Stress Creep Recovery Test. *Construction and Building Materials*, Vol. 93, 2015, pp. 514–521.
- [31] Mazumder, M., H. Kim, and S. J. Lee. Performance Properties of Polymer Modified Asphalt Binders Containing Wax Additives. *International Journal of Pavement Research and Technology*, Vol. 9, No. 2, 2016.
- [32] Pszczola, M., M. Jaczewski, D. Rys, P. Jaskula, and C. Szydłowski. Evaluation of Asphalt Mixture Low-Temperature Performance in Bending Beam Creep Test. *Materials*, Vol. 11, No. 1, 2018.
- [33] da Silva, L. S., M. M. de Camargo Forte, L. D. de Alencastro Vignol, and N. S. M. Cardozo. Study of Rheological Properties of Pure and Polymer-Modified Brazilian Asphalt Binders. *Journal of Materials Science*, Vol. 39, No. 2, 2004.
- [34] Planche, J.P., V. Mouillet, P. Dumas, and L. Lapalu. Aging Properties of Elastomer Modified Binders. *Proceedings of 4th Eurasphalt & Eurobitume Congress*, Presented at the 2008 Eurasphalt & Eurobitume, Congress, Copenhagen, 2008.
- [35] Planche, JP. Compatibility in Asphalt – A Moving Target with Sources, Modifications and Aging. Presented at 99th Annual Meeting of the Transportation Research Board, Washington, D.C., 2020.
- [36] Qabur, A. Fatigue Characterization of Asphalt Mixes with Polymer Modified Asphalt Binder. *University of Waterloo*. 2018.
- [37] Zhou, F., D. Newcomb, C. Gurganus, S. Banhashemrad, E. S. Park, M. Sakhaeifar, and R. L. Lytton. PROJECT NO. 9-57, FINAL REPORT: Field Validation of Laboratory Tests to Assess Cracking Resistance of Asphalt Mixtures: An Experimental Design, National Cooperative Highway Research Program, 2016.
- [38] Qiu, J. Self Healing of Asphalt Mixtures: Towards a Better Understanding of the Mechanism. *Delft University of Technology*, 2012.
- [39] Sun, D., F. Yu, L. Li, T. Lin, and X. Y. Zhu. Effect of Chemical Composition and Structure of Asphalt Binders on Self-Healing. *Construction and Building Materials*, Vol. 133, 2017, pp. 495–501.
- [40] Witczak, M., M. Mamlouk, M. Souliman, and W. Zeiada. PROJECT NO. 9-44, FINAL REPORT: Laboratory Validation of an Endurance Limit for Asphalt Pavements. National Cooperative Highway Research Program, 2013.
- [41] Islam, S., A. Sufian, M. Hossain, R. Miller, and C. Leibrock. Mechanistic-Empirical Design of Perpetual Pavement. *Road Materials and Pavement Design*, Vol. 21, No. 5, 2020.
- [42] Baghaee Moghaddam, T., and H. Baaj. The Use of Compressible Packing Model and Modified Asphalt Binders in High-Modulus Asphalt Mix Design. *Road Materials and Pavement Design*, Vol. 21, No. 4, 2020.

-
- [43] Bennert, T. Performance Testing for HMA Quality Assurance RFP Quarterly Progress Report. No. FHWA-NJ-2015-010, 2013.
- [44] Cooper S.B. Balanced Mix Design for Asphalt Mixtures 3 – Part Webinar Series Part 3: A case study of BMD implementation in Louisiana, Lessons learned Durability. Louisiana Transportation Research Center, 2017, pp. 1-29.
- [45] Chen, J. S., T. J. Wang, and C. te Lee. Evaluation of a Highly-Modified Asphalt Binder for Field Performance. *Construction and Building Materials*, Vol. 171, 2018, pp. 539–545.
- [46] Błazejowski, K., M. Wójcik-Wiśniewska, H. Peciakowski, and J. Olszacki. The Performance of a Highly Modified Binders for Heavy Duty Asphalt Pavements. *Transportation Research Procedia*, Vol. 14, 2016, pp. 679–684.
- [47] Habbouche, J., E. Y. Hajj, P. E. Sebaaly, and M. Piratheepan. A Critical Review of High Polymer-Modified Asphalt Binders and Mixtures. *International Journal of Pavement Engineering*, Vol. 21, No. 6, 2020, pp. 686–702.
- [48] Timm, D., M. Robbins, G. Huber, and Y. Yang. Analysis of Perpetual Pavement Experiment Sections in China. *Transportation Research Record*, No. 2226, 2011, pp. 94–103.
- [49] Hou, D., M. Han, Y. Muhammad, Y. Liu, F. Zhang, Y. Yin, S. Duan, and J. Li. Performance Evaluation of Modified Asphalt Based Trackless Tack Coat Materials. *Construction and Building Materials*, Vol. 165, 2018.
- [50] di Benedetto, H., C. de La Roche, H. Baaj, A. Pronk, and R. Lundstrom. Fatigue of Bituminous Mixtures. *Materials and Structures*, Vol. 37, No. 3, 2004, pp. 202–216.
- [51] Moreno-Navarro, F., and M. C. Rubio-Gómez. A Review of Fatigue Damage in Bituminous Mixtures: Understanding the Phenomenon from a New Perspective. *Construction and Building Materials*, Vol. 113, 2016, pp. 927–938.
- [52] Pérez-Jiménez, F. E., R. Botella, and R. Miró. Differentiating between Damage and Thixotropy in Asphalt Binder's Fatigue Tests. *Construction and Building Materials*, No. 31, 2012, pp. 212–219.
- [53] Wöhler, A. Über die Festigkeits-versuche mit Eisen und Stahl. 1870.
- [54] Tayebali, A. A., G. M. Rowe, and J. B. Sousa. SHRP-A-404: Fatigue Response of Asphalt-Aggregate Mixtures. Strategic Highway Research Program, Washington, D.C. 1994.
- [55] Perraton, D., H. Baaj, and A. Carter. Comparison of Some Pavement Design Methods from a Fatigue Point of View: Effect of Fatigue Properties of Asphalt Materials. *Road Materials and Pavement Design*, Vol. 11, No. 4, 2010, pp. 833–861.
- [56] Portillo, O., and D. Cebon. Fracture Mechanics of Idealised Bituminous Mixes. *International Journal of Pavement Engineering*, Vol. 17, No. 2, 2016, pp. 103–122.
- [57] Wen, H. Fatigue performance evaluation of WesTrack asphalt mixtures based on viscoelastic analysis of indirect tensile test. *North Carolina State University*, 2001.

-
- [58] Zhou, F., S. Im, L. Sun, and T. Scullion. Development of an IDEAL Cracking Test for Asphalt Mix Design and QC/QA. *Asphalt Paving Technology: Association of Asphalt Paving Technologists- Proceedings of the Technical Sessions*, Vol. 86, 2017, pp. 549–577.
- [59] Buttlar, B. Disk - Shaped Compact Tension Test. Vol. 7313, No. 07.
- [60] Kim, M., L. Mohammad, and M. Elseifi. Characterization of Fracture Properties of Asphalt Mixtures as Measured by Semicircular Bend Test and Indirect Tension Test. *Transportation Research Record*, No. 2296, 2012, pp. 115–124.
- [61] Park, S. W., Y. R. Kim, and R. A. Schapery. A Viscoelastic Continuum Damage Model and Its Application to Uniaxial Behavior of Asphalt Concrete. *Mechanics of Materials*, Vol. 24, No. 4, 1996, pp. 241–255.
- [62] Bessa, I. S., K. L. Vasconcelos, V. T. F. Castelo Branco, and L. L. B. Bernucci. Fatigue Resistance of Asphalt Binders and the Correlation with Asphalt Mixture Behaviour. *Road Materials and Pavement Design*, Vol. 20, No. sup2, 2019, pp. S695–S709.
- [63] Bahia, H. U., D. I. Hanson, M. Zeng, H. Zhai, M. A. Khatri, and R. M. Anderson. NCHRP REPORT NO. 459: Characterization of Modified Asphalt Binders in Superpave Mix Design. National Cooperative Highway Research Program, 2001.
- [64] Błazejowski, K., M. Wójcik-Wiśniewska, H. Peciakowski, and J. Olszacki. The Performance of a Highly Modified Binders for Heavy Duty Asphalt Pavements. *Transportation Research Procedia*, Vol. 14, 2016, pp. 679–684.
- [65] Zhou, F., P. Karki, and S. Im. Development of a Simple Fatigue Cracking Test for Asphalt Binders. *Transportation Research Record: Journal of the Transportation Research Board*, Vol. 2632, No. 1, 2017, pp. 79–87.
- [66] Apostolidis, P., C. Kasbergen, A. Bhasin, A. Scarpas, and S. Erkens. Study of Asphalt Binder Fatigue with a New Dynamic Shear Rheometer Geometry. *Transportation Research Record*, Vol. 2672, No. 28, 2018, pp. 290–300.
- [67] Bhasin, A., P. Apostolidis, R. Hajj, and T. Scarpas. Revisiting Measurement of Fatigue Cracking Resistance of Asphalt Binders. Presented at 99th Annual Meeting of the Transportation Research Board, Washington, D.C., 2020.
- [68] Shenoy, A. Fatigue Testing and Evaluation of Asphalt Binders Using the Dynamic Shear Rheometer. *Journal of Testing and Evaluation*, Vol. 30, No. 4, 2002, p. 303-312.
- [69] Hintz, C., R. Velasquez, C. Johnson, and H. Bahia. Modification and Validation of Linear Amplitude Sweep Test for Binder Fatigue Specification. *Transportation Research Record*, No. 2207, 2011.
- [70] Chen, H., Y. Zhang, and H.U. Bahia. “The Role of Binders in Cracking Resistance of Mixtures Measured with the IFIT Procedure”, *Proceedings, Canadian Technical Asphalt Association*, Vol. 64, 2019, pp. 401-421.
- [71] Soenen, H., L. Xiaohu, M. Uwe, and L. Olli-ville. The Influence of Aging on Binder Fatigue and Other Fracture Related Binders Test Results. No. August, 2018, pp. 1–13.

-
- [72] Safaei, F., and C. Castorena. Temperature Effects of Linear Amplitude Sweep Testing and Analysis. *Transportation Research Record: Journal of the Transportation Research*, Vol. 2574, 2016, pp. 92–100.
- [73] Tabaković, A., and E. Schlangen. *Self-Healing Technology for Asphalt Pavements*, Springer, Cham, 2015 pp. 285–306.
- [74] Leegwater, G., A. Tabokovi, O. Baglieri, and F. Hammoum. Terms and Definitions on Crack-Healing and Restoration of Mechanical Properties in Bituminous Materials. *Proceedings, RILEM International Symposium on Bituminous Materials*, 2020.
- [75] Bhasin, A., D. N. Little, R. Bommavaram, and K. Vasconcelos. A Framework to Quantify the Effect of Healing in Bituminous Materials Using Material Properties. *Road Materials and Pavement Design*, Vol. 9, No. SPECIAL ISSUE, 2008, pp. 219–242.
- [76] Khan, N. I., S. Halder, S. B. Gunjan, and T. Prasad. A Review on Diels-Alder Based Self-Healing Polymer Composites. *IOP Conference Series: Materials Science and Engineering*, Vol. 377, No. 1, 2018.
- [77] Sun, D., T. Lin, X. Zhu, Y. Tian, and F. Liu. Indices for Self-Healing Performance Assessments Based on Molecular Dynamics Simulation of Asphalt Binders. *Computational Materials Science*, Vol. 114, 2016, pp. 86–93.
- [78] Xie, W., C. Castorena, C. Wang, and Y. Richard Kim. A Framework to Characterize the Healing Potential of Asphalt Binder Using the Linear Amplitude Sweep Test. *Construction and Building Materials*, Vol. 154, 2017, pp. 771–779.
- [79] Baaj, H., P. Mikhailenko, H. Almutairi, and H. di Benedetto. Recovery of Asphalt Mixture Stiffness during Fatigue Loading Rest Periods. *Construction and Building Materials*, Vol. 158, 2018, pp. 591–600.
- [80] White, S. R., N. R. Sottos, P. H. Geubelle, J. S. Moore, M. R. Kessler, S. R. Sriram, E. N. Brown, and S. Viswanathan. Autonomic Healing of Polymer Composites. *Nature*, Vol. 409, No. 6822, 2001, pp. 794–797.
- [81] Bekas, D. G., K. Tsirka, D. Baltzis, and A. S. Paipetis. Self-Healing Materials: A Review of Advances in Materials, Evaluation, Characterization and Monitoring Techniques. *Composites Part B: Engineering*, Vol. 87, 2016, pp. 92–119.
- [82] Zhu, D. Y., M. Z. Rong, and M. Q. Zhang. Preparation and Characterization of Multilayered Microcapsule-like Microreactor for Self-Healing Polymers. *Polymer*, Vol. 54, No. 16, 2013, pp. 4227–4236.
- [83] Shen, J., S. Amirhanian, and J. Aune Miller. Effects of Rejuvenating Agents on Superpave Mixtures Containing Reclaimed Asphalt Pavement. *Journal of Materials in Civil Engineering*, Vol. 19, No. 5, 2007.
- [84] Xu, S., A. Tabaković, X. Liu, D. Palin, and E. Schlangen. Optimization of the Calcium Alginate Capsules for Self-Healing Asphalt. *Applied Sciences (Switzerland)*, Vol. 9, No. 3, 2019.
- [85] Garcia, A., J. Jelfs, and C. J. Austin. Internal Asphalt Mixture Rejuvenation Using Capsules. *Construction and Building Materials*, Vol. 101, 2015, pp. 309–316.

-
- [86] Cremaldi, J. C., and B. Bhushan. Bioinspired Self-Healing Materials: Lessons from Nature. *Beilstein Journal of Nanotechnology*, Vol. 9, No. 1, 2018, pp. 907–935.
- [87] Hamilton, A. R., N. R. Sottos, and S. R. White. Pressurized Vascular Systems for Self-Healing Materials. *Journal of the Royal Society Interface*, Vol. 9, No. 70, 2012, pp. 1020–1028.
- [88] Schlangen, E., A. García, M. van de Ven, G. van Bochove, J. van Montfort, and Q. Liu. Highway A58: The First Engineered Self Healing Asphalt Road. *3rd International Conference on Self-Healing Materials*, 2011.
- [89] Wu, S., L. Mo, Z. Shui, and Z. Chen. Investigation of the Conductivity of Asphalt Concrete Containing Conductive Fillers. *Carbon*, Vol. 43, No. 7, 2005, pp. 1358–1363.
- [90] García, Á., E. Schlangen, M. van de Ven, and Q. Liu. A Simple Model to Define Induction Heating in Asphalt Mastic. *Construction and Building Materials*, Vol. 31, 2012, pp. 38–46.
- [91] Li, C. H., C. Wang, C. Keplinger, J. L. Zuo, L. Jin, Y. Sun, P. Zheng, Y. Cao, F. Lissel, C. Linder, X. Z. You, and Z. Bao. A Highly Stretchable Autonomous Self-Healing Elastomer. *Nature Chemistry*, Vol. 8, No. 6, 2016, pp. 618–624.
- [92] Wang, D. P., J. C. Lai, H. Y. Lai, S. R. Mo, K. Y. Zeng, C. H. Li, and J. L. Zuo. Distinct Mechanical and Self-Healing Properties in Two Polydimethylsiloxane Coordination Polymers with Fine-Tuned Bond Strength. *Inorganic Chemistry*, Vol. 57, No. 6, 2018, pp. 3232–3242.
- [93] Abdullah, M. E., K. A. Zamhari, M. R. Hainin, E. A. Oluwasola, N. I. Nur, and N. A. Hassan. High Temperature Characteristics of Warm Mix Asphalt Mixtures with Nanoclay and Chemical Warm Mix Asphalt Modified Binders. *Journal of Cleaner Production*, Vol. 122, 2016.
- [94] Sun, G., D. Sun, A. Guarin, J. Ma, F. Chen, and E. Ghafoori-roozbahany. Low Temperature Self-Healing Character of Asphalt Mixtures under Different Fatigue Damage Degrees. *Construction and Building Materials*, Vol. 223, 2019, pp. 870–882.
- [95] Qiu, J., A. A. A. Molenaar, M. F. C. van de Ven, and S. Wu. Development of Autonomous Setup for Evaluating Self-Healing Capability of Asphalt Mixtures. *Transportation Research Record: Journal of the Transportation Research*, Vol. 2296, 2012, pp. 15–23.
- [96] Thomas Paul Grant. Determination of Asphalt Mixture Healing Rate Using the Superpave Indirect Tensile Test. *University of Florida*. 2001.
- [97] Daniel, J. S., and Y. R. Kim. Laboratory Evaluation of Fatigue Damage and Healing of Asphalt Mixtures. *Journal of Materials in Civil Engineering*, Vol. 13, No. 6, 2001.
- [98] Shirzad, S., M. M. Hassan, M. A. Aguirre, L. N. Mohammad, S. Cooper, I. I. Negulescu, L. N. Mohammad, and I. I. Negulescu. Laboratory Testing of Self-Healing Polymer Modified Asphalt Mixtures Containing Recycled Asphalt Materials (RAP/RAS). *MATEC Web of Conferences*, Vol. 271, 2019, p. 3003.
- [99] Norambuena-Contreras, J., E. Yalcin, A. Garcia, T. Al-Mansoori, M. Yilmaz, and R. Hudson-Griffiths. Effect of Mixing and Ageing on the Mechanical and Self-Healing Properties of Asphalt Mixtures Containing Polymeric Capsules. *Construction and Building Materials*, Vol. 175, 2018, pp. 254–266.

-
- [100] Santagata, E., O. Baglieri, L. Tsantilis, and D. Dalmazzo. Evaluation of Self Healing Properties of Bituminous Binders Taking into Account Steric Hardening Effects. *Construction and Building Materials*, Vol. 41, 2013, pp. 60–67.
- [101] Canestrari, F., A. Virgili, A. Graziani, and A. Stimilli. Modeling and Assessment of Self-Healing and Thixotropy Properties for Modified Binders. *International Journal of Fatigue*, Vol. 70, 2015, pp. 351–360.
- [102] Pang, L., H. Jiang, S. Wu, and S. Wu. Self Healing Capacity of Asphalt Binders. *Journal Wuhan University of Technology, Materials Science Edition*, Vol. 27, No. 4, 2012, pp. 794–796.
- [103] Leegwater, G. A., A. Scarpas, and S. M. J. G. Erkens. 8th RILEM International Conference on Mechanisms of Cracking and Debonding in Pavements. Vol. 13, 2016, pp. 247–252.
- [104] Qiu, J., M. F. C. van de Ven, S. Wu, A. A. A. Molenaar, and J. Yu. Self-Healing Characteristics of Bituminous Mastics Using a Modified Direct Tension Test. *Special Issue Article Journal of Intelligent Material Systems and Structures*, Vol. 25, No. 1, 2014, pp. 58–66.
- [105] Lee, J. N., C. Park, and G. M. Whitesides. Solvent Compatibility of Poly(Dimethylsiloxane)-Based Microfluidic Devices. *Analytical Chemistry*, Vol. 75, No. 23, 2003.
- [106] Aurilio, R. M., M. Aurilio, and H. Baaj. The Effect of a Chemical Warm Mix Additive on the Self-Healing Capability of Bitumen. *Proceedings, RILEM International Symposium on Bituminous Materials*, 2020.
- [107] Hofko, B., L. Porot, A. Falchetto Cannone, L. Poulikakos, L. Huber, X. Lu, K. Mollenhauer, and H. Grothe. FTIR Spectral Analysis of Bituminous Binders: Reproducibility and Impact of Ageing Temperature. *Materials and Structures*, Vol. 51, No. 2, 2018.
- [108] Chen, Y., and C. Wang. Oxidative Aging Effects on Damage-Healing Performance of Unmodified and Polymer Modified Asphalt Binders. *Lecture Notes in Civil Engineering*, Vol. 48, 2020, pp. 393-403.
- [109] Silva, F. A. B., F. A. Chagas-Silva, F. H. Florenzano, F. L. Pissetti, F. A. B. Silva, F. A. Chagas-Silva, F. H. Florenzano, and F. L. Pissetti. Poly(Dimethylsiloxane) and Poly[Vinyltrimethoxysilane- Co -2-(Dimethylamino) Ethyl Methacrylate] Based Cross-Linked Organic-Inorganic Hybrid Adsorbent for Copper(II) Removal from Aqueous Solutions. *Journal of the Brazilian Chemical Society*, Vol. 27, No. 12, 2016, pp. 2181–2191.
- [110] Aurilio, M., A. Qabur, P. Mikhailenko, and H. Baaj. Comparing the Ability of Different Tests and Rheological Indices to Evaluate the Cracking Resistance of Polymer Modified Asphalt Binders. *Proceedings, Canadian Technical Asphalt Association*, Accepted, 2020.
- [111] Gorsuch, C., S. Hogendoorn, Q. Zhou, C. Daranga, and J. McKay. Measuring Surface Tack of Modified Asphalt Binders and Emulsion Residues Using a Dynamic Shear Rheometer (DSR). *International Symposium on Asphalt Emulsion Technology*, 2012.
- [112] Huang, W., Q. Lv, and F. Xiao. Investigation of Using Binder Bond Strength Test to Evaluate Adhesion and Self-Healing Properties of Modified Asphalt Binders. *Construction and Building Materials*, Vol. 113, 2016, pp. 49–56.

Appendix

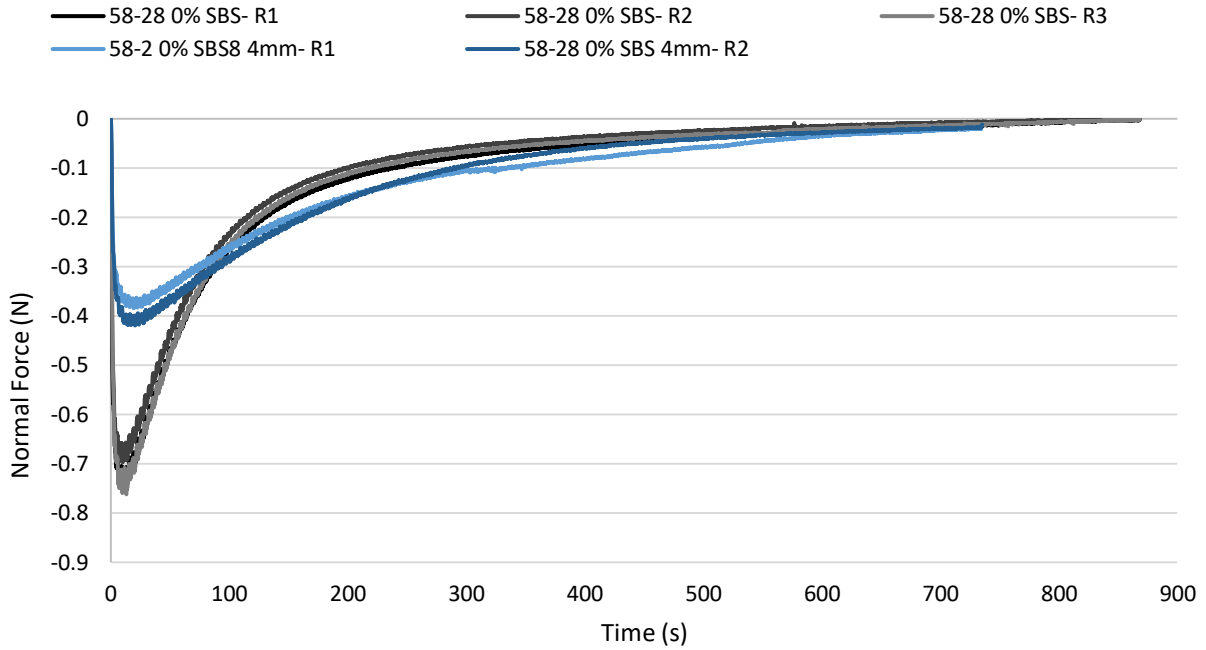


Figure A- 1 Comparison of Normal force versus time for No Gap and the 4mm gap for unmodified 58-28

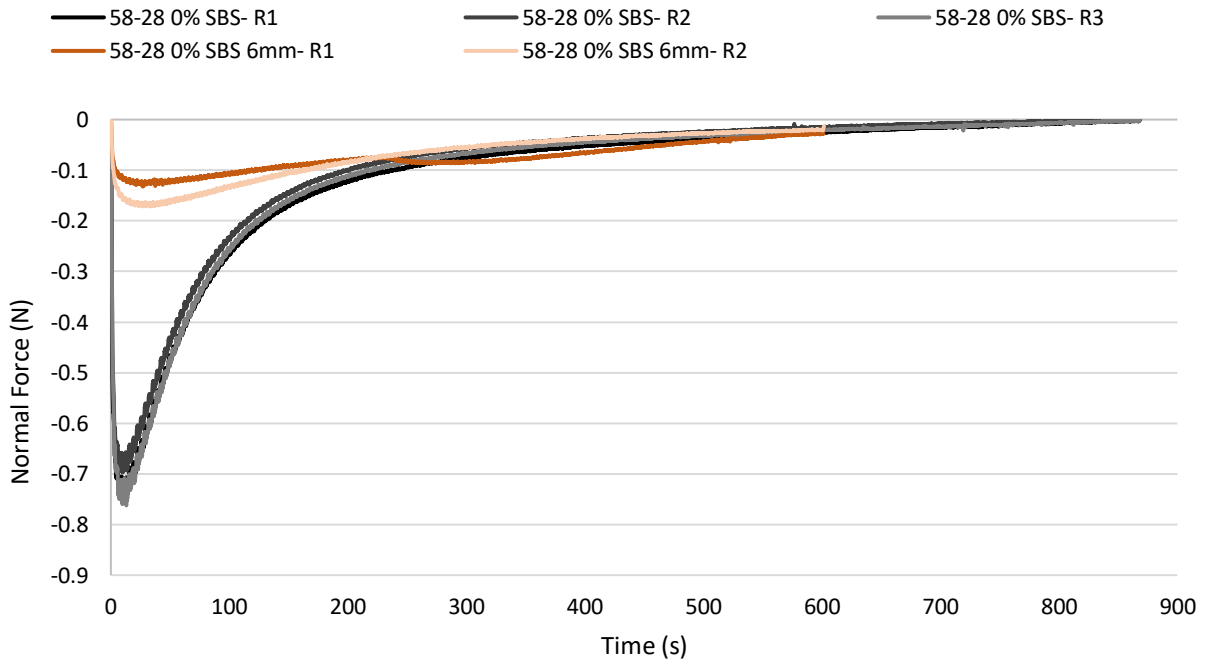


Figure A- 2 Comparison of Normal force versus time for No Gap and the 6mm gap for unmodified 58-28

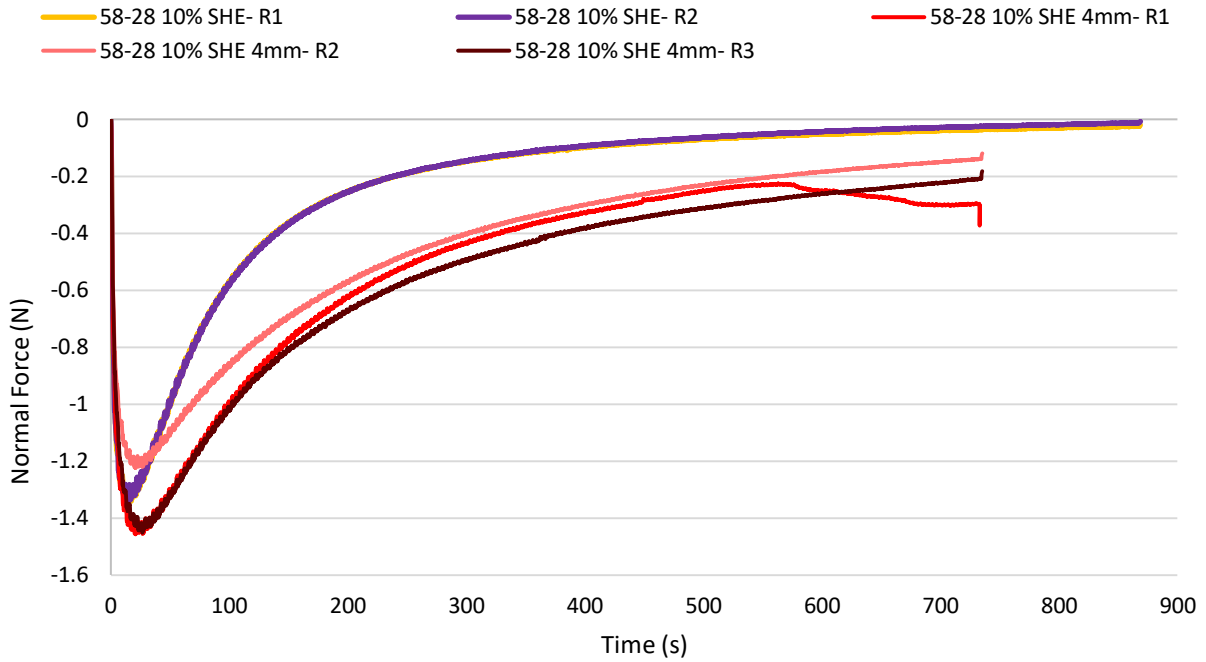


Figure A- 3 Comparison of Normal force versus time for No Gap and the 4mm gap for self-healing asphalt cement (10% SHE)

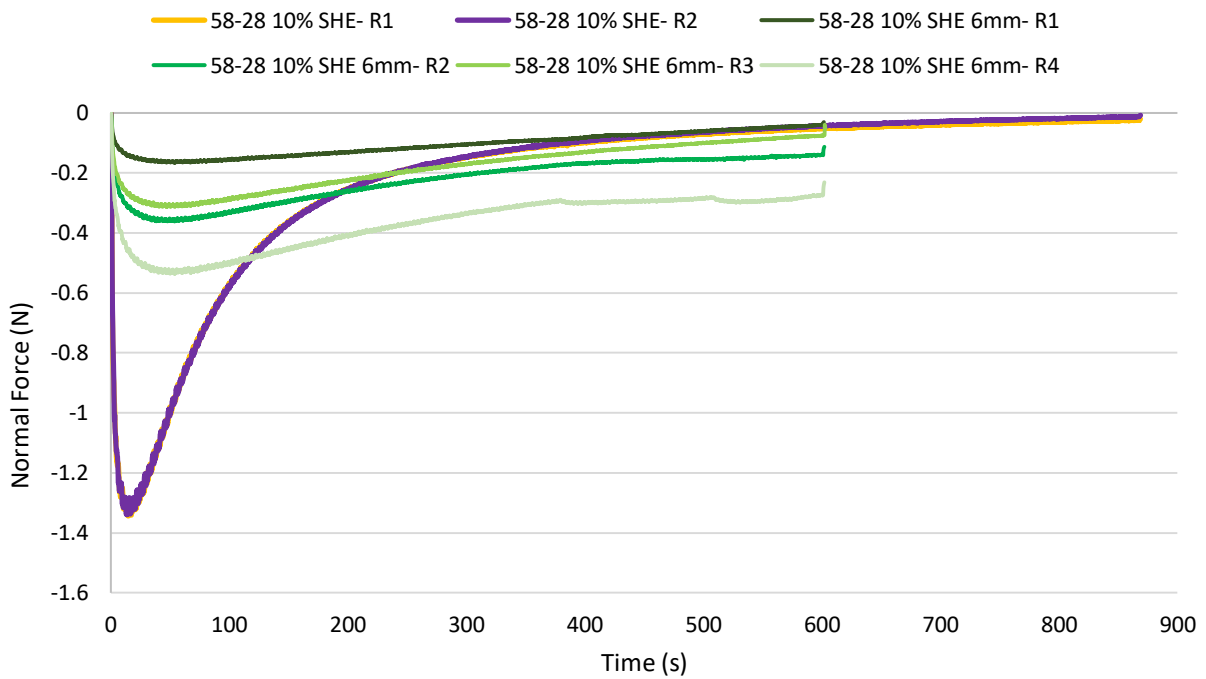


Figure A- 4 Comparison of Normal force versus time for No Gap and the 6mm gap for self-healing asphalt cement (10% SHE)

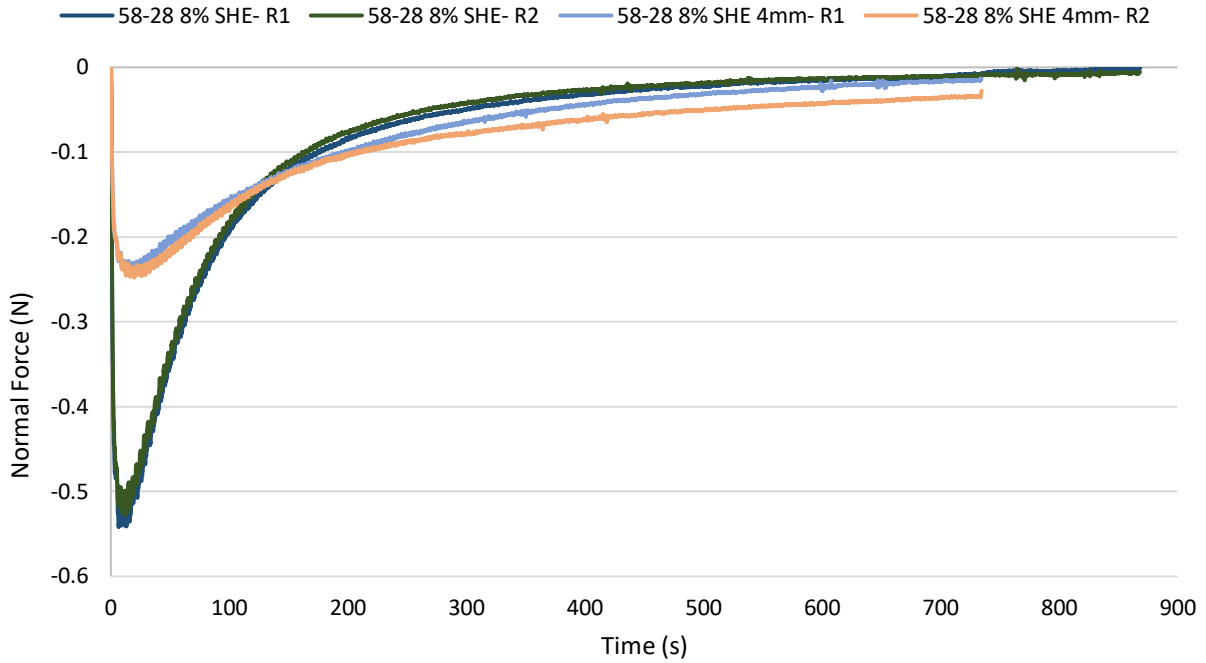


Figure A- 5 Comparison of Normal force versus time for No Gap and the 4mm gap for self-healing asphalt cement (8% SHE)

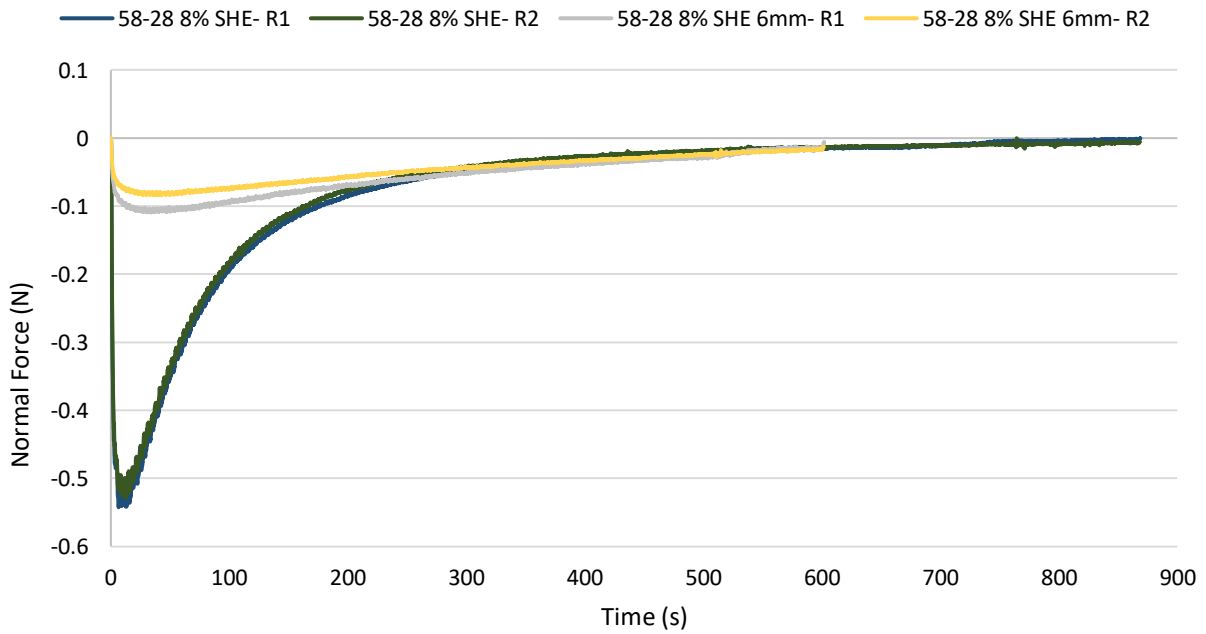


Figure A- 6 Comparison of Normal force versus time for No Gap and the 6mm gap for self-healing asphalt cement (8% SHE)

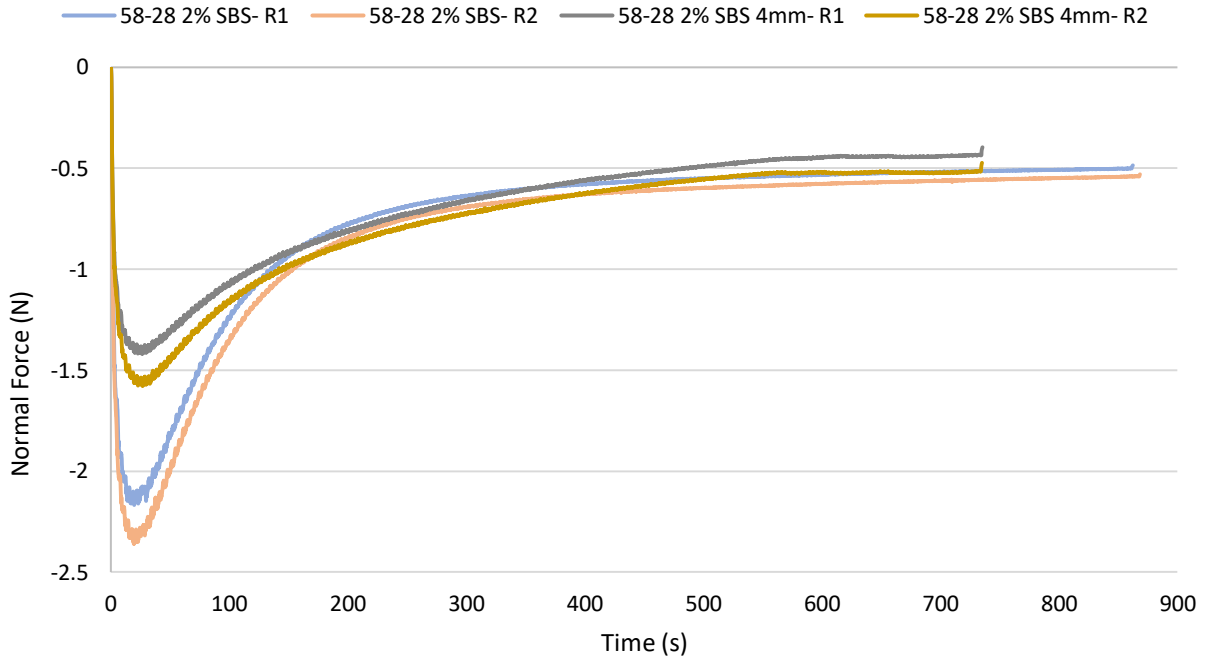


Figure A- 7 Comparison of Normal force versus time for No Gap and the 4mm gap for 58-28 2% SBS

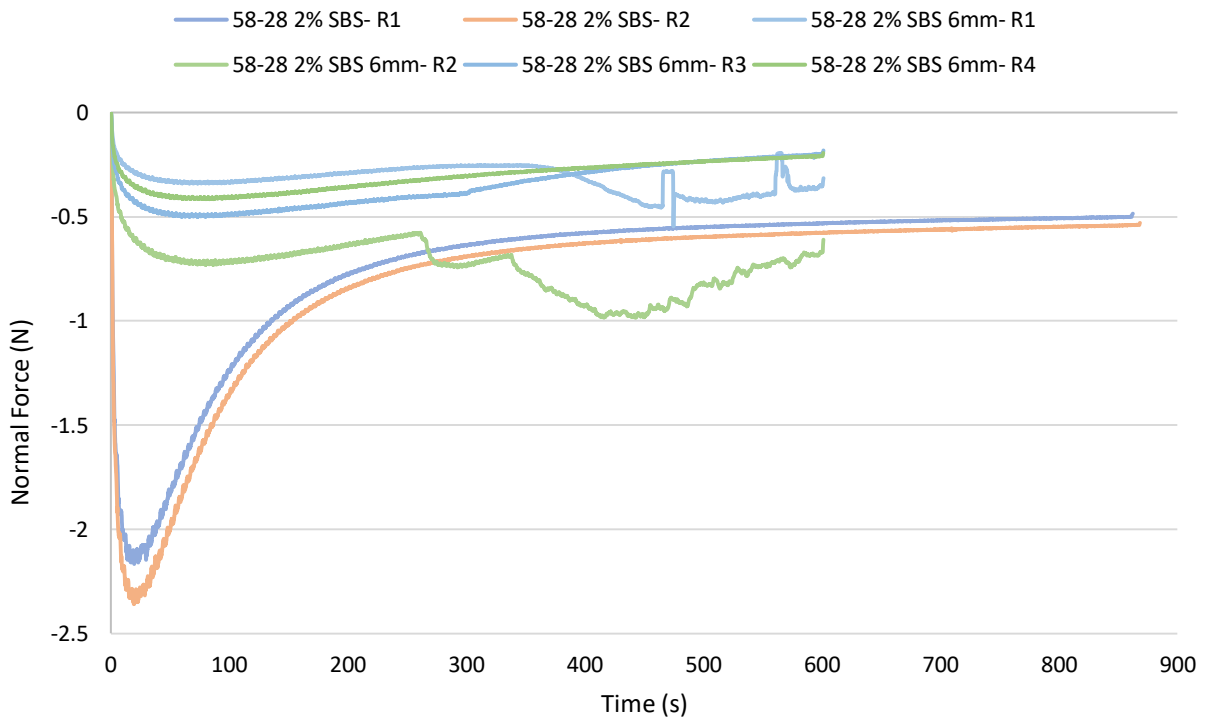


Figure A- 8 Comparison of Normal force versus time for No Gap and the 6mm gap for 58-28 2% SBS

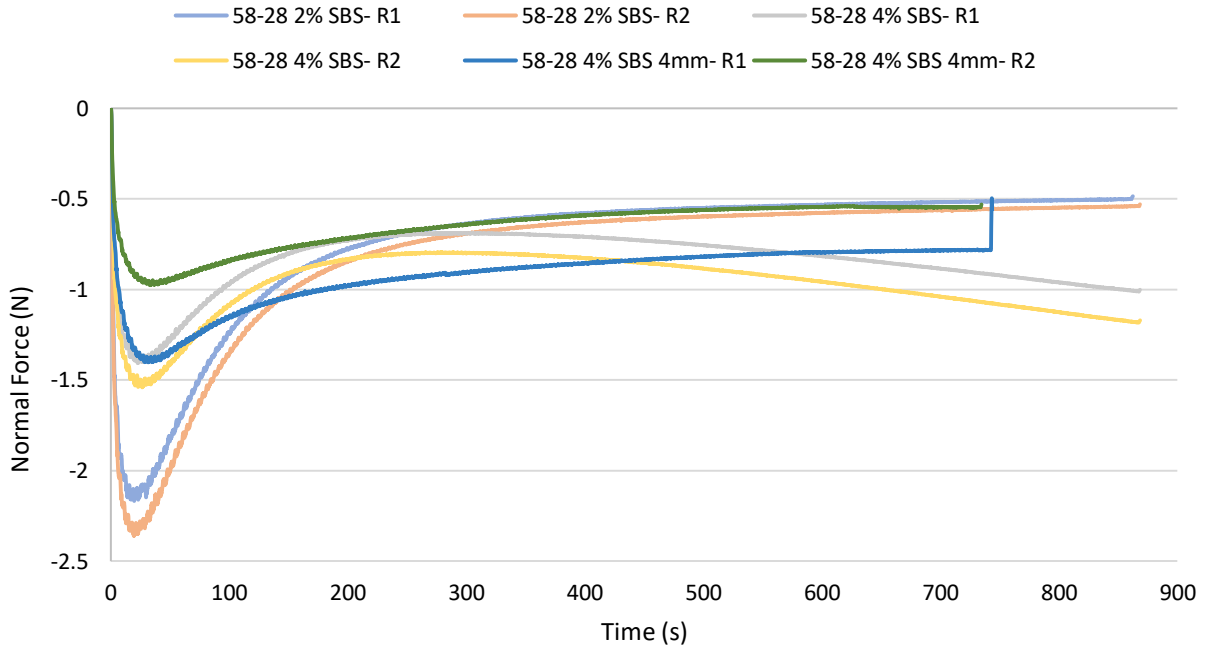


Figure A- 9 Comparison of Normal force versus time for No Gap and the 4mm gap for 58-28 4% SBS

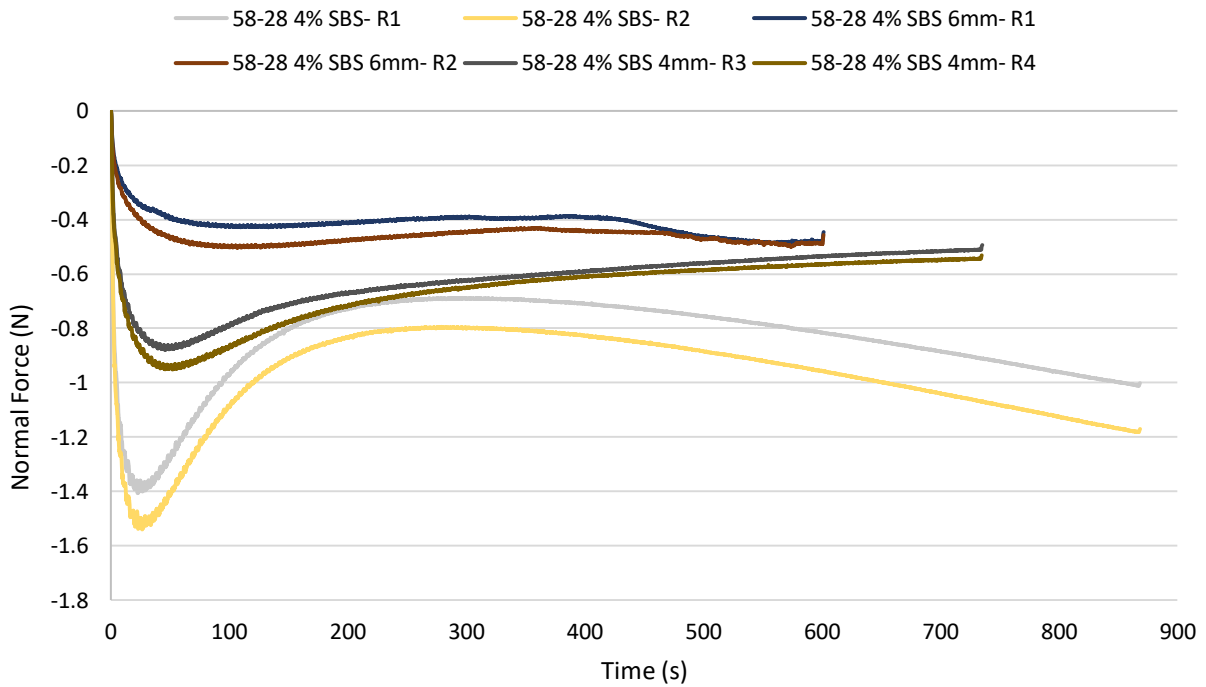


Figure A- 10 Comparison of Normal force versus time for No Gap and the 6mm gap for 58-28 4% SBS